SNOWCOVER

ACCUMULATION, RELOCATION AND MANAGEMENT

J.W. Pomeroy
and D.M. Gray

NHRI Science Report No. 7

Chapter 2 - Pg 6 - add the following row to Table 1

Table 1 *Snowpack Densities (after Seligman, 1980).*

SNOW TYPE	DENSITY (kg/m^3)
Hard wind slab	350

Chapter 4 - Pg 54 - 1st para., 3rd line, - Df should be D_f

Chapter 5 - Pg 73 - 1st para., 4th line, - Q_s (W/m^2) should be Q_s (W)

Chapter 5 - Pg 73 - $d\overline{m}(z)/dt$ should be $d(\overline{m}(z))/dt$

$$q_{subl} = \int_o^{z_b} \frac{d(\overline{m}(z))/dt}{\overline{m}(z)} \eta(z)\, dz, \quad and$$
$$q_{subl} = \int_o^{z_b} V_s(z)\eta(z)\, dz\,. \tag{48}$$

Chapter 5 - Pg 78 - x should be x in all cases

$$q_v(\mathrm{x},0) = \frac{dq_{salt}}{d\mathrm{x}}(\mathrm{x}) + \frac{dq_{susp}}{d\mathrm{x}}(\mathrm{x}) + q_{subl}(\mathrm{x}) + q_v(\mathrm{x}, z_b)\,, \tag{62}$$

Chapter 6 - Pg 95 - exp[-10(should be exp[-0.10(

$$\mathrm{TRAN}_m(25,1) = -8.26 + 0.89u_{10} + 5.70\exp[-0.10(T_{\max} + 20)] + 0.041RH_{\max} + 3.32\exp[\frac{-8.72}{d}]\,. \tag{67}$$

Chapter 6 - Pg 96 - 14.33 should be -14.33

$$\mathrm{TRAN}_m(1,1) = -14.33 + 2.26u_{10} - 0.25T_{\max} + 0.046RH_{\max} + 0.079P_m\,. \tag{69}$$

Environment Canada Environnement Canada

Canada

NATIONAL HYDROLOGY RESEARCH INSTITUTE
INSTITUT NATIONAL DE RECHERCHE EN HYDROLOGIE

National Hydrology Research Institute
11 Innovation Boulevard
Saskatoon, Saskatchewan
Canada S7N 3H5

Cat. En36-513/7E
NHRI Science Report No. 7

ISSN 0843-9052
ISBN 0-660-15816-7

Preface

Much of Canada's water supply is derived from snow. In most parts of the country, the annual spring freshet plays a key role in sustaining our aquatic ecosystems, while for semi-arid, boreal, alpine and arctic regions, snow is an important source of fresh water. In the context of sustainable development, i.e., the balanced management of natural resources to achieve a long-term, reasonable level of economic well-being while maintaining environmental values, snow plays a vital part. On the Canadian Prairies, for instance, snow management practices now often go hand-in-hand with no-tillage practices in the ongoing effort to sustain agricultural production over the long term. As another example, research conducted under the Canadian Model Forest Programme has highlighted the important role of snow in sustainable forestry management practices.

Snow can be considered as a physical resource, a raw material possessing properties that contribute to the production of food, fibre and other beneficial products for human use and enjoyment. As with the sun, the soil, the air and the rain, the natural behaviour of snow can be studied, understood and ultimately managed. In a country such as Canada, a better understanding of snow processes will make a significant contribution to hydrological science.

This scientific report on snowcover accumulation, relocation and management is a necessary step on the road to sustainable development. The dedication of the authors in preparing this comprehensive report that will be widely used by engineers, agriculture and forestry practitioners, scientists and university students is gratefully acknowledged.

R.A. Halliday

Director
National Hydrology Research Institute

Acknowledgements

The authors would like to acknowledge the contribution of many people to the publication of this Science Report. Dr. Walter Nicholaichuk, Chief, Hydrological Sciences Division, NHRI, continuously encouraged and supported the project. Colleagues at Environment Canada and the University of Saskatchewan, Saskatoon, the Rocky Mountain Forest and Range Experiment Station, Wyoming and the University of East Anglia, England have supported the research effort and participated in studies. Substantial contributions were made by those who designed instrumentation and collected field data, particularly Dell Bayne and Thomas Brown, Division of Hydrology, and Newell Hedstrom and Cuyler Onclin, NHRI. Dr. Leah Watson, NHRI and Simon Ommanney, International Glaciological Society, Cambridge edited the report. Elaine Wigham, Division of Hydrology and Philip Gregory, NHRI assembled the report text and figures, and Brenda Doell provided copy-editing services.

We gratefully acknowledge the financial support received from the National Hydrology Research Institute, the Canadian Global Energy and Water Cycle Experiment, the Prince Albert Model Forest Association, and the operating and strategic grants programme of the Natural Sciences and Engineering Research Council of Canada.

TABLE OF CONTENTS

LIST OF TABLES

LIST OF FIGURES

Chapter 1

INTRODUCTION

The seasonal snowcover exerts a major influence on the environment and on human activity at the Earth's surface. The presence of snowcover is associated with colder weather because snow efficiently reflects solar radiation back into the atmosphere and requires large amounts of heat to melt or sublimate. Sublimation of snow, while providing a winter source of water vapour to a relatively dry, mid-continental atmosphere, represents water lost to subsequent management and use. Large or unexpected accumulations of snow and reductions in visibility due to blowing-snow events interfere with human activities, particularly transport by road, rail and air. This has changed the course of historic battles and where persistent has impeded development of some mountain and northern regions. High snow loads can have deleterious effects on the structural integrity of buildings. Rapid melt of deep snow accumulation can lead to flooding, especially over frozen ground. Melt of heavily-polluted snow can lead to acid-shock upon entering aquatic ecosystems.

Conversely, snowcover serves many beneficial purposes. It is the basis of winter recreation industries, an insulator of flora and fauna throughout the winter, a sink for nutrients, and the host of various micro-organisms. In many semi-arid, boreal, alpine and arctic environments in Canada, melt of the seasonal snowcover is the most significant hydrological event of the year. Water derived from melting snowcovers often provides over 80% of the annual surface runoff, augments soil water reserves, and replenishes groundwater supplies. The entry of snowmelt water with its accompanying flux of heat and nutrients initiates and fosters spring biological activity in northern soils. Over the globe, snow supplies more than one-third of the water used in irrigation. In China, India, Pakistan,

Russia, Kazakhstan, Tajikstan, Turkmenistan, Uzbekistan, USA and Mexico, large desert areas are cultivated because snowmelt water flows in from adjacent snow-covered mountains.

Because snow has such widespread effects, there is a demand for information on the distribution, disposition and management of the seasonal snowcover. This Science Report aims to provide an understanding of major processes and factors affecting the spatial and temporal distribution of snowcover and its properties. The text focuses on the physical aspects of snow accumulation, relocation and management, documenting several decades of field and theoretical research from Canada and elsewhere. An attempt is made to link the physics of snow accumulation and relocation phenomena with practical guidelines for the management and control of snow.

Chapter 2

SNOWCOVER DEPTH, DENSITY AND WATER EQUIVALENT

Three of the most important physical properties of a snowcover are depth, density and water equivalent. Snow water equivalent, SWE, the equivalent depth of water of a snowcover, is not usually measured directly. Since a uniform depth of 1 mm of water spread over an area of 1 m^2 weighs 1 kg, SWE is calculated from snow depth, d_s, and density, ρ_s, by the expression:

$$SWE = 0.01 \; d_s \; \rho_s \; , \qquad (1)$$

in which SWE is in mm when d_s is in cm and ρ_s is in kg/m^3. Expressing snow water equivalent in mm and snow depth in cm is the practice of weather and water data collection agencies in Canada.

An average density for new snowfall equal to 100 kg/m^3 is often assumed. This gives 1 unit of water equivalent for 10 units of snow depth. It is not appropriate to use a common conversion for all environments, however. The density of freshly-fallen snow varies widely depending on the amount of air contained within the lattice of the snow crystals. Densities in the range of 50 to 120 kg/m^3 are common. Lower values are generally found in snowfalls formed under dry, cold conditions; higher values are found in wet snow at warm temperatures. The U.S. Army Corps of Engineers (1956) showed that the density of new-fallen snow decreases exponentially as the air temperature decreases below freezing (Figure 1).

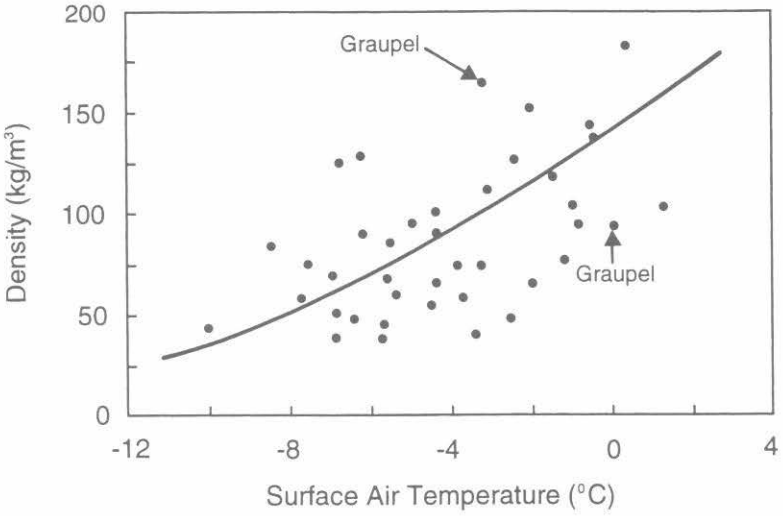

Figure 1. Relationship between density of new fallen snow and air temperature. Measurements were made at Central Sierra Snow Laboratory at an elevation of 2104 m in the Sierra Nevada Mountains of California. Air temperatures were taken at a height of approximately 1.22 m above the snow surface at about the same time as the density measurements.

2.1 Time Variation of Snow Density

Following deposition, the density of new snow increases rapidly with changes in the size, shape and bonding of snow crystals. This densification process is termed metamorphism, and is caused by temperature and water vapour gradients, crystal settlement and wind packing. Goodison *et al.*(1981) monitored average density increases between 8 and 13 kg/m^3/h during storms of less than 12 hours duration; increases in the range from 104 to 152 kg/m^3 in 6.5 h occurred after cessation of the storms. Their measurements were made under non-drifting conditions. The effect of wind packing is largest in exposed sites. Gray *et al.*(1970) reported a sixfold increase, from 45 kg/m^3 to 250 kg/m^3 in 24 hours, in the density of freshly-fallen snow during a blizzard on the Canadian Prairies.

The average density of a snowpack also varies seasonally (see Figure 2). The seasonal increase generally is largest in boreal forest and subarctic regions where densities increase from about 200 kg/m^3 in late winter to 350 kg/m^3 or greater as the snow ripens. These large increases are due to metamorphism caused by the strong temperature gradients that form in relatively shallow snowpacks (Sturm, 1991). Conversely, Pomeroy *et al.*(1993) report the halving of snow densities over winter near the bottom

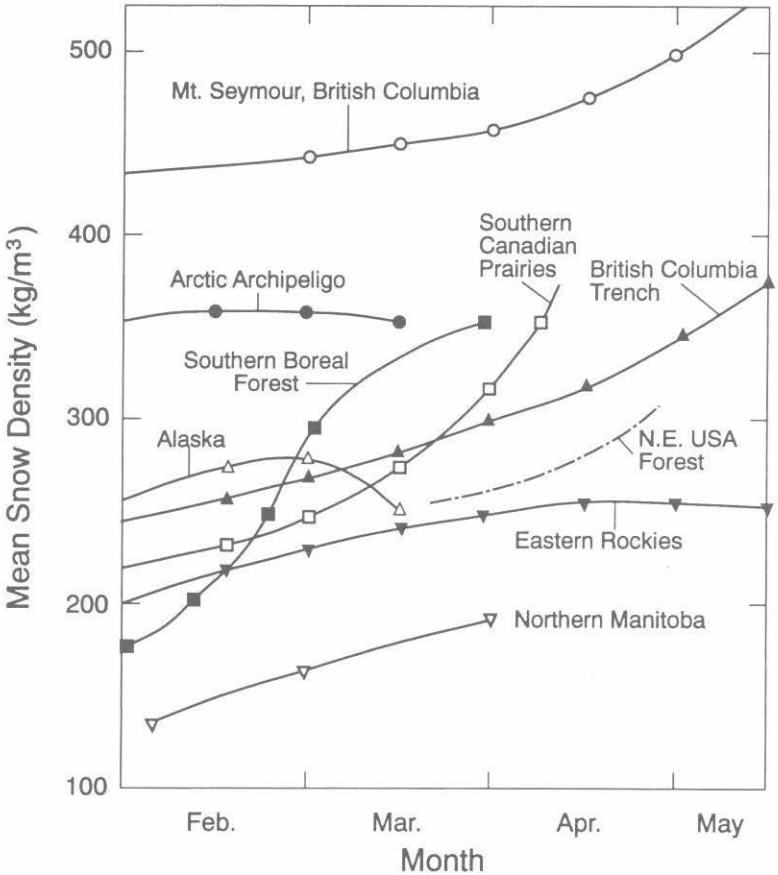

Figure 2 *Seasonal variation in average snowcover density.*

of shallow snowpacks near Inuvik, NWT, due to the upward flux of vapour along temperature gradients. Densities increased proportionately above this basal layer.

During snowmelt, the density of a snowpack may vary extensively due to storage and loss of meltwater. Melting snow densities commonly range between 350 and 500 kg/m^3. Lower densities occur in the morning, and density increases during the day as a snowpack becomes primed by infiltrating meltwater. Typical densities for dry snowcovers in a variety of environments are given in Table 1.

Table 1 *Snowpack Densities (after Seligman, 1980).*

SNOW TYPE	DENSITY (kg/m^3)
'Wild' snow	10 to 30
Ordinary new snow, immediately after falling in still air	50 to 65
Settling snow	70 to 190
Settled snow	200 to 300
Very-slightly-wind-toughened snow immediately after falling	63 to 80
Average wind-toughened snow	280

2.2 Density - Depth Interaction

Shallow Seasonal Snowcovers

Because for shallow snowcovers the density of snow in an area varies less than its depth, fewer density measurements are necessary to determine the areal mean snow water equivalent, $\overline{SWE}$. The $\overline{SWE}$ is related to the mean density $\overline{\rho_s}$ and mean depth $\overline{d_s}$ for a single set of measurements by the relationship noted by Steppuhn (1976):

$$\overline{SWE} = 0.01(\overline{\rho_s}\,\overline{d_s} + C) \qquad (2)$$

where SWE is in mm when $\overline{\rho_s}$ is in kg/m^3, $\overline{d_s}$ is in cm and C is the covariance of snow depth and density.

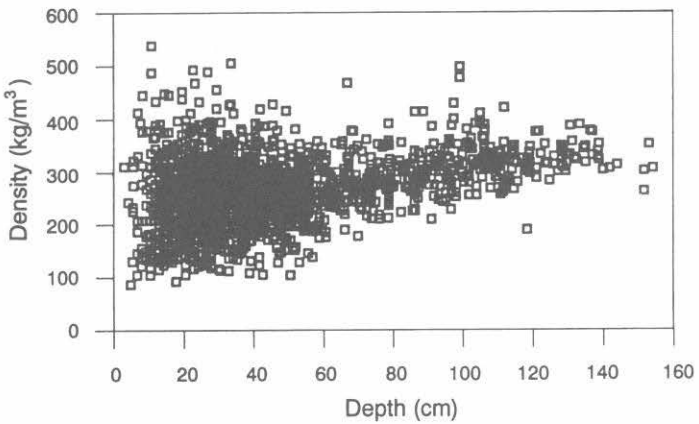

Figure 3 *Variation in density with depth for shallow prairie snowcovers that have not undergone appreciable melting.*

In those regions of the Canadian Prairies that do not experience major melt events during winter, the covariance between the density and depth of shallow snowcovers in late winter or early spring prior to active melting usually is very small. This is shown by Figure 3, in which snow density is plotted against depth for approximately 2,400 measurements taken over several years on a variety of landscapes in west-central Saskatchewan. For snow depths less than 60 cm, there is poor association between density and depth ($r^2 = 0.008$); for depths greater than 60 cm the association is stronger ($r^2 = 0.19$). When the covariance is small and need not be taken into account,the mean water equivalent of a snowcover can be calculated directly from the mean snow depth by Equation 1.

Figure 4 shows the linear association between the mean water equivalent

$$\overline{SWE}$$

(mm) and the mean depth

$$\overline{d_s}$$

(cm) for prairie snowcovers having a mean depth less than 60 cm. The best fitted values for equation 2 are:

$$\overline{SWE} = 2.39\,\overline{d_s} + 2.05\,. \qquad (3)$$

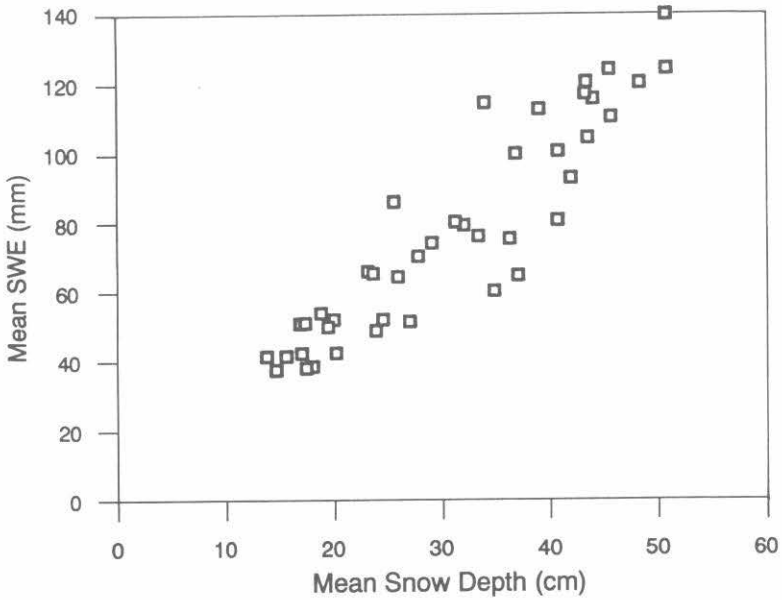

Figure 4 *Association between mean water equivalent and mean depth for shallow (≤ 60 cm) prairie snowcovers that have not undergone appreciable melting.*

The slope corresponds to a mean density, ρ_s = 239 kg/m^3, which is very close to the measured average density of 246 kg/m^3. The intercept (2.05) typifies the low covariance between density and depth.

When the process is repeated for snowcovers having a mean depth greater than 60 cm (see Figure 5), the parameters of the linear relationship change: the coefficient increases to 3.41 whilst the intercept declines to -45.6.

The coefficients of Equation 2 for greater and lesser than 60 cm depth are not significantly different at the 5% level; however, the intercepts are significantly different, indicating an increasing covariance between density and depth as depth increases (Shook and Gray, 1994). This increasing covariance means that simple relationships such as Equation 3 are only valid for snowcovers more shallow than 60 cm.

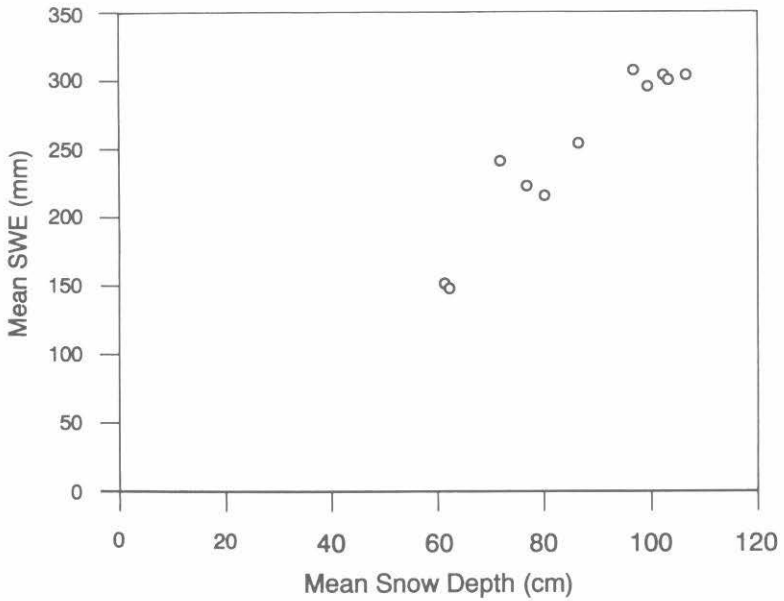

Figure 5 *Association between mean water equivalent and mean depth for deep (> 60 cm) prairie snowcovers that have not undergone appreciable melting.*

Deep Seasonal Snowcovers

Tabler *et al.* (1990b) found from extensive field measurements that the integrated density of deep snow drifts, ρ_s (kg/m^3), increased with depth, d_s (cm), as:

$$\rho_S = 522 - \frac{20470}{d_S}[1 - \exp(-\frac{d_S}{67.3})]. \quad (4)$$

An analogous expression for non-melting snowcovers in the central and northern zones of the agricultural region of the Canadian Prairies that are continuous over winter is:

$$\rho_S = 488 - \frac{20470}{d_S}[1 - \exp(-\frac{d_S}{67.3})]. \quad (5)$$

Combining Equations 4 and 5 with Equation 1 leads to the following expressions for the water equivalent of accumulations of wind-transported snow as a function of depth. The expressions follow the form of Equation 2 with a function that increases the covariance of depth and density as depth increases:

$$SWE = 5.22 d_S - 204.7\,[1 - \exp(-\frac{d_S}{67.3})], \quad \text{and} \quad (6)$$

$$SWE = 4.88 d_S - 204.7\,[1 - \exp(-\frac{d_S}{67.3})]. \quad (7)$$

For snow drifts and snowcovers greater than 60 cm in depth, Equations 6 and 7 respectively are recommended to calculate SWE from depth of snow.

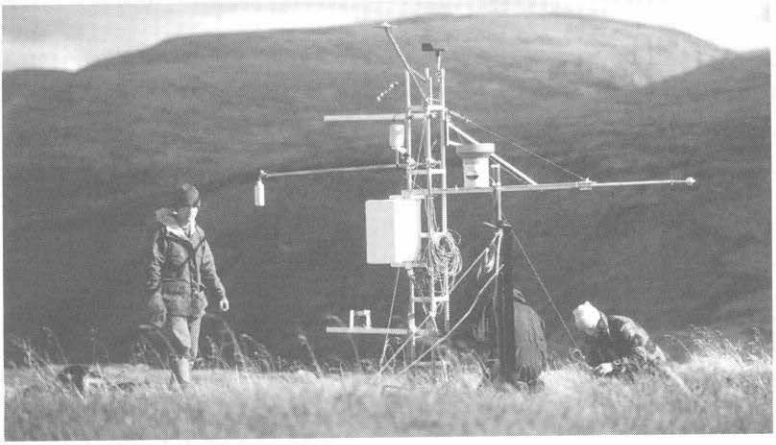

Figure 6 *Ultrasonic snow-depth sensor, Wolf Creek, Whitehorse, Yukon.*

2.3 Snowcover Measurement

There are no universally accepted instruments for measuring snow depth, density, and water equivalent and even methodologies may vary widely with the user and with site conditions. Several methods used in North America to measure these snow parameters are summarized below. The references should be consulted for complete descriptions.

Point Measurements

Snowcover Depth

Method: Snow ruler, graduated rod and aerial snow markers

Principle: A ruler or rod is pushed through the snowpack to the ground surface and the depth measured directly. In remote regions, snow markers may be used. The depth of snow at a marker is observed from distant ground points or from aircraft by means of binoculars or telescopes. The technique is normally straightforward and accurate but becomes labour-intensive for frequent sampling. During periods of intense solar radiation, preferential snow melt/evaporation may occur around permanently installed snow rulers.

Reference: Goodison *et al.* (1981).

Method: Sonar (Figure 6)

Principle: An ultrasonic pulse is emitted from a fixed, downward-facing horn placed from 0.5 to 10 m above the snow surface and the timing of its echo is recorded by a co-located receiver/micro-processor. Concomitant measurements of air temperature are used to calculate the speed of sound in air, which, together with the travel time of the ultrasonic pulse, is used to calculate the distance from horn/receiver to the snow surface. Anomalous measurements may occur during falling or blowing snow. Also, an ultrasonic pulse cannot distinguish newly-fallen, low-density snow. A resolution of 0.1 cm in depth can be achieved at other times. Advantages of the technique are non-disturbance of measured snow and a spatial average of depth over a circular area that may vary from 0.2 to 2 m in diameter. The spatial averaging compensates for the presence of snow dunes and changes in microstructure.

Reference: Gubler (1981), Goodison *et al.* (1984; 1988).

Snowcover Density

Method: Gamma ray attenuation

Principle: Attenuation of gamma radiation by a snow sample placed between a radioactive source (usually 5 millicurie ^{137}Cs) and a detector. The method uses the principle that the attenuation of radiation emitted by a source follows an exponential decay whose rate depends on the density, absorptivity and length of the intervening material. To obtain the density from the measured gamma particle count rate one must know the intensity of the source, the extinction coefficient of ice and sample length. Horizontal layers, approximately 2-cm thick, 5-cm wide and 60-cm long, are sampled. Profiling gauges monitor changes in density occurring within thin layers of a snowpack over time. The attenuation principle has also been used in instruments designed to measure the snow density of shallow snow packs (1 m deep) from a portable source/detector arrangement. The low-intensity source is located on a snow rod driven vertically through the snowpack to the ground surface. A portable detector is placed on top of the pack for measurement. Increasing concerns about the security of, and human exposure to, radioactive sources have limited the use of this method.

Reference: Smith *et al.* (1972)

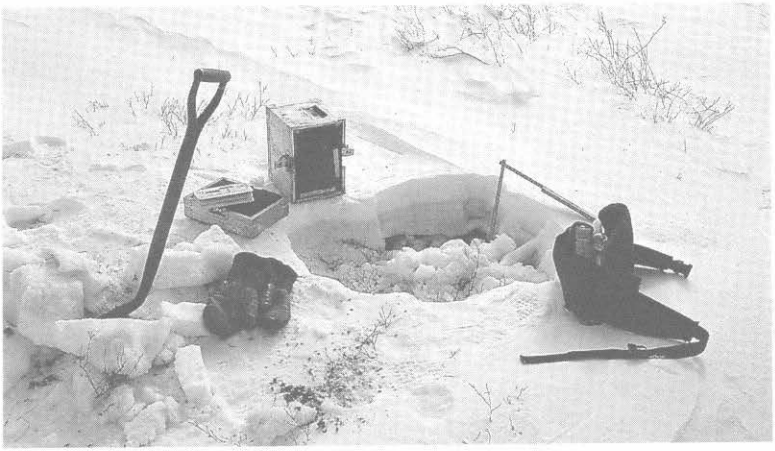

Figure 7 Gravimetric sampling of snow water equivalent, Inuvik, N.W.T.

Method: Snow pit and gravimetric samples (Figure 7)

Principle: A pit is dug to the bottom of the snowpack and individual snow strata (layers of snow having distinctive properties such as density, hardness and grain-size) are identified and their thickness measured. A small scoop (100 to 250 ml) is used to remove samples of snow from each layer and these samples are weighed to determine density. The average density for a snowpack can be obtained by dividing the sum of the densities for the layers weighted according to layer thickness by the depth of snow. This technique is straightforward and very accurate but destroys the snowpack and is quite labour-intensive.

Reference: IASH/Unesco/WMO (1970).

Method: Microwave radar
(Frequency Modulated Continuous Wave, FMCW) (Figure 8)

Principle: Microwave radiation is transmitted vertically into the snowpack at frequencies sweeping from 3.6 to 18 GHz. A collocated antenna receives the reflected radiation. The difference between the spectra of transmitted and received frequencies is used to calculate the "electrical depth" of various reflecting surfaces within the snowpack (usually stratum interfaces) which is related to the density of the intervening snow. The FMCW radar unit may be stationary or carried on

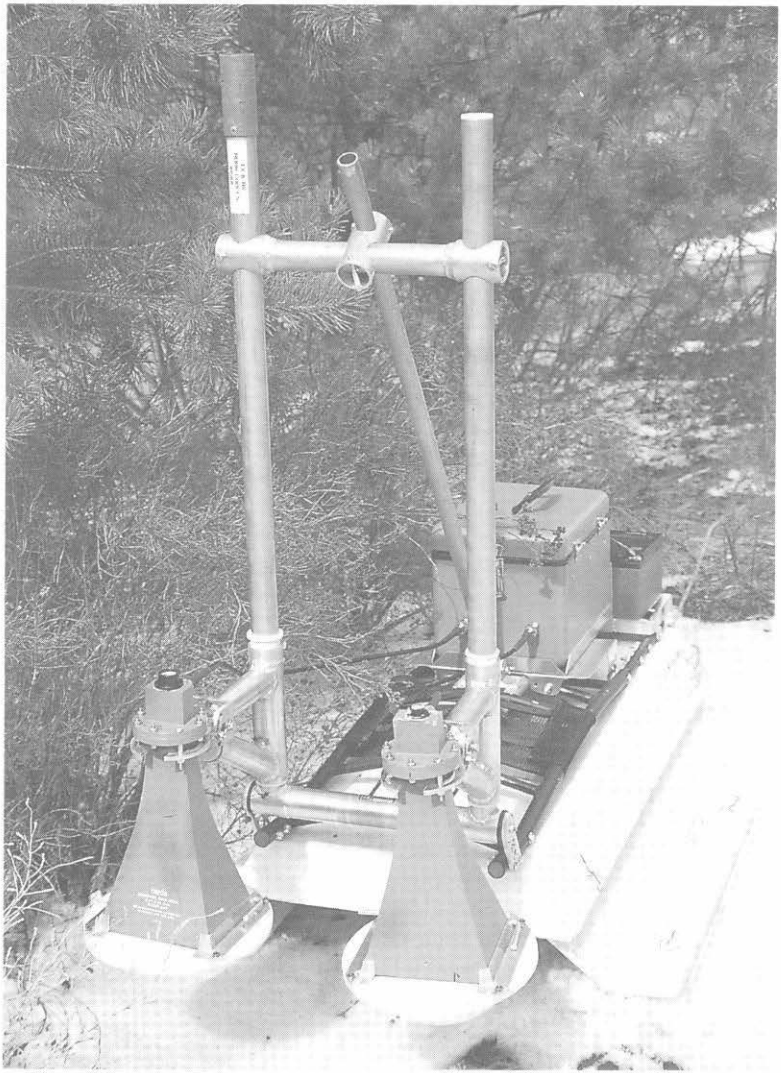

Figure 8 *NHRI's microwave (FMCW) radar unit.*

a sled. Estimates of the dielectric constant and concomitant measurements of depth provide profiles of density and water equivalent. The non-destructive sampling and continuous profiling of this technique during snow surveys are useful for measurement of the vertical variation of snow density over large time and space scales.

Reference: Ellerbruck and Boyne (1979), Gubler and Hiller (1984).

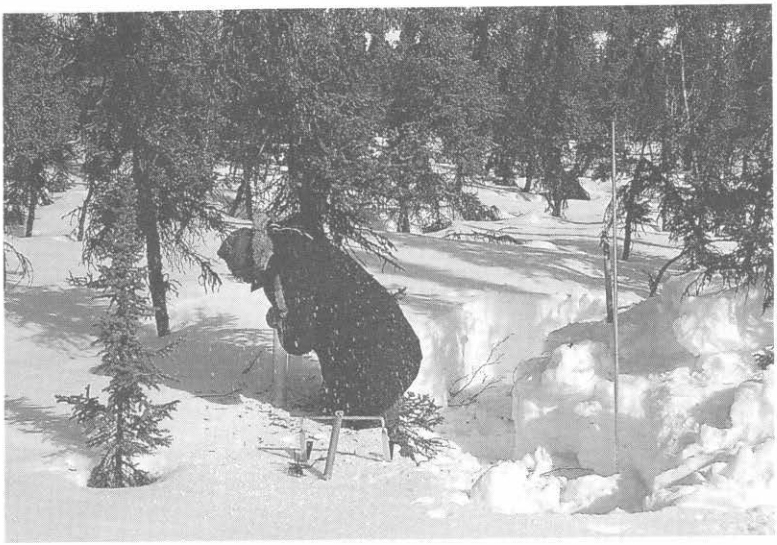

Figure 9 *Snow sampling tube and scale, Inuvik, N.W.T.*

Snowcover Water Equivalent

Method: Gravimetric

Principle: A snow tube, a graduated, hollow tube with a cutter fitted to the end, is used to obtain a vertical core of snow. The water equivalent of the core is determined either by melting it or by weighing it (Figure 9). The operator must be careful to obtain a full core of snow without spillage. This is often difficult where woody vegetation underlies the snowpack or where a layer of large, unconsolidated snow crystals exists at the base of the pack. Water may drain from extremely wet snow in the tube. The gravimetric technique is presently the most commonly-used snow water equivalent measurement and with an experienced operator can be very accurate.

Reference: Goodison *et al.* (1981).

Method: Snow pillow (Figure 10)

Principle: A mattress-type apparatus filled with fluid (antifreeze) and installed below the snowpack is used to monitor snow water equivalent by responding to the weight of snow accumulated on its surface. The pressure changes usually are measured with a manometer or a pressure transducer. Pillows come in various shapes (octagonal and circular), sizes (~3.5 m^2 to ~11.5 m^2), and materials (butyl rubber, sheet metal and

Figure 10 *Snow pillow, Carcross, Yukon Territory. Photograph by M. Jasek.*

stainless steel). Snow pillows are most effective for monitoring relatively-deep snowpacks in sheltered environments. Bridging of snow due to ice or hard-snow layers and wet, draining snow makes interpretation of snow pillow measurements difficult. Their low maintenance requirements have led to frequent installation in remote areas; however they can be destroyed or disturbed by large mammals.

Reference: Goodison *et al.* (1981).

Areal Measurements

Surface-based Depth and Density

Method: Snow surveying

Principle: Snow surveys are made at regular intervals throughout winter at designated stations along a permanently-marked traverse (snow course) to determine depth, vertically-integrated density, and snow water equivalent. The length of a snow course and the distance between sampling points vary depending on site conditions and uniformity of snowcover. In hilly terrain, a snow course generally is 120 to 270 m long with observations taken at about 30-m intervals. In open environments, a snow course may be longer with density measurements taken 100 to 500 m apart and depth measurements made at about five equally-spaced points between the density locations. Figure 11 and Table 2 provide details required for proper documentation of snow course information.

Reference: Goodison *et al.* (1981).

888-81

Province of British Columbia
Ministry of Environment

SURFACE WATER SECTION
WATER MANAGEMENT BRANCH
Parliament Buildings
Victoria British Columbia
V8V 1X5

SNOW SURVEYS

Snow Course No. 3A01 — 81/03/01 (Yr./Mo./Da.)

Snow Course Name Grouse Mountain

Observer's Name J. Atkinson

No. Of Tube Sections Used: 5 Driving Wrench Used: Yes ✓ No ___

Station No.	Snow Depth cm: with dirt plug	Snow Depth cm: without dirt plug	Core Length cm	Weight Tube and Core	Wt. Tube Only Before Sampling	Water Equivalent cm	Density %
1		76	74	80	48	32	
	302	300	221	147	48	99	
1		300	295			131	44
2		95	91	86	48	38	
	318	315	216	140	48	92	
2		315	307			130	41
3		54	51	71	48	23	
	283	282	223	145	48	97	
3		282	274			120	43
Total							
Average							

FOR REGIONAL OFFICE VERIFICATION ONLY

___ cm ___ mm ___

Verified By: _____ Date: _____ Density: _____

FOR VICTORIA USE ONLY

Approved By: _____ Date: _____ Density: _____

Figure 11 Basic form for recording snow course measurements, (B.C. Ministry of the Environment).

Method: Stratified sampling (unitized sampling).

Principle: This method is based upon the association between average snowcover depositional patterns and landscape features. A watershed is divided into land units on the basis of terrain, land use and vegetative

characteristics. Random samples of snow density and depth are taken from a few units of a specific class and these are used to calculate the average snow water equivalent for that class. Mean depth of water on a watershed is obtained by weighting the values for various classes according to area. The number of depth and density measurements taken on a given landscape class should attempt to define the mean snow depth with a relative error of about 5% and the standard deviation with a relative error of about 10%. Sampling of snow density around a central depth (mean, median or mode) is recommended. Where the coefficients of variation for snow depth and density are available, these should be used to calculate the number of samples required for the specified basin-wide accuracy. The method is most successful in relatively-homogeneous climatological zones where the seasonal snowcover does not melt noticeably over the winter and where terrain, ground cover and weather patterns tend to cause snow to accumulate in recurring patterns each year. Ground cover data can be updated annually with Landsat imagery.

Reference: Adams and Findlay (1966), McKay (1970), Steppuhn and Dyck (1974), Steppuhn (1976), Granberg (1978), Woo *et al.* (1983).

Remote Sensing

Method: Visible, near-infrared and mid-infrared imagery.

Principle: These images may be collected from sensors mounted on specially-commissioned airplanes or from satellites. When corrected for atmospheric conditions, the images display the emittance and/or reflectance by the Earth's surface of electromagnetic radiation. The application of these data to determine snow-covered area can be limited by clouds, mountainous terrain, vegetation and atmospheric haze. The desired spatial resolution of the images must be balanced by the required frequency of coverage of the satellite. The most commonly-used images in Canada are distributed by the US-NASA (Landsat) and US-NOAA (NOAA series, GOES and TIROS N). Landsat thematic mapper (TM) band 1 (blue $\lambda = 0.45$ to 0.52 μm) is used to distinguish snow in shadowed areas, whereas TM bands 2 (green $\lambda = 0.53$ to 0.61 μm) and 5 (short-wave infrared $\lambda = 1.57$ to 1.78 μm) are used to distinguish snow from cloud, rocks and vegetation in sunlit areas. Landsat TM bands 1, 2 and 5 provide 30-m resolution; however its 16-day (at best) return period usually makes it unsuitable for operational snow-coverage mapping. NOAA satellites have a resolution of about 1 km and provide daily returns. Visible ($\lambda = 0.55$ to 0.75 μm) band GOES imagery has been used operationally by NOAA to provide area maps of snowcover for the US and southern Canadian basins. Over high latitudes, it is often difficult to distinguish snow from cloud. These images can also be significantly distorted. NOAA Advanced Very High Resolution Radiometer (AVHRR) data can be used

to simulate the reflected infrared of Landsat band 5 by subtracting AVHRR Band 4 (thermal infrared λ = 10.3 to 11.4 μm) from AVHRR Band 3 (mid infrared λ = 3.5 to 3.95 μm). Comparing AVHRR Band 1 (red λ = 0.57 to 0.7 μm) to the reflected infrared signal makes it possible to distinguish snow in both open and coniferous forest areas from snow-free zones and from clouds. Presently, NOAA AVHRR is the best operational tool to distinguish snow-covered area using satellite platforms.

Reference: Dozier and Marks (1987), Carroll (1991), Holroyd and Carroll (1990), Rees (1990).

Remote Sensing - Depth

Method: Visible imagery

Principle: The ratio of snow surface visible reflectance to bare ground reflectance increases with increasing snow depth for depths from 0 to about 0.3 m. In areas of shallow and discontinuous snowcover over open, relatively-level terrain, relationships have been developed between NOAA-GOES visible reflectance and snow depth for depths less than 0.2 m. These relationships work best when the snow has been redistributed by wind or undergone some melting.

Reference: McGinnis *et al.* (1975), Donald *et al.* (1991).

Remote Sensing - Snow Water Equivalent

Method: Visible and near-infrared imagery.

Principle: For mountainous regions, empirical relationships between the elevation above which there is a continuous snowcover (snow-line) and the mean snow water equivalent above this line may be developed. These relationships are based upon the sequence of areal depletion of snowcover during melt. Therefore, the snow-covered area/snowline must be followed from premelt through melt to calculate the pre-melt snow water equivalent. Visible or near-infrared imagery can be used to determine snow-covered area and the elevation of the snowline. When a series of clear images is available during melt, a bulk snow water equivalent for the snow-covered area can then be calculated. This method is quite useful in inaccessible mountain regions where surface data are often sparse and non-representative.

References: Hall and Martinec (1985), Martinec and Rango (1991), Martinec *et al.* (1991).

Method: Natural gamma radiation

Principle: Natural gamma radiation ($\lambda = 10^{-12}$ to 10^{-10} m) emitted by the Earth's surface is detected by a spectrometer mounted in an aircraft. Terrestrial gamma radiation originates primarily from natural ^{40}K, ^{238}U and ^{208}TI radioisotopes. Snow water equivalent is calculated from spectrometer counts and soil-moisture data. Initially, a background count (no snowcover) is established over a prescribed flight line (typically 16-km long by 300-m wide). Flights are made along the same line(s) during winter and, as snow accumulates, the attenuation of gamma radiation emitted by the Earth's surface increases and the count rate monitored by the spectrometer decreases. "Raw" radiation data must be corrected for: background (e.g., radon gas) and other extraneous effects (aircraft, pilots), the mass of air between the sensor and the snowcover, and soil moisture changes (primarily those occurring in the upper 20-cm layer of the soil). The difference between the transformed (geometric) mean of SWE derived from gamma attenuation and the true mean becomes large when the ratio of the snow water equivalent in deep drifts to shallow snow approaches 0.5. Corrections are available for this error, which may be of the order of 10 to 15% in the prairie region. Root mean square errors in snow water equivalent ranging from 5 to 8 mm over flat, agricultural landscapes and 23 mm over forest landscapes are reported. This method can be used in snowpacks with water equivalents up to 300 mm.

Reference: Cork and Loijens (1980), Goodison *et al* (1981), Carroll (1987).

Method: Passive microwave

Principle: The Earth emits microwave radiation as a near black-body in that its radiant intensity depends largely on the temperature of its surface. Snow as a porous medium scatters radiation and has a lower emissivity than the Earth, this emissivity being a function of its complex dielectric scattering coefficient. Since the dielectric properties of snow vary with several snow properties, the microwave emissivity likewise varies with these properties. For example, microwave emissivity increases with increasing snow-surface roughness, temperature, underlying frozen soil and snow wetness, and decreasing snow-particle radius and snow depth. Successful estimates of snow water equivalent have been made using the 37 GHZ brightness temperature for cold, dry snowpacks over open agricultural land with frozen soils. The Nimbus 7 satellite (NASA) detects vertically and horizontally polarized microwave radiation for $\lambda = 4.55$, 2.81, 1.67, 1.43 and 0.81 cm with a 20-km resolution and 48-hour flyover

time. Microwave radiometers mounted on airplanes give a resolution of the order of 100 m x 100 m. Present research is directed towards prediction of SWE in mountainous, arctic and forested landscapes using a variety of microwave bands; however, interpreting the large pixels in these inhomogeneous landscapes is a difficult task.

References: Chang *et al.* (1982), Goodison *et al.* (1986), Wankiewicz (1991).

Chapter 3

SNOWCOVER DISTRIBUTION

The areal variability of snowcover is studied at three spatial scales:

1. Macroscale or regional: areas up to 10^6 km^2 with characteristic distances of 10 km to 1,000 km depending on latitude, elevation, orography and the presence of large water bodies. At this scale, dynamic meteorological effects such as standing waves in the atmosphere, the directional flow around barriers, and lake effects are important.

2. Mesoscale or local (within region): characteristic linear distances ranging from 100 m to 10 km in which redistribution of snow along relief features may occur because of wind or avalanches, and deposition and accumulation of snow may be related to terrain variables and to vegetative cover.

3. Microscale: characteristic distances of 10 to 100 m over which differences in accumulation patterns result from variations in air flow patterns and transport.

In the absence of a complete understanding of the physical processes governing snowcover distribution, hydrologists use empirical relationships to estimate snow water equivalent and snow depth from topography, vegetation and land use. This approach assumes consistent patterns in annual snowcover characteristics as related to landscape features and climate. Extrapolation of relationships outside the region where they are developed is not recommended.

3.1 Effect of Topography

Effect of Elevation, Slope and Aspect

Where vegetation, micro-relief and other factors do not vary with elevation, the depth of seasonal snowcover usually increases with increasing elevation because of concomitant increase in the number of snowfall events and decrease in evaporation and melt. At a specific location in a mountainous region, therefore, a strong linear association is often found between seasonal snow water equivalent and elevation within a selected elevation band (U.S. Army Corps of Engineers, 1956). As demonstrated by Meiman (1970), however, even along specific transects the rate of increase in snow water equivalent with elevation may vary widely from year-to-year.

Elevation alone, however, is not a causative factor in snowcover distribution. A host of other variables such as slope, aspect, vegetation, wind, temperature and characteristics of the parent weather systems must be considered. Orographic precipitation is more related to terrain slope and wind-flow than elevation. Rhea and Grant (1974) studied the effects of large-scale vertical air mass movement, convective activity, and orographic lift on mountain snowfall. From an analysis of Colorado winter precipitation, they found that the long-term average snowfall at a point was strongly correlated with the topographic slope located 20-km upwind. They also found that long-term average precipitation is not well correlated with station elevation except for points along the same ridge.

Figure 12 *Snow field of wind-scoured, alpine terrain, Cairngorms, Scotland.*

More frequent winds of high speed and long duration at the higher elevations cause additional redistribution and sublimation. Figure 12 shows the snow field of a wind-scoured alpine region. Pomeroy (1991) found that in the Scottish mountains vertical transport and sublimation of snow led to large wind-scoured, snow-free areas on a high-elevation plateau, whereas large accumulations developed on the slopes leading up to the plateau. The accumulations on the slopes were related more to antecedent snowfall on the plateau and wind direction, wind speed and temperature during snow redistribution than to direct snowfall received by the slopes. The effects of greater snow redistribution at higher elevations are demonstrated by Killingtveit and Sand (1991). They examined variations in the mean depth and coefficient of variation of water equivalent as a function of elevation for snowpacks in Norwegian mountains (Figure 13). Mean snow water equivalent in open areas decreased or remained the same as elevation increased, whereas in forests the depth increased with elevation (Figure 13a). The coefficient of variation, CV, for open areas increased dramatically with elevation, whereas in forests CV did not change appreciably (Figure 13b). The increase in the coefficient of variation and the decrease in mean depth with increasing elevation in open areas suggest that wind redistribution of snow is important at high elevations. The greater losses due to blowing snow processes in open areas more than compensated the increase in precipitation received at the higher elevations.

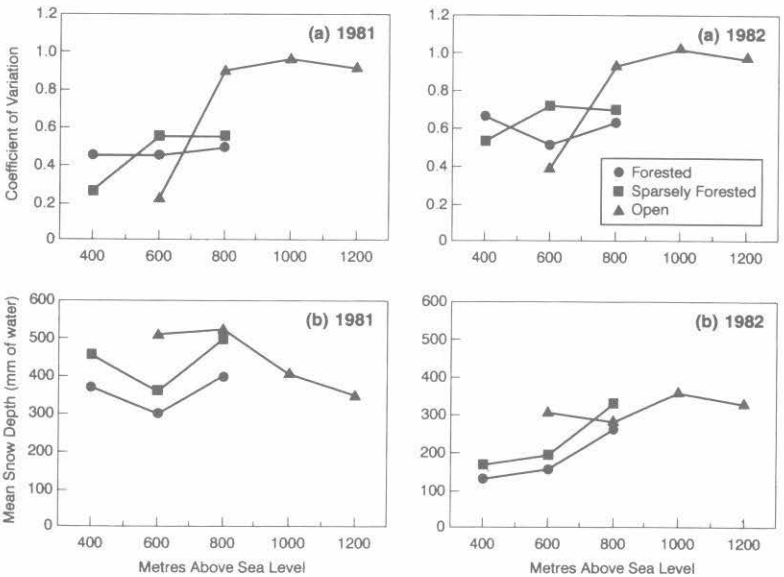

Figure 13 *Variation in:* ***(a)*** *coefficient of variation of snow depth and* ***(b)*** *mean snow depth with elevation in forested, sparsely forested and open terrain in Norway (after Killingtveit and Sand, 1991).*

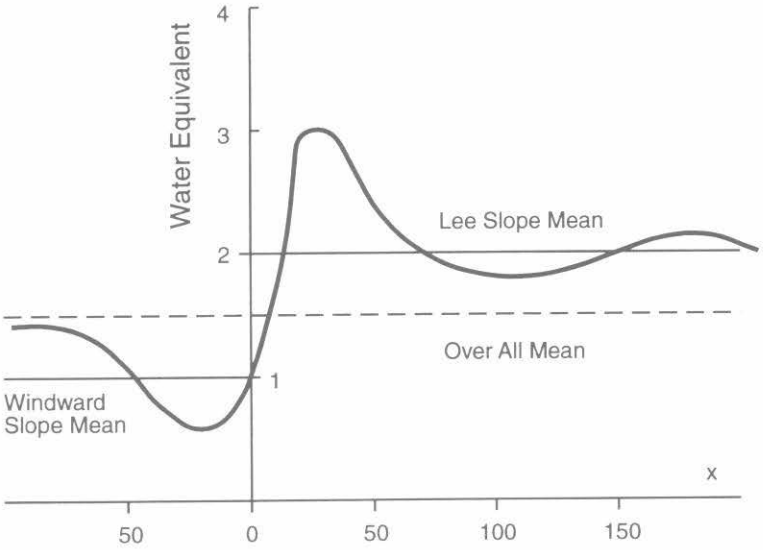

Figure 14 *Pattern of snow deposition on ridges and the relationship to mean mass accumulation on windward and lee slopes. The pattern is generalized from several snow survey transects made in Switzerland on ridges with crest angles greater than 25° and wind-flow from left to right (after Föhn and Meister, 1983).*

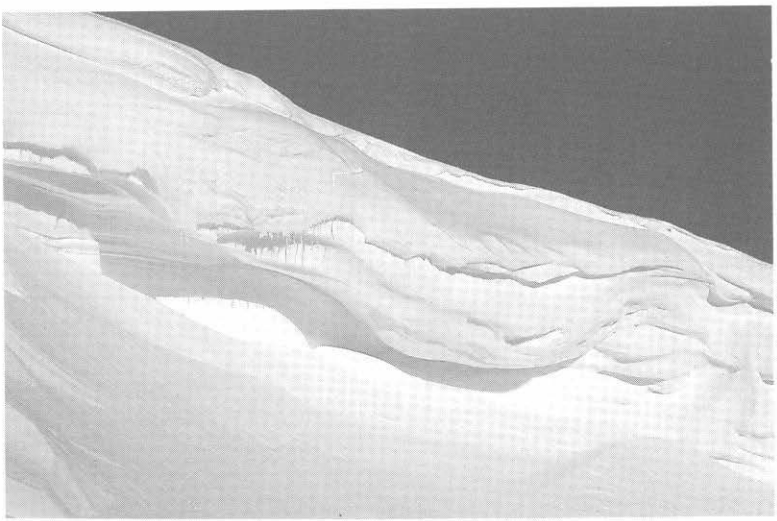

Figure 15 *Cornice, Resolute Bay, N.W.T.*

Föhn and Meister (1983) examined snow distribution patterns along exposed mountain ridges in Switzerland, showing that the regular patterns are a result of blowing-snow plume dispersion over ridge crests and subsequent settling. Figure 14 shows the snow-depth pattern on the lee-slope of a ridge resembles a dampened sine wave. The results of plume modelling indicate that the amplitude of the wave is a function of ridge-size and crest-sharpness. Cornices (Figure 15) form on lee slopes with slope angles greater than 25° and crest edges facing the lee-side. A scoured zone forms on the windward slope adjacent to the crest. For ridges oriented perpendicular to the predominant snow-bearing wind direction, slopes to the lee of the crest accumulate twice as much snow as adjacent windward slopes. However, the ridge system as a whole accumulates the same quantity of snow as adjacent level terrain.

The effects of slope and aspect on snow depositional patterns, under conditions where the effects of orography on precipitation formation and distribution are insignificant, are illustrated in Figure 16. This figure plots observations of snow water equivalent along a transect in the Canadian Arctic that encompassed an upland tundra plateau, a valley side-slope and a lowland tundra region. The survey line is oriented along one of the dominant snow transport directions. The lowest snow accumulation is on the upland tundra with the highest accumulation along the upper valley side slope. Accumulation then decreases down-slope reaching a moderate value for the lowland tundra (valley bottom). Similarly-configured upland/valley-side-slope/lowland transects monitored in the area, whose

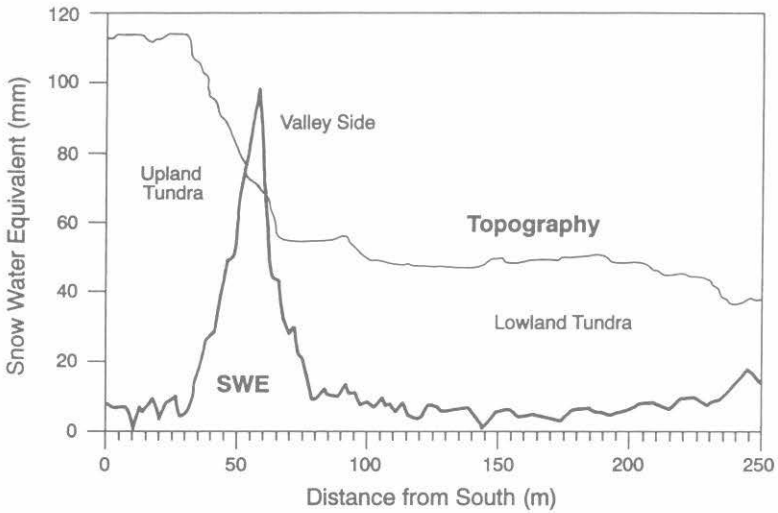

Figure 16 *Snow water equivalent transect. Cross-section along a wind-swept upland tundra plateau, down a valley side (incline greater than 25°) to a sheltered tundra lowland, Trail Valley Creek, N.W.T.*

Figure 17 *Intercepted snow - oblique photograph of snow-covered black spruce canopy, Prince Albert National Park, Saskatchewan.*

aspects do not follow a major snow transport axis, did not display massive drift formations along the valley sides. The size of a drift is determined by snow transport to the edge of the plateau and the sharpness of the transition from plateau to valley.

Aspect also affects snow distribution patterns due to its influence on the surface energy exchange processes. The effects are most evident during snowmelt. Snow disappears first from those slopes that receive the highest radiation and from those that are exposed to the movement of warm winds. In regions where snowmelt occurs shortly after snow deposition, it is often difficult to distinguish snow patterns caused by snow deposition processes from those caused by energy-exchange and snowmelt processes (Toews and Gluns, 1986).

3.2 Effect of Vegetation[1]

Snow falling into a vegetation canopy is redistributed by two phenomena:

1. Turbulent air flow above and within the canopy (Hoover and Leaf, 1967; Jeffrey, 1968; Steppuhn, 1981; Troendle *et al.*, 1988) that may lead to variable snow input rates to the canopy and microscale variation in snow loading on the ground;

2. Direct interception of snow by the canopy elements (see Figure 17) (Meiman, 1970; Calder, 1990; Schmidt and Gluns, 1991).

During the accumulation season, intercepted snow may sublimate or fall to the ground. Both processes affect the distribution of snowcover under a canopy. Sublimation reduces the amount of snow available for accumulation whereas snow that falls from the canopy affects the spatial distribution in depth and density of a snowcover. The latter is strongly influenced by atmospheric turbulence within the canopy during release. In particular regions, the combination of these processes may produce distribution patterns that are reasonably similar from year-to-year. The geometries of these patterns are related to vegetation type, vegetation density (projected area of canopy, trunk density or stalk density) and the presence of nearby open areas.

---

1 Short vegetation such as the stubble of cereal grain crops and short native grasses typically fill with snow over winter. Once filled they behave aerodynamically as open, non-vegetative snow fields in relation to the erosion and deposition of wind-transported snow (Steppuhn, 1981; Pomeroy and Gray, 1990). The distribution of snow in regions with short vegetation is treated in Section 3.4 and the accumulation and management of snow in these vegetative zones are discussed in Sections 6 and 7. The material within this sub-section focuses on snow accumulation in forests, particularly coniferous forests.

Within forest canopies, snow depth and water equivalent vary:

1. In relation to distance to trees (see Figure 18) where generally they decrease with decreasing distance to a coniferous tree trunk and increase slightly with decreasing distance to a deciduous trunk (Woo and Steer, 1986; Sturm, 1992),

2. Between stands of different tree species, with higher accumulations under deciduous trees and least accumulations under coniferous species (Patch, 1981, Barry, 1991).

Using a stochastic approach, Woo and Steer (1986) simulated the variation in snow depth in a coniferous forest by creating a model forest on the basis of probability distributions of natural variables. The distance between trees, the radii of trees, and the variation in snow depth with distance from a tree were simulated statistically using Gaussian distributions. When applied to two sites in a spruce forest in northern Ontario, the simulation was able to produce frequency distributions of snow depth resembling those found in nature. Differences of less than 3% between the observed

Figure 18 *Snowcover distribution under a mixed-wood canopy, Prince Albert National Park, Saskatchewan.*

and simulated snow depth over the forest were obtained. The measurements by Woo and Steer (1986) indicate (a) snow depths within 2-m of tree trunks are about 40% of snow depths monitored at locations away from the trunks, and (b) the standard deviation of snow depth decreases with increasing distance from the trunk.

Sturm (1992) presented the following model for snow depth as a function of distance from a tree trunk in a northern coniferous forest:

$$d_s(x) = d_s(300) + [d_s(0) - d_s(300)]\exp[-(\frac{x}{k})^2], \quad (8)$$

where $d_s(x)$, $d_s(300)$ and $d_s(0)$ are snow depths at distances of x, 300 and 0 cm from the central trunk respectively and k (cm) is a parameter representing the radius of the circle of snow affected by the individual tree crown. Sturm related k(cm) to the diameter of the trunk of a tree measured at chest height, D(cm), from measurements at two Alaskan sites and from Woo and Steer's data to obtain:

$$k = 57.3 + 3.1D, \quad r^2 = 0.64. \quad (9)$$

k was found to be relatively invariant over winter up to the beginning of spring melt. Sturm's (1992) model requires knowledge of the diameter of a tree trunk at chest height, which may be obtained from certain operational forest-stand inventories.

Several attempts have been made to establish relationships between forest stand parameters and snow water equivalent. Meiman (1970) reported increases of 8 to 56 mm of snow water due to a 10% decrease in canopy density, i.e., the proportion of the ground surface protected (shaded) by vegetation, depending on tree species. Kuz'min (1963) found the snow water equivalent in a fir forest decreased from 56 mm to 34 mm for cover densities increasing from 10 to 100% in a winter with little snow. For a winter with heavy snow, the corresponding decrease was from 230 mm to 150 mm. Jones (1987, 1991) tested correlations between snow depth and water equivalent and 16 forest stand parameters in mixed coniferous and deciduous stands in the Forêt Montmorency, north of Québec City. The most significant correlations for predicting snow water equivalent, SWE (cm), used the basal area of conifers, A_c (cm^2), and the mean distance from the sampling point to a coniferous trunk, x_c (cm), in the expression:

$$SWE = 185.6 - 841.9\frac{A_c}{x_c}, \quad r^2 = 0.75. \quad (10)$$

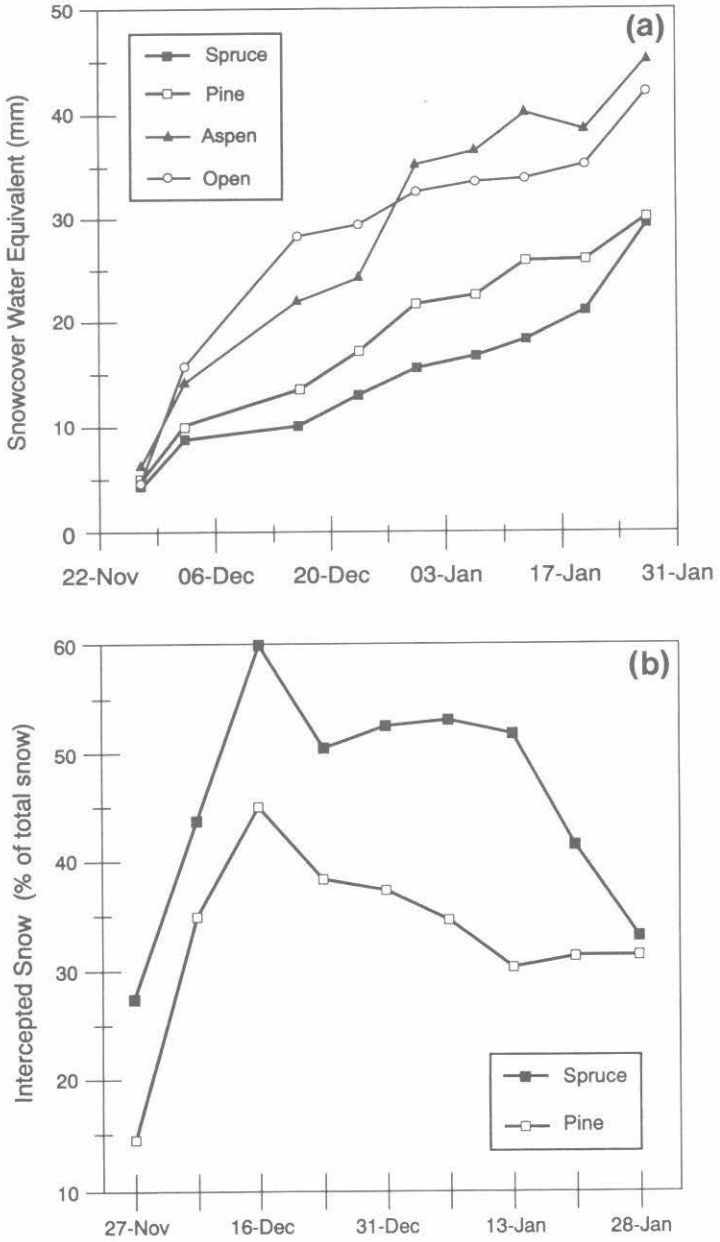

Figure 19 *Variations in:* ***(a)*** *water equivalent of snowcover under spruce, open-aspen, open jack pine canopies and in a clearing, and* ***(b)*** *intercepted snowfall in spruce and jack pine canopies during winter months in the southern boreal forest, Prince Albert National Park, Saskatchewan, 1992/93.*

Equation 10 is specific to a mixed forest and relatively humid, high-precipitation climate. Because of the lack of leaves, deciduous forests have greater accumulations of snow on the ground than do coniferous forests. The effect of increasing the deciduous content of a mixed forest on SWE is considered by Equation 10 in the ratio, A_c/x_c. As the proportion of deciduous trees increases, A_c decreases and x_c increases. This causes A_c/x_c to decrease and SWE to increase.

Small differences in snow accumulation in forests with different species of conifers usually can be accounted for by a stand density model on the basis of differences in tree size and spacing. On the other hand, large differences in accumulations are likely between coniferous and deciduous stands. Barry (1991) compared snow water equivalent in open, aspen and coniferous canopies in north-eastern Ontario, a region that experiences infrequent wind transport of snow. He reported:

1. The mean ratio of snow water equivalent in the open to that in the aspen forest ranged from 1.16 to 1.14 for wet and dry snow. These data suggest losses to interception of the order of 12 to 14% of snow accumulations measured in the open.

2. The mean ratio of snow water equivalent in aspen to that in conifers reached a high of 2.75 in an early wet snowfall. A mean of 1.7 for dry snowfall characterized the ratio-values for the remainder of the winter.

3. The coefficient of variation of snow water equivalent in the conifers, CV = 0.43, was much higher than in the aspen, CV = 0.07. The higher CV in conifers is attributed mainly to greater interception by the canopies.

4. The loss of annual snowfall in the conifers was about 50%, over four times greater than that experienced by the aspen.

Surveys of snow water equivalent in the boreal forest of Prince Albert National Park in central Saskatchewan in 1992/93 compared accumulations at identical positions in stands of dense black spruce, open-canopy jack pine, open-canopy aspen, and the centre of a small clearing (500 m wide) (see Figure 19a). The winter was cold with air temperatures ranging from -20 to -45°C between mid-December and mid-January. This cold period was followed by above-freezing temperatures at the end of January. Early in the winter, the open site held 12-20% more snow than the open aspen site. However, the release of intercepted snow by the aspen canopy and the wind transport of snow from the open site resulted in the water equivalent at the aspen site being 6-12% higher than the snowcover water equivalent at the open site from late-December onwards. This difference in findings from Barry's observations is attributed to the colder, drier snowcovers and higher winds in Saskatchewan that enhance the wind transport of snow from open areas.

By mid-January, the pine canopy had lost most of its intercepted snow. Conversely, large amounts of snow were retained by the spruce canopy until warming occurred in late-January.

The total intercepted snowfall (sum of snow held by and sublimated from the canopy) was estimated by the difference between the mean water equivalent for the snowcovers at aspen and open sites (total snowfall) and the water equivalent of the snowcover under a canopy. Intercepted snowfall calculated in this manner and expressed as a percentage of total snowfall for the spruce and pine sites is plotted in Figure 19b. As shown in the figure, in mid-December a maximum of 60% of total snowfall in spruce and a maximum of 45% of total snowfall in pine was intercepted. The spruce canopy retained more than 50% of total snowfall until mid-January whereas the pine canopy steadily lost snow due to unloading, and interception declined to 32% of total snowfall by mid-January. In early-December, most of the "intercepted" snow was retained in the canopies of the conifers; however, by the end of January, the canopies were relatively snow-free. Any "intercepted" snow remaining at that time represents snow that has sublimated. Interestingly, despite the wide difference in canopy density of the spruce and pine forests, the estimated total proportion of snowfall that sublimated as intercepted snow was roughly the same for the two canopies: that is, one-third of total snowfall.

Figure 20 *Depth hoar, Eureka, N.W.T. Photograph by P. Marsh.*

3.3 Other Factors - Water Vapour Fluxes

In subarctic and arctic environments, strong temperature gradients may form within shallow snowcovers and in the underlying soil during winter due to persisting low-air temperatures, the loss of energy by long-wave radiation, and the release from the soil of stored heat and the latent heat of fusion. These gradients can cause the transfer of water vapour from warm to cold layers in porous soils and in snow, and from porous soils to snow (see Figure 20). Pomeroy *et al.* (1993) measured temperature gradients greater than 50°C/m in shallow (50 cm deep or less) tundra snowcovers near Inuvik, N.W.T. The high ice content of the underlying tundra soils resulted in low porosity during the winter. Average overwinter decreases in density of 50% in snow layers near the soil surface were reported. Using SO_4^{-2} concentrations as a tracer, they suggested the sublimated water that had been relocated to upper layers of the snowpack resulted in no net loss of mass. Sturm (1991) modelled temperature gradients and water vapour fluxes in snowcovers in central Alaska. He found large spatial variations in moisture fluxes at small scales (one to two metres) because of the movement by convection of cold air into the pack and of warmer air from the pack into the atmosphere. Santeford (1978) monitored the exchanges of water vapour between wet frozen organic soils and subarctic snowcovers in central Alaska. Over a winter, approximately 30 mm of water, which represented 30% of the total water equivalent of the snowcover, moved from the soil into the snow. Gray *et al.*(1985) measured *in situ* the redistribution of water in freezing soils on the Canadian Prairies. They found that most prairie soils experience a loss of water from the depth increment, 0 to 50 cm, over winter. The existence of layers of round grains of metamorphosed snow adjacent to the soil surface corroborated the movement of water vapour from soil to snowcover.

The movement of water vapour from soil into a snowcover is a complicated process that depends on all factors affecting heat and mass flow in the two materials and transfers across the soil-snow interface. To date, the process has not been adequately enough described to allow simple prediction of the flux. However, vapour movement may be anticipated in environments where temperature gradients in the snowcover greater than 10°C/m (necessary for "kinetic metamorphism" as described by Colbeck, 1986) persist over several months in the winter and where soil structure and ice content permit soil macropores to exist in mid-winter.

3.4 Distribution of Snow in Heterogeneous Environments

Predominantly Forested Environments

Much of the research on snowcover distribution in forested environments has concentrated on the differences between amounts of snow collected in forests and in clearings. The results of these studies have demonstrated larger amounts of snow in clearings. In southeastern British Columbia, Toews and Gluns (1986) reported that increases in snow accumulations in clear-cuts over accumulations in adjacent coniferous forests ranged from 4 to 118%, with a mean difference of 37%. In Alberta, Golding and Swanson (1986) reported snow accumulation increased from 20 to 45% from forest to clearing.

One confusing aspect of most studies concerns the causative processes. Are the relatively higher amounts of snow in clearings due to:

(a) redistribution of intercepted snow by wind to the clearings,

(b) reduced amounts of snow reaching the forest floor because of interception, or

(c) the sublimation of intercepted snow before it is unloaded or redistributed from the canopy?

Recent studies suggest that most of the difference in snow accumulation between clear-cuts and forests develops during storms, not between storms. Therefore, redistribution of intercepted snow is not the primary cause of the larger accumulations in clearings. Wheeler (1987) provides additional evidence against wind transport and redistribution as causal factors. He found no significant difference between the average snow water equivalent monitored at forest sites located upwind and downwind of a clearing. He concluded that interception and sublimation were the major factors contributing to the difference between snow accumulations in the forest and clearing.

Kuz'min (1963) suggests that the snow water equivalent in a fir forest, SWE_f, and in a clearing, SWE_c, can be related to forest canopy cover density, p, (expressed as a decimal fraction) as:

$$SWE_f = SWE_c(1-0.37p)\,. \qquad (11)$$

This expression compares forest- to open-area accumulation without reference to the wind domain or size of the clearing.

Gary (1974) and Dickinson and Theakston (1982) support the thesis that wind fields within clearings affect the snow distribution patterns in the openings. They show greater snow accumulation on the windward side of a clearing than on the leeward side.

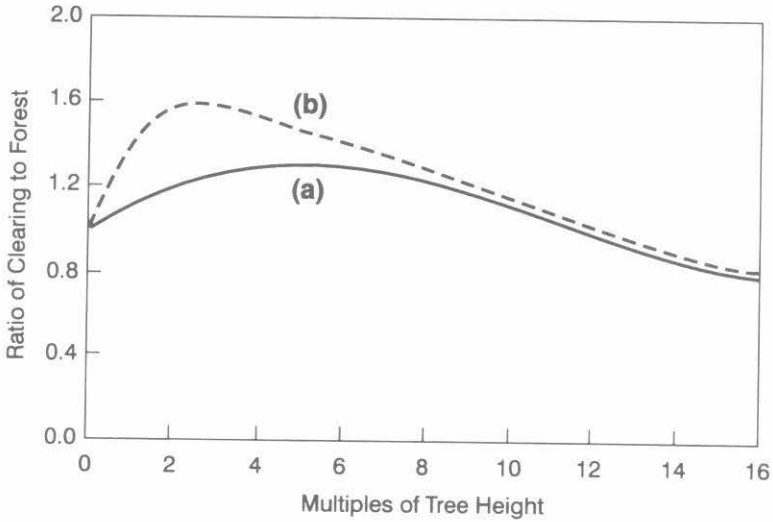

Figure 21 *Snow retention as a function of size of clear-cut opening: **(a)** after Troendle and Leaf (1980) in Colorado and **(b)** after Swanson (1988) in Alberta.*

The average depth of snow in a clearing varies with the size of the opening: increasing the size decreases the average depth (Dickinson and Theakston, 1982; Troendle and Meiman, 1984). Troendle and Leaf (1980) note that an opening with a fetch equal to five times the height of the surrounding forest canopy (5H), aligned in the direction of the prevailing wind, accumulates the maximum amount of snow (see Figure 21). According to their model, snow retention decreases from this maximum with increasing or decreasing size of clearing. When the size of clearing is greater than 12H, the clearing retains less snow than the adjacent coniferous forest. Swanson (1988) found a slightly different retention curve for snowcovers in forests in the foothills of the Rocky Mountains in Alberta. Maximum accumulation occurred in clearings with sizes of 2H or 3H and retention decreased more rapidly with increasing fetch. For clearings with openings greater than 7H, the curve approaches the relationship proposed by Troendle and Meiman (1984). The trend for retention to decrease with increasing fetch is a manifestation of the greater likelihood for gusts of wind to erode snow from the clearing as the fetch length increases.

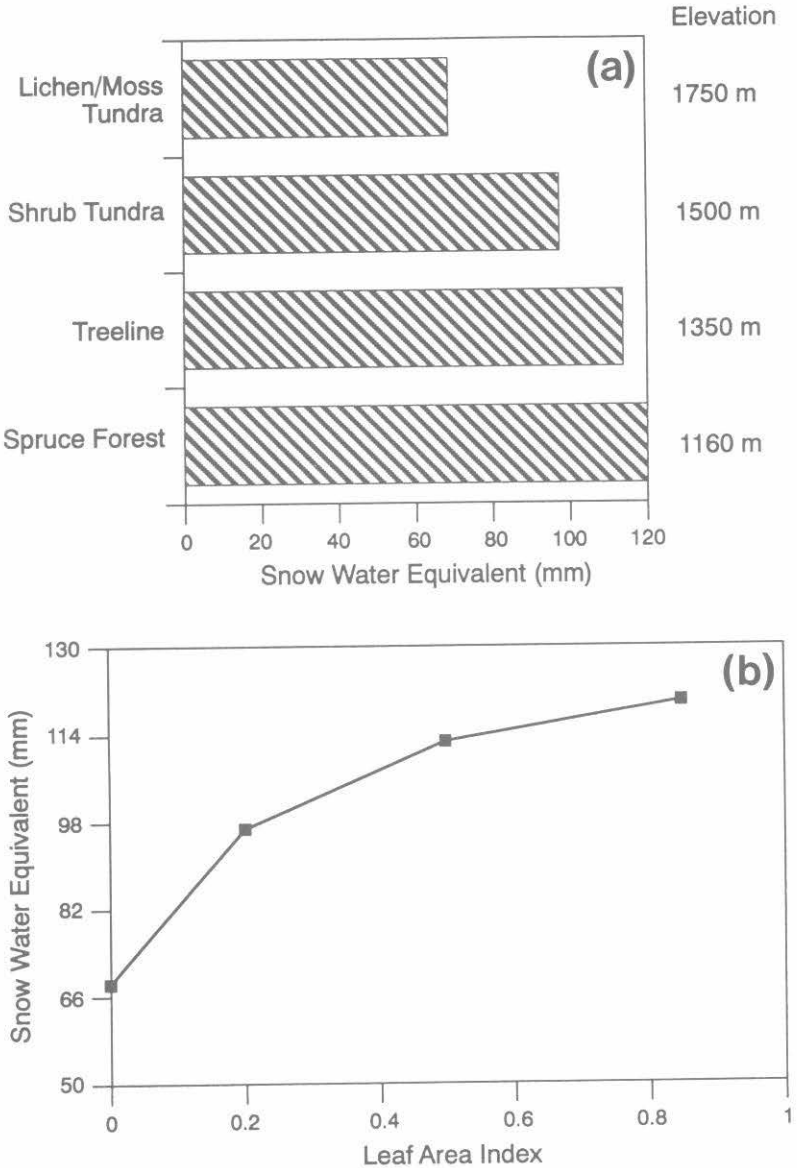

Figure 22 *Variation in:* ***(a)*** *snowcover water equivalent with type of vegetation and elevation and* ***(b)*** *snowcover water equivalent with leaf area index in Wolf Creek Research Basin located in the Coast Mountains near Whitehorse, Yukon Territory - March 31, 1993. Leaf area index is the ratio of the plan area of leaves (branches, stems, needles and other vegetative matter) to the area of ground under the canopy.*

Predominantly Open Environments

Over highly-exposed terrain, the effects of meso- and micro-scale differences in vegetation and terrain features may produce wide variations in accumulation patterns due to the effects of surface roughness on air-flow patterns and snow transport. Maximum snow water equivalent as a function of vegetation and elevation in the Coast Mountains of the southern Yukon Territory is shown in Figure 22a. This wind-swept region does not normally experience melt at lower elevations during winter. Also, it has a long snow accumulation season and relatively shallow snow packs for a subalpine to alpine mountain environment. Figure 22a shows snow water equivalent decreasing with increasing elevation, a trend opposite to the association found between these variables in most mountainous environments. Accumulation could be based on vegetation and exposure to the wind. Figure 22b shows snow water equivalent increasing with increasing "winter" stem area index (plan area of plant material, including stems, per unit area of ground). The effect is probably exacerbated by higher wind speeds at the higher elevations where the leaf area index is small.

Table 2 lists the relative amounts of snow water equivalent retained by various landscapes in the Canadian Prairies near maximum accumulation in years of normal or above normal snowfall. It is evident from these data that the combination of terrain and vegetation types provides landscape classes that have distinctive influences on snow accumulation. Included in the table are representative values for the coefficients of variation of depth and water equivalent for the various classes. These data can be used to establish the number of measurements required to be confident that the true mean falls within $\pm\Delta$ units of the sample mean. That is,

$$N = \left(\frac{tCV\overline{d_s}}{\Delta} \right)^2 \text{ or } N = \left(\frac{tCV\overline{SWE}}{\Delta} \right)^2, \qquad (12)$$

where: N = number of samples,

t = the statistic Student's "t" for a selected probability level (Haan, 1977),

CV = coefficient of variation of snow depth or water equivalent (Table 2),

$\overline{d_s}$, $\overline{SWE}$ = sample mean snow depth and water equivalent, respectively.

In contrast to the Prairies and the mountains, vegetation in high arctic regions is uniformly short and snow depth and snow density vary solely with terrain features (Woo and Marsh, 1978). Figure 23 shows that although gullies and valleys may occupy only a very small portion of the area of a basin (5%), their accumulations may contain a supply of snow that is at least as important as the snow accumulated on hilltops, which occupy 40-50% of the basin area.

Table 2 *Relative snow water retention and coefficients of variation of depth and water equivalent of snowcover on various landscapes in an open grassland environment in years of normal or above normal snowfall (Gray and others, 1979).*

Landscape	Relative Accumulation[a]	Coefficient of Variation	
		Depth	SWE[b]
Level Plains			
fallow	1.00	0.35	0.45
stubble	1.15	0.25	0.35
pasture (grazed)	0.60		
Gradual Hill and Valley Slopes			
fallow	1.0 - 1.10	0.40	0.50
stubble, hayland	1.0 - 1.10	0.30	0.40
pasture (ungrazed)	1.25	0.30	0.40
Steep Hill and Valley Slopes			
pasture (ungrazed)	2.85	0.45	0.55
brush	4.20	0.40	0.45
Ridge and Hilltops			
fallow, ungrazed pasture	0.40 - 0.50	0.45	0.55
stubble	0.75	0.30	0.40
Small Shallow Drainageways			
fallow, stubble, pasture (ungrazed)	2.0 - 2.15	0.45	0.55
Wide Valley Bottoms			
pasture (grazed)	1.30	0.33	0.43
Farm Yards			
(mixed trees)	2.40	0.40	0.50

[a] Snow water equivalent normalized to snow water equivalent monitored on level plains under fallow.

[b] SWE = snowcover water equivalent.

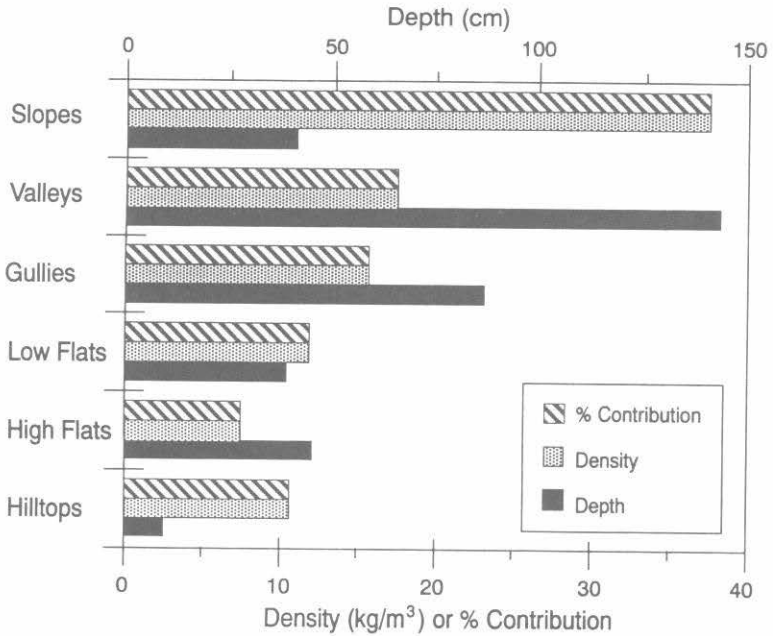

Figure 23 *Mean snow depth and density for various types of terrain in the High Arctic (after Woo and Marsh, 1978).*

Chapter 4

INTERCEPTION

Interception of snowfall by vegetation plays a major role in the snow hydrology of forests. Interception storage is controlled by the accumulation of snow falling in the canopy. The disposition of this snow is affected by sublimation, melt, unloading from branches and wind redistribution. Figure 24 shows that intercepted snow acts both as a sink and source of water, receiving snow primarily from snowfall and snow unloaded from upper branches, and, to a lesser extent, by drip from melting snow on upper branches and vapour deposition. As a source, intercepted snow sublimates, melts and evaporates, becomes suspended by atmospheric turbulence (and either sublimates or redeposits), melts and drips to the surface snowpack, or is unloaded from a branch and falls to the surface of the snowpack. The relative proportion of intercepted snow that eventually accumulates on the ground rather than returning to the atmosphere can strongly affect local water supply.

The importance of various processes affecting the collection and disposition of intercepted snow varies with climatic region, local weather pattern, tree species and canopy density. An example of the result of a complex combination of snow loss and accumulation processes on a single tree is illustrated in Figure 25. In the boreal forest of Prince Albert National Park, Saskatchewan, a 9-m tall black spruce tree with its intercepted snow was continuously weighed from January to February, 1993. Over 10 kg of snow accumulated on the tree in December and January during cold periods (-10 to -45°C). In warmer periods (-20 to +10°C), all this snow was lost. The primary loss mechanism was sublimation, though when the temperature approached or exceeded 0°C, melt/drip and unloading dominated and are identified by rapid losses in

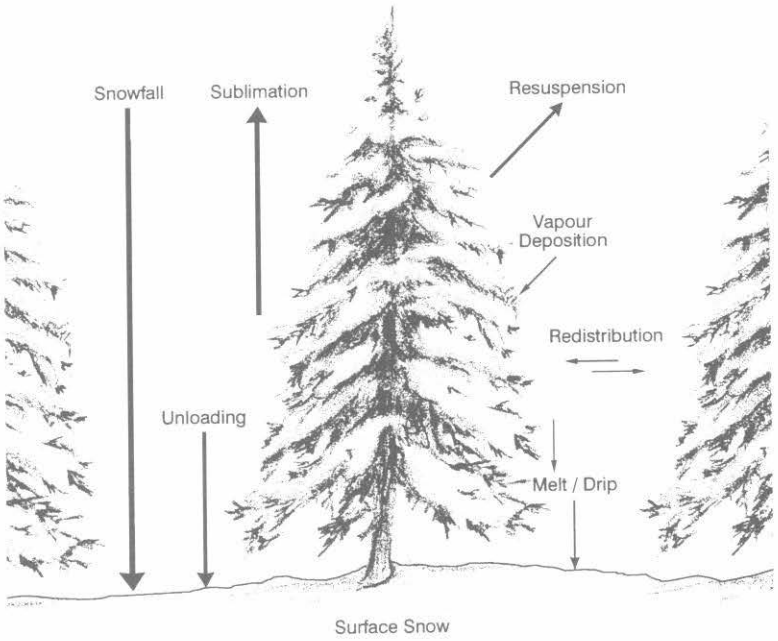

Figure 24 *Disposition of intercepted snow in a coniferous forest canopy. Sketch by R.J. Gillman, Waskesiu, Saskatchewan.*

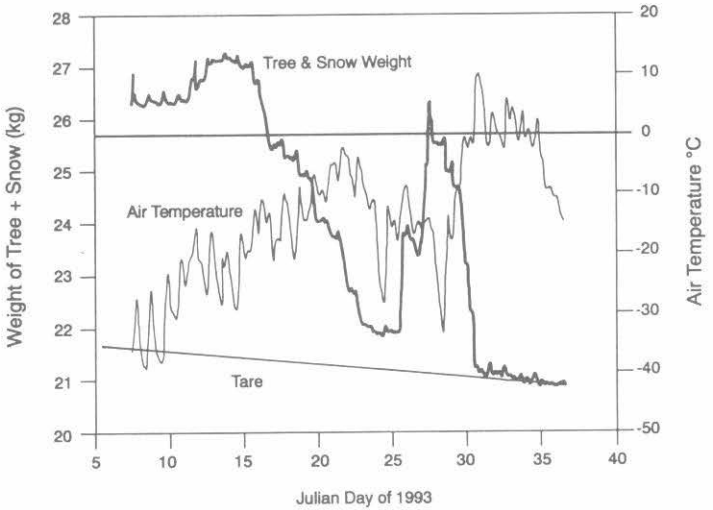

Figure 25 *Combined weight of a 9-m black spruce tree and its intercepted snow and the ambient air temperature in January and February, 1993 in a black spruce stand near Waskesiu Lake, Saskatchewan. The tare denotes the estimated weight of the tree itself which slowly desiccated and lost needles during the experiment.*

snow mass. To predict and manage snow interception, an understanding of the relevant physical processes is required. The physics of snow interception in coniferous (softwood) forests is discussed below.

4.1 Accumulation in Coniferous Forest Canopies

The interception efficiency of a canopy, the ratio of the amount of snow intercepted to the total snowfall, is a synthesis of the collection efficiencies for individual branches that compose the canopy. The collection efficiency is the proportion of snowfall received by the projected horizontal area of a branch during a storm that is retained by the branch. Early in a storm, snowflakes fall through the spaces between branches and needles, lodging in the smallest spaces until small bridges form at narrow openings. These snow bridges increase the collection area and the efficiency with which a branch accumulates snow. Additional snow is retained on the bridges by cohesion. *Cohesion* of snow crystals results from the formation of microscale ice-bonds between crystals. These bonds form due to the freezing of water at the points of contact or the re-formation of crystals due to small-scale vaporization and condensation (Langham, 1981). Cohesion increases rapidly following initial contact of the crystals, the rate increasing as air temperatures approach the freezing point. Therefore, the collection efficiency of a branch due to cohesion of snow increases with increasing temperature, other factors being equal.

Factors affecting the collection efficiency of a branch are:

1. *Elastic rebound* of snow crystals falling on branch elements and snow held by the branch. Rebound is most pronounced at air temperatures below -3°C, declining rapidly as the temperature rises from -3 to 0°C (Schmidt and Gluns, 1991). Rebound occurs most effectively near the edge of a branch; therefore, large branches (small ratio of perimeter to horizontal area) lose proportionately less snow to rebound than do small branches (large ratio of perimeter to horizontal area).

2. *Branch bending* under a load of snow. Bending decreases the horizontal area of a branch exposed to falling snow. It also increases the vertical slope of a branch, thereby increasing the probability that falling snow crystals will bounce off. The degree to which a branch will bend under a given load increases with branch elasticity. Branch elasticity at sub-freezing temperatures is related to the ice crystal content of the branch and increases linearly with increasing temperature (Schmidt and Pomeroy, 1990).

3. *Strength* of the snow structure. As intercepted snow accumulates, the extent to which it bonds to itself and the branch is related to the strength of the interlocking snow crystals. As air temperature increases, the rate at which the structure of snow "simplifies" (reducing number of bonds) due to metamorphism increases. Therefore, snow strength decreases with increasing temperature. When accumulations are large, the reduction in snow strength may lead to decreased interception efficiency (Gubler and Rychetnik, 1991).

A conception of snow interception on a single branch, showing the effect on interception efficiency of bridging of snow, elastic rebound and branch bending is illustrated in Figure 26. The amount of intercepted snow on a branch, air temperature, snow density and wind speed strongly influence subsequent interception. For steady meteorological conditions, interception is most efficient during bridging of the smallest branches. As accumulation continues, bending decreases the horizontal area of a branch

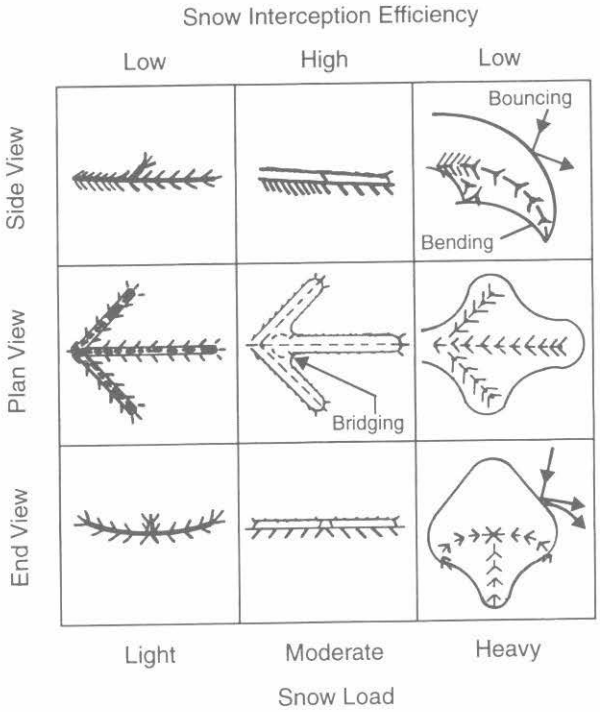

Figure 26 *Snow interception efficiency of a conifer branch as a function of elastic rebound of snow crystals, branch-bending, cohesion and snow-strength for various snowloads (after Schmidt and Gluns, 1991).*

exposed to falling snow and increases avulsion of intercepted snow. These processes result in decreases to the interception rate and loading greater than the increases produced by bridging. As interception approaches its maximum for a specific set of conditions of snow cohesiveness, horizontal area of branch and intercepted snow, the sharp vertical angles of the snow surface promote crystal rebound and erosion rather than continued accumulation.

Low air temperatures affect snow interception in the following ways:

1. They improve the rebound efficiency. The highest rate of change of rebound efficiency with change in air temperature occurs in the temperature range from 0 to -3°C,

2. They stiffen branches and lower branch bending. The greatest rate of change in the elasticity of conifers with temperature occurs in the range from -12 to 0°C.

3. They produce a stronger snow structure.

The net result of these factors is to increase the interception efficiency (Hoover and Leaf, 1967; Gubler and Rychetnik, 1991).

At air temperatures above -3°C, when intercepted snow loads are light, it has been observed that a canopy initially has a relatively high interception efficiency due to high cohesion of snow and poor particle rebound. Highly cohesive snow is intercepted by tree trunks as well as branches for short periods of time. However, in time, as snowfall and interception continue, the unloading of intercepted snow due to branch bending and weakening in snow strength may overcome the increased retention by cohesion. When this occurs, lower interception efficiencies result.

Schmidt and Gluns (1991) suggest that interception efficiency is inversely related to the density of freshly fallen snow (see Figure 27). They propose that accumulations of low-density snow in a forest canopy promote interception because (1) falling snow particles do not rebound efficiently off poorly-bonded (low-density) snow, and (2) the horizontal area of branch and snow increases rapidly during the early phase of snow accumulation.

High winds during accumulation may induce snow redistribution, thereby reducing the apparent interception efficiency. Schmidt and Gluns (1991) observed that the lowest interception efficiencies occurred during the highest wind speeds. Their observations concur with the measurements by Wheeler (1987) of small differences between accumulations under a forest, and in a clearing, after snowfalls with high winds. Release of intercepted snow, triggered by branch movement, has been observed during highly-turbulent winds.

One may conclude that interception efficiency generally increases with increasing size of falling snow crystals, decreasing temperature, decreasing wind speed, and decreasing density of intercepted snow. Satterlund and Haupt (1970) and Schmidt and Gluns (1991) show that these meteorological and precipitation parameters can be more important than conifer type in determining interception efficiency for single branches or single trees.

Scaling the observations from a single branch or a single tree to a forest is difficult because the effects of the bulk properties of the canopy on snowfall interception may override many of the factors important to interception on a branch or tree. Calder (1990) recounts an experiment designed to measure the quantity of snow intercepted by a spruce stand in

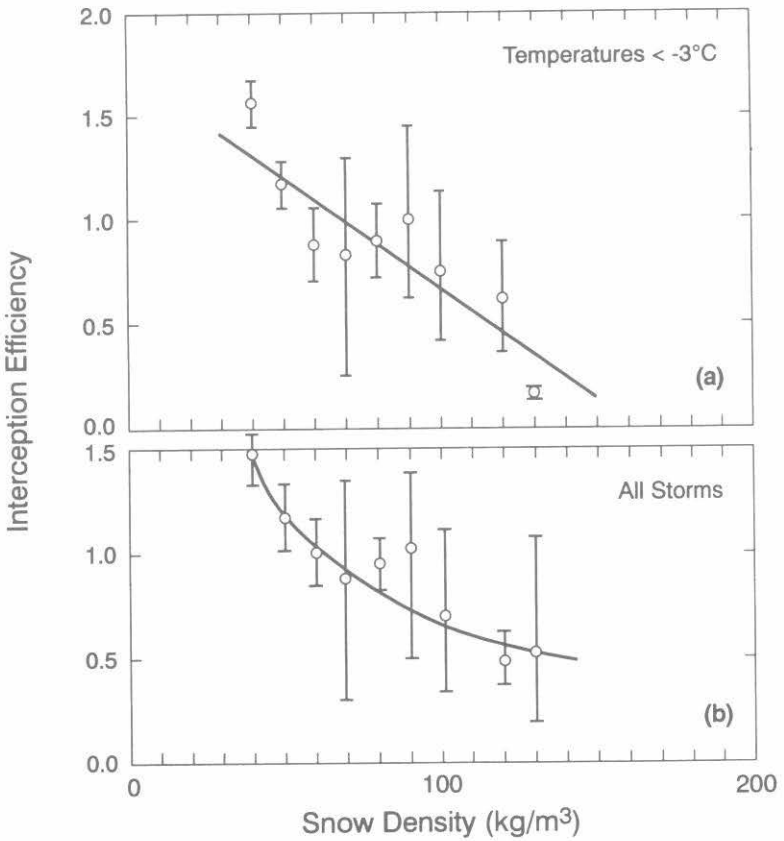

Figure 27 Variation in interception efficiency of a single artificial conifer with density of accumulated newly-fallen snow: (a) for dry snow and (b) for all snowfalls (after Schmidt and Gluns, 1991).

Scotland, using measurements of gamma-ray attenuation in a transect through about 20 trees. The results show the rate of increase in snow interception with storm snowfall decreases as snowfall increases. A similar association between storm interception and storm precipitation for forests of varying crown density was found by Strobel (1978) in Switzerland (see an example of the application of Strobel's model in Figure 28). Strobel's measurements are based upon snow surveys conducted after snowfalls in forests and in adjacent open areas not subject to wind transport of snow. On the basis of the measurements, Strobel presents a model for interception during an individual storm, I (mm SWE), as a function of the maximum interception for the forest stand, I^* (mm SWE) and the total storm precipitation, P (mm SWE):

$$I = I^* \arctan(\frac{P}{b}), \tag{13}$$

in which b is an empirical coefficient. This relationship must be derived for individual forest stands.

McNay *et al.* (1988) conducted snow surveys in forested and open areas following individual snowfall events in upland Douglas fir and western hemlock forests on Vancouver Island in British Columbia. They related the depth of new snow under the forest canopy, d_s(forest)(cm), to the depth of new snow in open areas, d_s(open)(cm), and canopy coverage, C_c (%):

$$d_s(\text{forest}) = -1.29 + 1.08 d_s(\text{open}) - 0.006 d_s(\text{open}) C_C , \tag{14}$$

Equation 14 has a coefficient of determination, $r^2 = 0.97$. The model can be modified for predicting interception snow water equivalent per unit area of canopy, I (mm), as:

$$I = 1.935 + P(0.006 C_C - 0.08) . \tag{15}$$

Equation 15 assumes (a) a density for newly-fallen snow equal to 150 kg/m^3, and (b) depth of storm precipitation, P = 1.5 d_s(open). The expression was developed from storms producing up to 60-mm water equivalent. It is plotted for "old growth," C_c = 90%, and "commercially-thinned," C_c = 40%, forest in Figure 28 where it is compared to Strobel's function, which has been empirically fitted to similar forest stand conditions. Although the equation defines a linear relationship between I and P, McNay et al. note that because of its limited range, in terms of Strobel's data, the relationship does not necessarily contradict the curved form described by Strobel (1978) and Calder (1990).

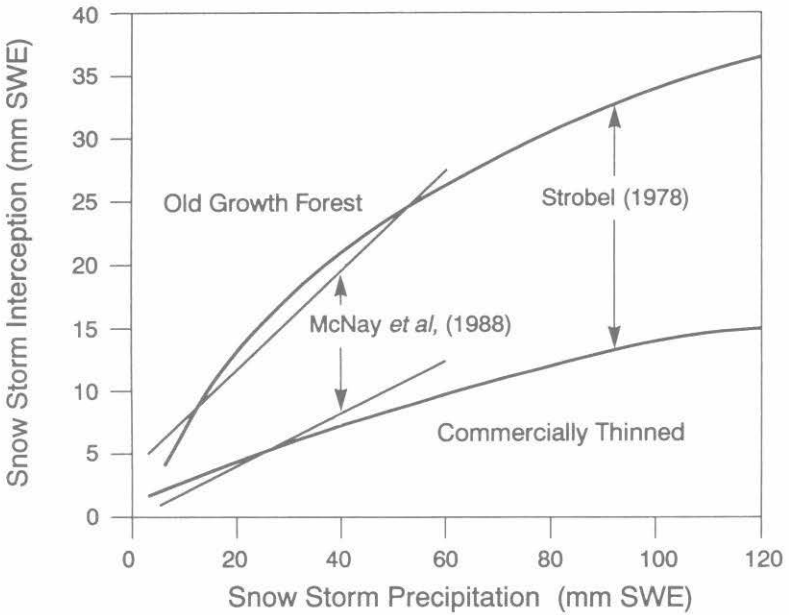

Figure 28 Variation in snow-storm interception with snow-storm precipitation for old-growth forest and commercially-thinned forest of Douglas fir and hemlock calculated using Strobel's (1978) model and McNay et al's (1988) linear model.

4.2 Sublimation of Intercepted Snow

Sublimation of snow involves the conversion of ice to water vapour. This change consumes 2.84 MJ of energy per kilogram of ice at 0°C and standard atmospheric pressure - a large amount of energy for a winter environment to yield. Most intercepted snow is distributed over the lower 10 to 20 m of the atmosphere and its ratio of surface area to mass is large. These features offer the potential for the turbulent transfer of large amounts of heat from the atmosphere to the intercepted snow and concomitant sublimation. The long period of exposure of snow-covered canopies to the atmosphere during northern winters provides ample time for sublimation to occur. Field measurements of sublimation losses show the rates vary widely from one climatic region to another. For example, in humid northern Idaho, Satterlund and Haupt (1970) estimated annual sublimation losses of intercepted snow during two winters at only 4.5% for Douglas fir and 5.2% for white pine. Wilm and Dunford (1945) in more arid Colorado and Miner and Trappe (1957) in Oregon reported sublimation of snow from coniferous canopies to be 32% and 24% respectively of the seasonal snowfall. In central Colorado, Schmidt *et al.* (1988) reported that one-third of the snow intercepted by an artificial

conifer sublimed during a six-hour warming period. Recent measurements in the boreal forest near Waskesiu, Saskatchewan showed that one-third of the annual snowfall sublimated from coniferous canopies in two months.

The sublimation rate for a sphere of ice is controlled by the turbulent transfer of heat to the particle, the turbulent transfer of water vapour from the particle, and the radiation exchange (see Section 5.4). Sublimation may be expressed as a rate coefficient, c_{subl}, defined as,

$$c_{subl} = \frac{\frac{dm}{dt}}{m}, \qquad (16)$$

where m is the mass of a single ice sphere and t is time. Solar radiation, air temperature, humidity and wind speed affect the sublimation rate coefficient. Because of the high albedo of snow, the effect of short-wave radiation on c_{subl} is small relative to the effects of the other factors. Figure 29a shows the effect of air temperature and humidity on c_{subl} of an ice particle having a radius of 500 μm. The coefficient increases sharply as air temperature rises towards the freezing point and declines sharply as relative humidity increases towards 100%. Figure 29b shows the sublimation rate coefficient increasing with increasing wind speed. For wind speeds greater than 1 m/s the increase is approximately linear.

Scaling sublimation rates for a single ice sphere so they apply to snow intercepted by a forest canopy requires knowledge of the number density of trees in the forest, the mass of intercepted snow in a tree, and the proportion of snow exposed to atmospheric ventilation available to sublimate. Presuming uniform atmospheric conditions surrounding a tree, the sublimation flux from a single tree, q_{subl}(tree), is given by:

$$\frac{dM}{dt} = q_{subl}(\text{tree}) = c_{subl}\, c_e(M) M, \qquad (17)$$

where c_e(M) is an exposure coefficient that corrects for the difference in the ratio of surface area to mass between the single ice sphere and the snow intercepted by a tree, and M is the mass of snow on a tree. Adding a term to correct for the spatial density of trees and accounting for varying tree size and intercepted load provides the sublimation flux for a forest, q_{subl}(forest) as:

$$q_{subl}(\text{forest}) = \int c_{subl} c_e(M)\, n_T(M) M\, dM, \qquad (18)$$

where n_T(M) is the number density of trees (#/m^2) having an intercepted mass of snow M.

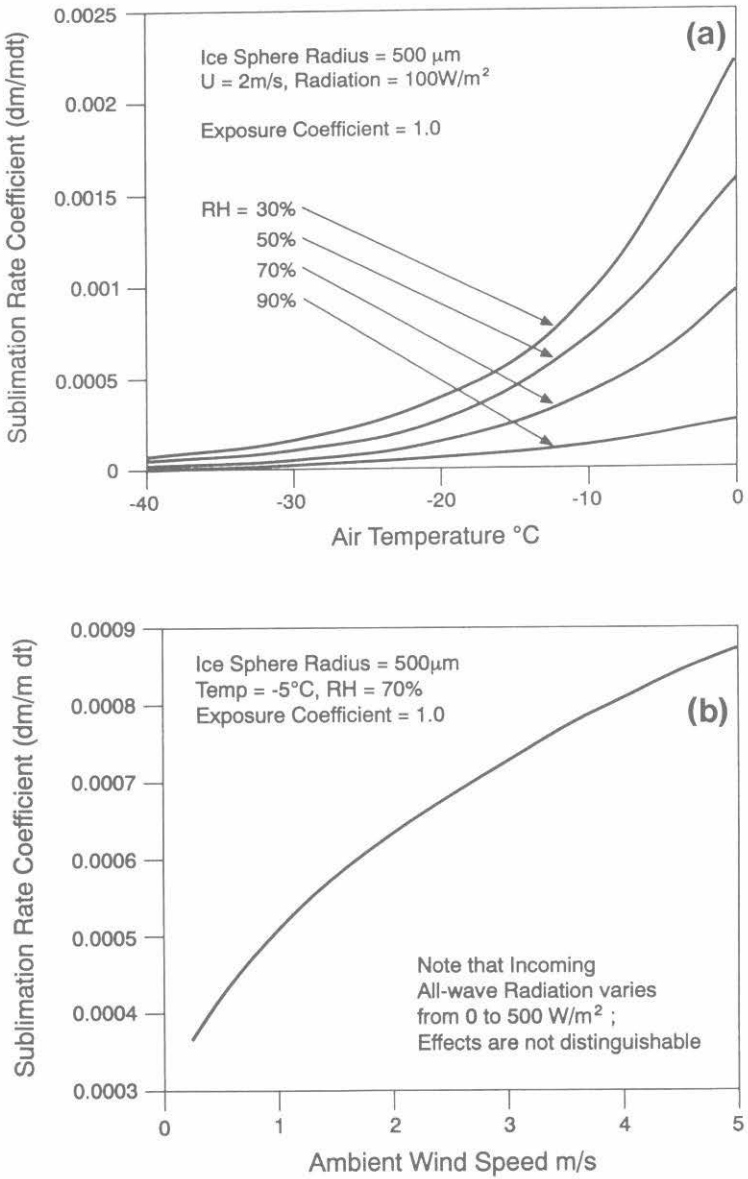

Figure 29 *Variation in the sublimation rate coefficient of a 1-mm diameter ice sphere with:* ***(a)*** *air temperature and relative humidity when subjected to a wind speed of 2 m/s, an incident radiation flux of 100 W/m² (ventilation velocity calculated as $0.3u_2$, particle albedo taken as 0.9) and* ***(b)*** *wind speed for an ambient temperature of -5 °C, a relative humidity of 70% and all-wave radiation flux varying from 0 to 500 W/m² (ventilation velocity calculated as $0.3u_2$, particle albedo taken as 0.9).*

Snow in the forest is not so well-exposed to the atmosphere as a single snow particle. The exposure coefficient may be effectively defined as a geometric ratio (Pomeroy and Schmidt, 1993):

$$c_e(M) = \frac{\frac{A_M}{M}}{\frac{A_m}{m}}. \tag{19}$$

where A is the exposed surface area of snow in a tree (M) and for an ice sphere (m).

Assuming that the difference in sublimation rate coefficients for a mass of snow intercepted by a tree and a single ice sphere is primarily due to the difference in the ratio of surface area to mass between the two, the exposure coefficient may be determined empirically as the ratio of sublimation rate coefficient for snow intercepted on a tree to that for a "standard" ice sphere (radius of 500 μm), i.e.,

$$c_e(M) = \frac{m\frac{dM}{dt}}{M\frac{dm}{dt}}. \tag{20}$$

Schmidt(1991) measured the mass of intercepted snow that sublimated from a small artificial conifer (1 m high by 0.5 m wide) over several sequences of accumulation and sublimation of intercepted snow. For the same period, he calculated sublimation of an ice sphere from the ambient atmospheric conditions. Relative to the sublimation from the ice sphere, sublimation of intercepted snow increased rapidly as snow filled a snow-free canopy, and doubled for freshly-fallen snow as opposed to well-aged snow. Schmidt developed an expression for the sublimation rate of snow on the artificial tree as a function of the sublimation rate of an ice sphere, the mass of snow on the tree and a parameter, a, that indicates the age of snow on the tree as:

$$\frac{dM}{dt} = \frac{dm}{dt} a M^{(0.7-5x10^{-5}M)}. \tag{21}$$

Schmidt's function for dM/dt may be used with Equation 20 to derive an empirical expression for $c_e(M)$ as a function of a dimensionless ratio of snow mass on the tree to the maximum snow mass that may be held by the tree. Assuming an ice sphere mass, m = 5.236 x 10^{-7} kg (r = 500 μm), dm/dt follows the sublimation model (Equation 47), M and dM/dt are

equal to the values measured by Schmidt (1991), and M^*, the maximum snow load for a given tree (taken as 5.5 kg for the artificial conifer) provides:

$$c_e(M) = k_1(\frac{M}{M*})^{-F}, \quad (22)$$

where k_1 is a coefficient indexing the age (structure) of snow (for Schmidt's tree (k_1 = 0.0001099 for fresh snow and 0.0000549 for old snow) and F is an exponent having the value of 0.3 for snow on the artificial tree. The exposure coefficient is plotted as a function of the ratio of intercepted snow mass to the maximum mass that might be held by the tree in Figure 30. Even though the mass of intercepted snow is expressed as a dimensionless ratio, M/M^*, the values for k_1 and F shown are not necessarily applicable to mature trees because of the dependence of the ratio of surface area to mass for intercepted snow on the size and and shape of a tree and the differences in branch morphology between artificial and natural conifers.

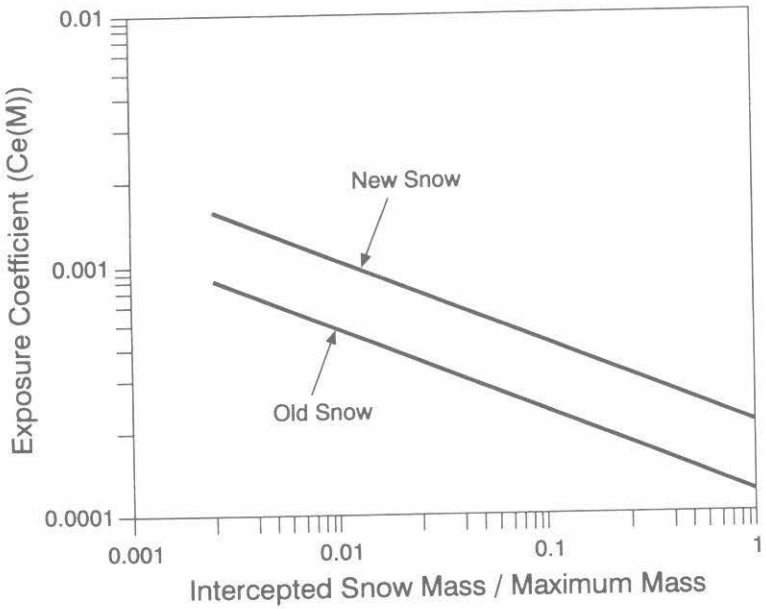

Figure 30 *Exposure coefficient for an artificial conifer as a function of the ratio of intercepted snow mass to the maximum snow mass for fresh snow and aged snow.*

Fractal Analysis of Intercepted Snow

Fractal geometry may be used to extrapolate the results of natural phenomena from small to large scales. Fractal objects are complex, convoluted and irregular but have certain intrinsic patterns that govern their form (Mandlebrot, 1983). They have no characteristic spatial scale, in that their degree of roughness is independent of the scale of measurement. Forest canopy, snow crystal and snow patch shapes have been shown to behave as fractals over useful ranges of spatial scales (Barnsley, 1988; Shook *et al.*, 1993). Pomeroy and Schmidt (1994) showed that intercepted snow is also fractal, and that fractal geometry may be used to extrapolate geometrical characteristics of intercepted snow from a small artificial conifer to a forest or from individual branches to a forest.

The dimension, D, is commonly used in fractal mathematics to evaluate the degree of irregularity of an object. For classical Euclidean objects this dimension is an integer; however, the more convoluted an object is, the greater its dimension is in excess of an integer and the more difficult it is to describe using Euclidean geometry. For fractal objects, D is composed of Euclidean (integer), D_E, and fractal (non integer), D_f, components, i.e.,

$$D = D_E + D_f \,. \tag{23}$$

If the fractal object is self-similar in all directions then the fractal component of the dimension is the same if we are considering the perimeter of a cross-section of the object or the surface area of the objects volume; only the Euclidean component is incremented by integers depending on whether a line or area is specified.

Pomeroy and Schmidt (1993) used a combination of dimensional analysis and fractal mathematics to evaluate $c_e(M)$ from its geometric definition (see Equation 19). Setting the reference ice sphere as Euclidean ($D = D_E$) and intercepted snow as fractal ($D = D_E + D_f$),

$$c_e(M) = \frac{\dfrac{A_f}{V_f \rho}}{\dfrac{A_E}{V_E \rho}} = \frac{L_E}{L_f} = \frac{L^1}{L^{(1+D_f)}} = L^{-D_f} \,, \tag{24}$$

in which A = area, V = volume, ρ = density, L = length and the subscripts f and E refer to fractal and Euclidean objects respectively. As M/M^* and k_1 in Equation 22 are truly dimensionless, then $D_f \equiv F$. Pomeroy and Schmidt used the perimeter-area relationships from digitized, cross-sectional photographs of snow on pine and spruce branches and in

a 12-m tall black spruce canopy to establish the fractal dimension of intercepted snow (Mandelbrot, 1983) (see Figure 31). From these data they calculated the fractal component, Df, and hence F. Their results show:

1. The exponent F for individual branches and the lower canopy centred on 0.3 and varied from 0.22 to 0.36. Therefore, Equation 22 can be used with Schmidt's (1991) measurements from an artificial conifer to estimate the exposure coefficient for lower parts of spruce and pine trees.
2. The exponent F for the upper spruce canopy (height >10 m) varied from 0.26 to 0.44, usually remaining well above 0.37.

The important aspects of these findings with respect to calculations of sublimation are:

1. Sublimation of intercepted snow may be indexed to sublimation of a single ice sphere if a correction for the ratio of exposed surface area to mass of intercepted snow (exposure coefficient) is applied,
2. The exposure coefficient is of the order of 0.001 to 0.0001,
3. The exposure coefficient decreases with increasing intercepted load,
4. The exposure coefficient decreases with the mass of intercepted snow that has sublimated, and
5. Because intercepted snow behaves as a fractal, the exposure coefficient does not vary significantly over the scale from individual branches to canopies.

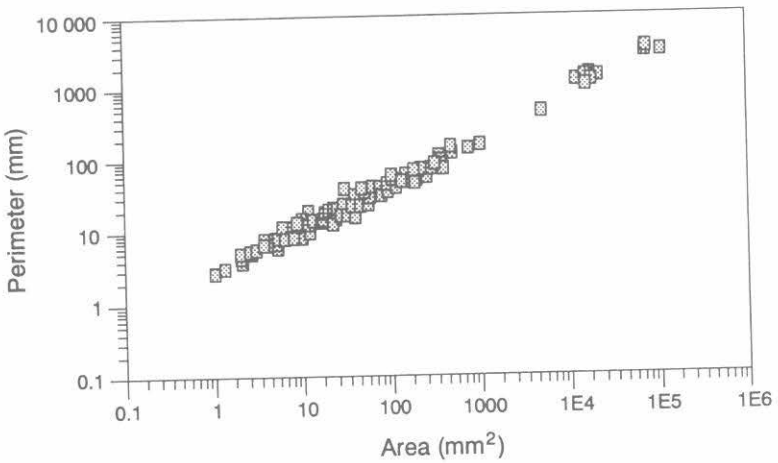

Figure 31 *Perimeter-area relationship for intercepted snow.*

4.3 Melt of Intercepted Snow

Melt of intercepted snow is considered to be a relatively unimportant process of intercepted snow ablation in continental North America (Schmidt, 1991). Snow, when warmed to near-melting levels, develops a weakened structure and tends to unload from the canopy before melt can occur (Gubler and Rychetnik, 1991). Calder (1990) suggests that intercepted snow can retain a maximum liquid water content of 15% by mass. Meltwater in excess of this limit is considered to drip from the canopy.

4.4 Unloading of Intercepted Snow

Unloading of intercepted snow may occur as a result of failure in the strength of branch or in the strength of the intercepted snow. Weakening in snow structure may be triggered by an increase in the angle of the branch-stem (change in angle of repose), melting along the snow-branch interface, a decrease in the number of inter-crystal bonds, or wind-induced vibration. Unloading may also be caused by the atmospheric shear stress exerted by wind on the branch and snow.

Schmidt and Pomeroy (1990) examined the effects of temperature on the flexure of conifer branches by measuring the force necessary to deflect a branch 10 cm at various temperatures. They found that branches are substantially stiffer at colder temperatures, with the modulus of elasticity, E (N/mm^2), increasing with decreasing branch temperature, T_b (°C), in the range $-12°C < T_b < 0$ as:

$$E = 2650 - 842 T_b \, . \qquad (25)$$

The effects of the variation in E with T_b on the bending action of a fir branch loaded with 0.25 kg of snow are shown in Figure 32. At a temperature of -12°C, the branch is stiff and easily retains the load; when T_b equals -2°C, bending occurs that would induce unloading.

Gubler and Rychetnik (1991) suggest that unloading associated with increasing air temperature is affected more by the decrease in snow strength than the increase in bending. They observed unloading of intercepted snow in coniferous forests in Switzerland, an environment dominated by high winds and a relatively-small range in air temperature. They concluded that wind triggers the unloading of weakened snow that has been warmed by rising temperatures before snow is unloaded by increased branch-bending. Observations by Pomeroy of branch temperature, intercepted snow temperature, wind speed and the timings of accumulation and release of snow in spruce trees in the Rocky Mountains

near Canmore, Alberta suggest that branches warm more rapidly than intercepted snow. During warming periods, branch flexibility increased several hours before intercepted snow warmed and metamorphosed. Similar visual observations of the process in the boreal forest of northern Saskatchewan (an environment with relatively low wind speeds) showed that unloading associated with warm air temperatures occurred first due to increased branch bending and later due to weakened snow structure. The difference in findings between Switzerland and western Canada is most probably due to differences in the night-time long-wave radiation losses experienced by forest canopies in the two regions. Because of the maritime climate in Switzerland the losses from forests are smaller than those experienced by forests in continental regions where clear skies and high atmospheric transmissivities predominate during the nocturnal hours. Following cold, clear nights, larger amounts of energy are required to warm the intercepted snow in continental forests.

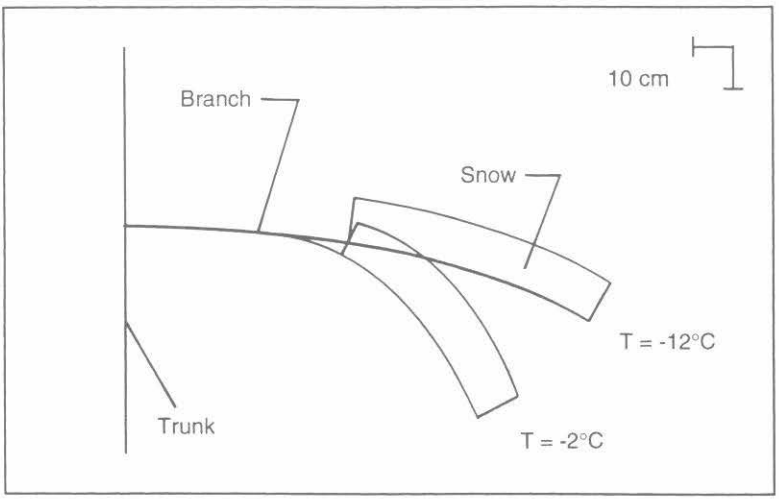

Figure 32 *Bending of a fir branch predicted by a branch elasticity model under a snow load of 0.25 kg per 0.1 m segment of the branch, at temperatures of -2 and -12°C (after Schmidt and Pomeroy, 1990).*

4.5 Wind Redistribution of Intercepted Snow

Wind affects interception by disrupting the bridging process, by reducing the amount of snow intercepted because of vibration of the vegetation, by eroding of intercepted snow and by retaining snow particles in suspension. Miller (1962) reports that interception declines notably when wind speeds during snowfall exceed 2 m/s. Because of mechanical removal of snow by vibration and increased erosion due to increased turbulence, high winds may decrease the amount of snow intercepted along exposed windward edges of a forest and at the top of the canopy.

Plumes of snow are sometimes visible above forest canopies during high winds. Schmidt and Troendle (1992) suggested snow particles suspended in plumes are less than 500 μm in radius, much smaller than the original snow crystals. Because of the small fraction of intercepted snow particles that fall within the narrow size range of particles suspended in plumes and the intermittent nature of snow removal in plumes, the mass of suspended snow likely is much smaller than the amount initially intercepted by the canopy. On the basis of measurements in Colorado, Troendle *et al.* (1988) suggest that during periods without snowfall the mass of snow suspended in plumes did not contribute significantly to the snow accumulation in a downwind clearing. Most intercepted snow removed by wind fell in large clumps that accumulated on the snow surface within a few tree heights of the canopy from which they originated. This finding contradicts the observations of Hoover and Leaf (1967) that the differences between snow accumulations in clearings of a coniferous forest and in the forest are due to redistribution by wind of intercepted snow.

Schmidt and Troendle (1989) found that the flux of snow at the canopy top and the percentage of snow particles that enter the canopy and fall to a lower level during snowfall increases with increasing wind speed. Therefore, high winds may change the vertical distribution of intercepted snow. Wheeler's (1987) comparative accumulation measurements between forest stands and clearings show smaller differences for higher wind speeds during snowfall. Considered together with Schmidt and Troendle's finding, Wheeler's results confirm reduced interception during snowfalls with high winds.

Chapter 5

WIND TRANSPORT

The effects of wind on the evolution and distribution of a snowpack are most pronounced in open environments. Dyunin *et al.* (1991) suggest that wind erosion of snow can be the primary process of "desertification" in northern steppe environments. They strongly correlate this desertification with the suppression of natural vegetative cover in Russian steppes and forests. Wind hardens and densifies a snow cover because of the drag forces exerted on the surface by the moving air. When snow is transported by wind, the crystals undergo changes to their shape, size and other physical properties and, on re-deposition, form drifts and banks of higher density than the parent material. Most hydrological studies of wind transport have focused on the influence of redistribution on the areal measurement of snowcover water equivalent. Equal attention has not been given to the loss of water by sublimation that occurs during movement (Dyunin, 1961; Tabler, 1971; Schmidt, 1972; Pomeroy 1988) and the effect of this loss on the amount of snow water available for runoff and management.

The transport of snow particles by wind involves three modes of movement:

1. *Creep* - the movement by rolling along the surface of those particles too heavy to be lifted by the prevailing wind. Migrating snow waves or dunes develop from creeping snow and these dunes travel downwind at a rate proportional to the wind speed. Tabler et al. (1990) recount that with the 10-m wind averaging 8 m/s, snow waves were observed to move at 5 m/h, and to transport about 45 kg of snow per hour per metre of width across the wind. Kobayashi (1971)

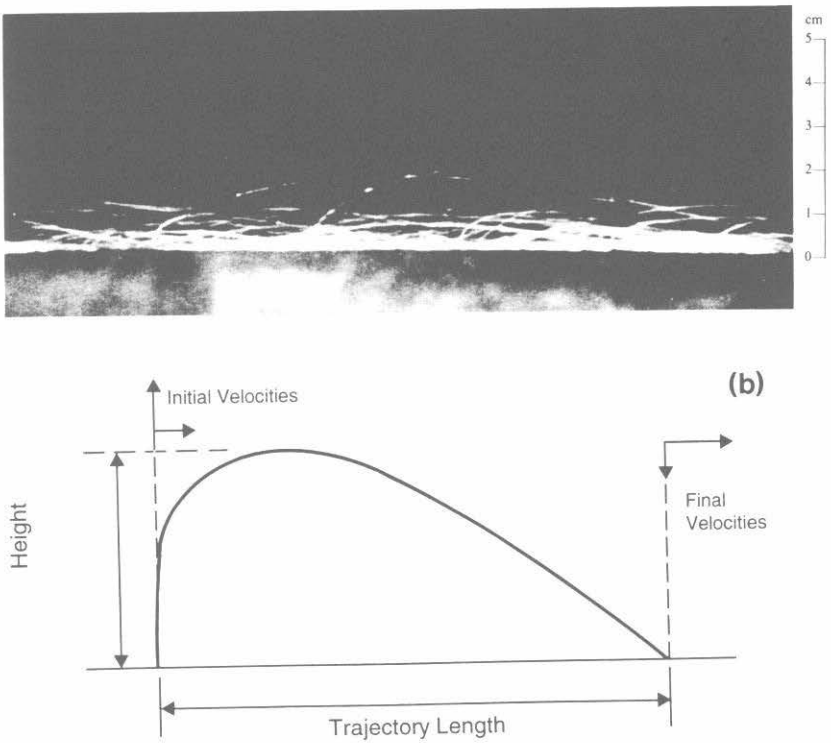

Figure 33 ***(a)*** *Photograph of trajectories of saltating snow particles; $u = 3.9$ m/s at $z = 1$ m (after Kobayashi, 1972) and* ***(b)*** *Initial and final velocity components of a saltating particle.*

reported snow-wave celerities of 1.2 to 6 m/h, with wave lengths varying from 3 to 15 m and heights from 0.05 to 0.2 m. Creeping particles usually comprise a very small portion of the total transport of blowing snow, except at very low wind speeds.

2. *Saltation* - the movement of snow particles by a "skipping" or "jumping" action along the snow surface. The "bed" of saltating snow is not a layer of uniformly-shaped particles; it is a mixture of bonded crystals metamorphosed by the impact of saltating particles and vapour transfer during transport. The trajectories of the saltating particles vary with wind speed, particle size and surface conditions. They follow a path exhibiting an abrupt, near-vertical ascent and a flat, near-horizontal descent (see Figure 33). A typical "jump" may be 1 cm high and 20 cm long. Most saltating particles attain a maximum trajectory in the range from a few millimetres to 5 cm.

3. *Turbulent Diffusion (Suspension)* - the movement of snow particles in suspended flow at a mean horizontal velocity close to that of the moving air. The source of suspended particles is the saltation layer. A saltating particle becomes suspended when the drag force imposed on it by upward-moving air exceeds the gravitational force.

5.1 Saltation

In the first few centimetres above the snow surface, particles move in saltation and the mass concentration appears to decrease exponentially with height. Erosion of snow particles occurs when the drag force exerted on the snow surface by the wind exceeds the surface shear strength. When air moves over flat landscapes, the atmospheric shear stress imparted to the surface by the moving air, τ, is considered to be composed of three components: τ_n, the shear stress applied to non-erodible surface elements, such as vegetation and mechanical barriers; τ_s, the shear stress applied to the stationary erodible surface; and τ_p, the shear stress applied to the saltating bed of snow particles. Thus:

$$\tau = \tau_n + \tau_s + \tau_p, \quad and \tag{26}$$

$$\tau_p = \tau - \tau_n - \tau_s . \tag{27}$$

The total atmospheric shear stress, τ, is equal to $\rho_a u^{*2}$, where ρ_a is the air density and u^* is the friction (shear) velocity. u^* can be determined using measurements of the vertical profile of the mean horizontal wind speed in the Prandtl logarithmic expression:

$$u^* = \frac{u_z k}{\ell n\left(\frac{z}{z_o}\right)}, \tag{28}$$

where: k = von Kármán constant (0.4),

u_z = mean horizontal wind speed (m/s) at height z (m), and

z_o = aerodynamic roughness height (m).

The aerodynamic roughness height during blowing snow differs from that for non-transport conditions because of the particles of saltating snow. Pomeroy (1988) found *for blowing snow* over complete snowcovers:

$$z_o = \frac{u^{*2}}{163.3} + 0.5\, N_s\, A_s\ , \qquad (29)$$

in which N_s is the number of vegetation elements per unit area (stalks/m^2) and A_s is the exposed silhouette area (m^2), the product of the stalk diameter and the exposed height of stalk of a single typical vegetation element. The second term on the right side of Equation 29 is the roughness created by exposed vegetation (Lettau, 1969). A typical value of N_s for wheat fields in Saskatchewan is 320 stalks/m^2.

When profiles of wind speed are not available one of the following expressions may be used to approximate u^* from the 10-m wind speed, u_{10}.

For the Antarctic Ice Sheet,

$$u^* = \frac{u_{10}}{26.5}, \qquad \textit{Budd et al.} (1966) \qquad (30)$$

For a snow-covered lake,

$$u^* = \frac{u_{10}^{1.18}}{41.7}, \qquad \textit{Tabler} (1980) \qquad (31)$$

For a snow-covered fallow field,

$$u^* = \frac{u_{10}^{1.30}}{44.2}, \qquad \textit{Pomeroy} (1988) \qquad (32)$$

in which u^* is in m/s with u_{10} in m/s.

For complete snowcovers with no vegetation protruding above the snow surface, the shear stress applied to non erodible elements is zero; that is, $\tau_n = \rho_a u_n^{*2} = 0$, in which u_n^* is the friction velocity for the non-erodible elements. When stalks and branches of short vegetation are exposed to the moving air, the atmospheric shear stress applied to these elements can be estimated by the empirical relationship (Lyles and Allison, 1976):

$$\left(\frac{\tau}{\tau_s+\tau_p}\right)^{0.5} = 1.638 + 17.04\,N_s A_s - 0.117\left(\frac{L_y}{L_x}\right), \qquad (33)$$

in which L_y is the distance between stalks in the direction parallel to the wind (m), and L_x is the distance between stalks perpendicular to the direction of the wind (m). Equation 33 is used in Equation 26 to derive an expression for, τ_n, as a function of τ, N_s, A_s, L_y, and L_x.

The shear stress applied to the erodible surface, τ_s, is the force per unit area required to maintain particle ejection; it does not contribute to supporting the weight of the saltating snow. When $\tau_n = 0$, τ_s is approximated by $\rho_a u_t^{*2}$, where u_t^* is the threshold friction velocity at the termination/initiation of transport. Determination of u_t^* at the cessation of movement is recommended because the processes of particle impact, rebound and ejection are fully operational, whereas at the time saltation begins they are not. u_t^* is lower (0.07-0.25 m/s) for fresh, loose, dry snow and during snowfall and higher (0.25-1.0 m/s) for older, wind-hardened, dense or wet snow and when interparticle bonds and cohesive forces are strong. Figure 34 (Kind, 1981) shows the influence of hardness of the snow surface at a temperature of ≈ -15°C on the threshold shear velocity.

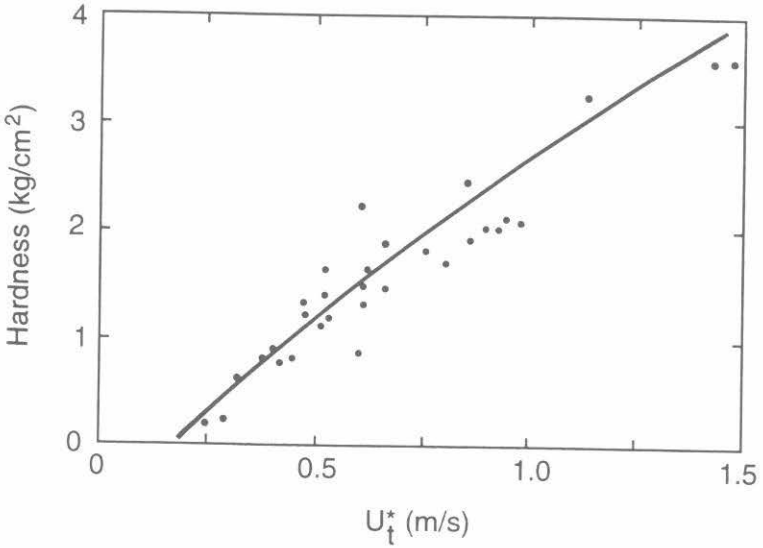

Figure 34 *Influence of the hardness of the snow surface at a temperature of ≈-15°C on threshold shear velocity (based on Antarctic field data reported by Kotlyakov, 1961).*

Transport Rate

The transport rate of saltating snow per unit width in the direction perpendicular to the prevailing wind, q_{salt}, depends on the vertical distribution of wind, the roughness and hardness of the snow surface, the size and density of roughness elements protruding above the snow surface, fetch distance and other factors. q_{salt} for several threshold conditions and exposed heights of wheat stubble is plotted against wind speed in Figure 35. The data show that the increase in the saltation transport rate with increasing wind speed is approximately linear, except for wind speeds near the threshold level. High threshold conditions inhibit transport at low wind speeds, but they enhance transport at high wind speeds because of more-efficient, particle-surface interaction. Exposed stubble substantially raises the minimum wind speed at which transport can be sustained and reduces the saltation transport rate for a given wind speed.

q_{salt} can be expressed as:

$$q_{salt} = u_p \frac{W_p}{g}, \tag{34}$$

where: u_p = mean horizontal velocity of the snow particles in the saltating layer (m/s),

W_p = mean weight of snow saltating over a unit area of the snow surface (N/m^2), and

g = acceleration due to gravity (m/s^2).

The saltation velocity, u_p, is the mean horizontal velocity of snow moving in the saltation layer. Photographs of saltating snow particles, reproduced by Maeno et al. (1979), show that the horizontal velocities of ascending particles increase to match the ambient horizontal wind velocity, whereas the velocities of descending particles decelerate slightly. Therefore, the saltation velocity is approximately proportional to a wind speed within the saltation layer. Measurements of saltating sand in water suggest a centre of fluid drag at 0.8h, where h is the mean saltation trajectory height (Abbott and Francis, 1977).

Bagnold (1941) and Chepil(1945) show that the vertical profiles of wind speed above layers of saltating sediment in the atmosphere meet at a constant wind speed focus within the saltation layer. The focus height is of the order of, or greater than, 80% of the mean height of the trajectories of the saltating particles. During saltation, the wind speed at the height of the focus remains constant at the threshold value; below the focus height, the wind speed profile is fairly uniform. Because the focus wind speed is proportional to the threshold wind speed, and, therefore, to the threshold

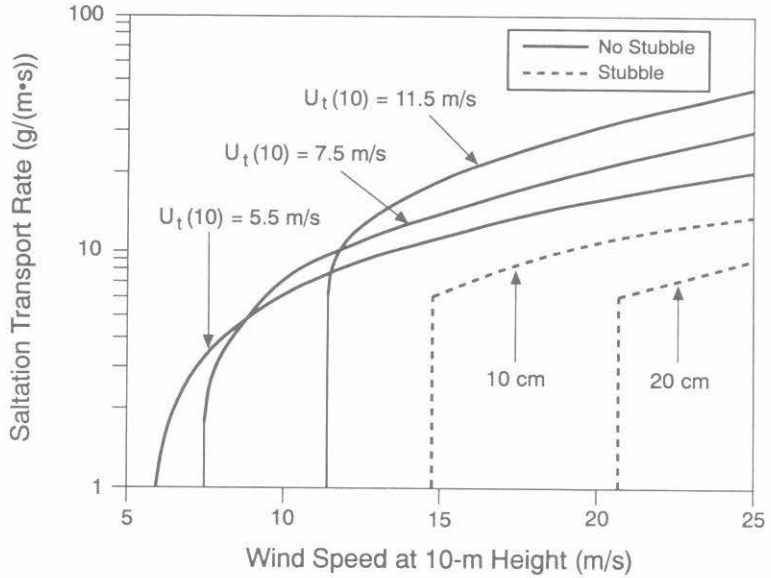

Figure 35 *Variation in the snow saltation transport rate with 10-m wind speed for various threshold 10-m wind speeds ($u_{t\,10}$) given no exposed stubble and for two heights of exposed wheat stubble given $u_{t\,10}$ = 5.5 m/s.*

friction velocity, the saltation velocity, u_p, is proportional to the threshold friction velocity as:

$$u_p = c\, u_t^* , \tag{35}$$

in which c is a proportionality constant. Equation 35 implies that for saltation with constant threshold conditions the saltation velocity is constant and independent of wind speeds above the saltation layer.

Pomeroy and Gray (1990), following on Bagnold's (1941) and Schmidt's (1986) concepts, related the weight of saltating snow, W_p, to the flow shear stress applied to the particles, τ_p, by the expression:

$$W_p = e\,\tau_p = e\left(\tau - \tau_n - \tau_s\right), \tag{36}$$

in which e, the efficiency of saltation, is inversely related to the kinetic energy resulting from particle impact, rebound and the ejection of shattered crystals.

Using Equations 34, 35 and 36 and field measurements, Pomeroy and Gray (1990) derived the general equation for steady-state saltation of a prairie snowcover as:

$$q_{salt} = \frac{0.68\rho_a}{u^* g} u_t^* \left(u^{*2} - u_n^{*2} - u_t^{*2}\right), \tag{37}$$

in which ρ_a is the air density (kg/m^3), u_t^* is the threshold shear velocity (m/s), u^* is the atmospheric shear velocity (m/s), and u_n^* is the shear velocity for non erodible elements (m/s).

Attempts have been made to derive empirical expressions for estimating q_{salt} directly from point measurements of wind speed. A relationship of this type is given by Pomeroy and Gray (1990):

$$q_{salt} = \frac{u_{10}^{1.295}}{2118} - \frac{1}{17.37 u_{10}^{1.295}}. \tag{38}$$

In Equation 38, q_{salt} is in kg/s per metre of width perpendicular to the wind when u_{10}, the wind speed at a height of 10 m is in m/s. The expression applies to flat, non-vegetative land surfaces with complete snowcover and wind speeds $\geq$ 6.5 m/s.

5.2 Suspension

Suspended snow is carried by moving air at a velocity approximately equal to that of the mean horizontal wind. Saltating snow particles are generally considered the source of suspended particles. Hence, suspension of snow cannot proceed until the threshold friction velocity for saltation has been exceeded and a saltation layer exists. A particle becomes suspended when the time-averaged drag force, imposed on it by upward-moving eddies, exceeds the gravitational force. Because the drag force exerted on a particle is proportional to the square of the particle diameter, whereas the mass of a particle increases with the cube of its diameter, movement by diffusion favours the transport of small particles. Therefore, suspended particles are smaller than those moving in saltation.

It is difficult to define the range in height over which the change from movement by saltation to movement by suspension occurs. For practical applications, empirical relationships have been developed for the thickness of the saltation layer, h^*. They assume that above this height particles move by turbulent diffusion. A useful expression for this purpose is (Greely and Iversen, 1985):

$$h^* = \frac{u^{*2}}{12.25}, \tag{39}$$

in which h^* is in metres and u^*, the shear velocity, is in m/s.

The mass concentration of suspended snow (drift density) reaches a maximum just above the saltation layer and decreases with height at a rate that depends on the wind speed (Figure 36). Assuming 100% of snow transport (saltation + suspension) occurs within 10 m of the surface, Pomeroy (1988) shows that 77% and 40% of this total would occur below a height of 1 m, when the 10-m wind speed was 10 m/s and 30 m/s, respectively. Under severe blowing conditions and over terrain where the upstream fetch is several kilometres in length, the layer of suspended snow may extend to heights of hundreds of metres. Therefore, although the mass

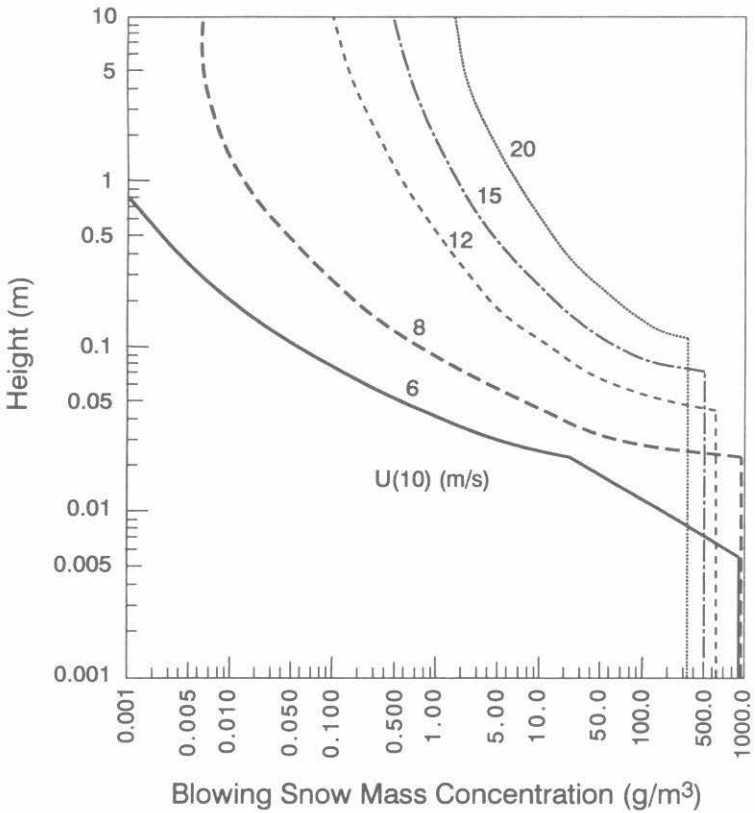

Figure 36 *Vertical profiles of the variation in blowing snow drift density due to saltation and suspension with height and 10-m wind speed assuming a threshold 10-m wind-speed of 5 m/s.*

concentration of blowing snow may be smaller at higher elevations, the total mass of snow moving in suspension may be large because of the thickness of the layer. Figure 36 also shows that the higher the wind speed the more uniform the vertical distribution in mass concentration.

Transport Rate

The transport rate of suspended snow is found by integrating the mass flux over the depth of flow, which extends from the top of the saltation layer to the top of the surface boundary-layer. The mass flux is the mass concentration multiplied by the mean downwind particle velocity; on average this velocity is equal to the velocity of a parcel of air (Schmidt, 1982). Using Equation 28, the transport rate of suspended snow per unit width perpendicular to the wind, q_{susp} (kg/m·s), can be expressed as:

$$q_{susp} = \frac{u^*}{k} \int_{h^*}^{z_b} \eta(z)\, \ell n(\frac{z}{z_o})\, dz\,, \qquad (40)$$

where: k = von Kármán constant,

h^* = height of the top of the saltation layer (m) (Equation 39),

z_b = height of the top of the surface boundary layer for suspended snow (m),

$\eta(z)$ = mass concentration of suspended snow at height, z, (kg/m^3), and

z_o = roughness height (m).

Mass concentration of suspended snow, $\eta(z)$

The steady-state mass concentration of suspended snow at a specific height may be approximated as (Pomeroy and Male, 1992):

$$\eta(z) = \eta(z_r)\, e^{-1.55[(0.05628u^*)^{-0.544} - z^{-0.544}]}\,, \qquad (41)$$

in which $\eta(z_r)$ is the reference mass concentration for suspension. Pomeroy and Male suggest $\eta(z_r)$ = 0.8 kg/m^3, based on measured concentrations in the saltation layer (Pomeroy and Gray, 1990).

Height of the top of the surface boundary layer for suspended snow, z_b

The upper boundary height for suspended snow, exclusive of inversions or flow separation due to upwind topography, is determined by the time available for diffusion of a snow particle from the lower boundary. The top of a plume of diffusing particles, z_p, may be found from the elapsed time and turbulence characteristics if the variance of particle velocity is approximately equal to that of an atmospheric fluid point velocity. Following Pasquill (1974),

$$z_p(t) - z_p(0) = ku^* t \,, \tag{42}$$

where t is elapsed time. Assuming $z_p(t) \equiv z_b$, the top of the surface boundary layer for suspended snow may be expressed in terms of the logarithmic wind profile as:

(43)

$$z_b = z_p(t) = z_p(0) + k^2 [x(t) - x(0)][\ell n(\frac{z_p(0)}{z_o}) \ell n(\frac{z_p(t)}{z_o})]^{-0.5} \,,$$

where x is the distance downwind from the leading edge of the fetch over which the surface roughness and the aerodynamic roughness height can be considered uniform. Pomeroy (1988) demonstrates that the assumption of equal particle and wind velocity variance is not met at heights near to or below the saltation layer.

Suspension transport rates modelled by Equation 40 for a 500-m fetch distance, a threshold 10-m wind speed of 5.5 m/s, and various heights of exposed grain stubble are shown in Figure 37. They show suspension rates increasing exponentially with 10-m wind speed. Exposed stubble increases the minimum wind speed necessary to sustain transport(by suppressing saltation) and decreases the suspension transport rate at a given wind speed.

Tabler *et al.* (1990a) reported reasonable agreement between modelled values of q_{susp} to a height of 5 m with estimates by the equation:

$$q_{susp} = \frac{u_{10}^{4.13}}{674{,}000} \,, \tag{44}$$

in which q_{susp} is in kg/s per metre width perpendicular to the wind when u_{10}, the wind speed at a height of 10 m, is in m/s. The increase in transport rate with roughly the fourth power of wind speed is in agreement with theoretical considerations that suggest the mass concentration is proportional to the kinetic energy expended by turbulence, and therefore

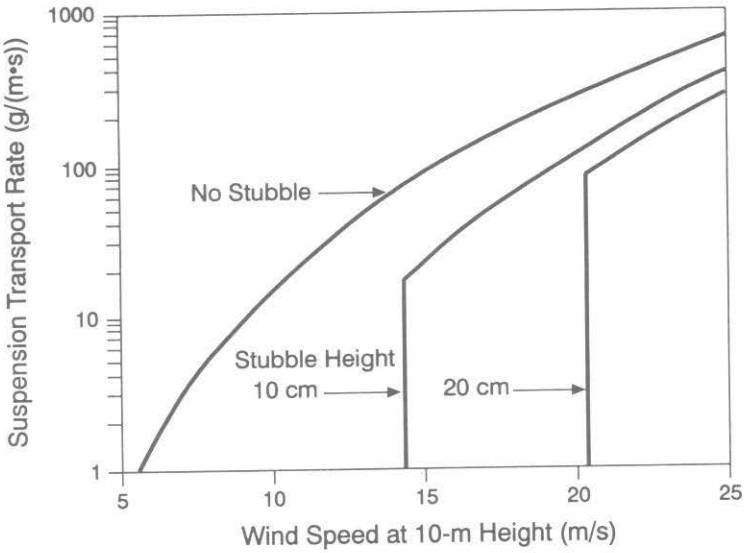

Figure 37 Variation in snow suspension transport rate with wind speed and stubble height on a 500-m fetch with the threshold 10-m wind speed of 5.5 m/s.

to the third power of wind speed. Transport rate would be roughly proportional to mass concentration times wind speed and therefore roughly proportional to the fourth power of wind speed.

5.3 Total Snow Transport

The total snow transport rate, q_T, can be estimated by summing the saltation and suspension components. Alternatively, empirical expressions are available that may be used to estimate the rate from wind speed. Table 3 compiles models for q_T that have been developed from extensive measurement programs.

The transport rates by these expressions are plotted against the 10-m wind speed in Figure 38. Differences between the estimated transport rates at a specific wind speed are due to many factors. For example: (a) the expressions integrate the mass flux to different heights and (b) they are based on varied assumptions, measurement techniques and snow surface conditions. Budd *et al.* (1966) presume higher saltation rates than normally measured. This expression was adjusted by Tabler *et al.* (1990b) to provide a better estimate of the saltation flux, and as shown in Figure 38, the transport rates by the modified expression more closely agree with the results from Japan, Siberia and Canada.

Table 3 *Expressions for calculating the transport rate of blowing snow, q_T, in kg/s per metre perpendicular to the wind over a specified range of height. u is the wind speed in m/s at the height indicated by the subscript in metres.*

Equation	Height (m)	Reference	Comments
$\log q_T = -1.82 + 0.089u_{10}$	0.001 - 300	Budd *et al.* (1966)	Antarctica
$q_T = 0.000077(u_{10} - 5)^3$	0 - 2	Dyunin & Kotlyakov (1980)	Siberia
$q_T = 0.0002u_1^{2.7}$	0 - 2	Takeuchi (1980)	Japan: old, firm snow
$q_T = 0.0000014u_{10}^{4.2}$	0 - 10	Tabler *et al.* (1990)	Antarctica/ prairie synthesis
$q_T = 0.0000022u_{10}^{4.04}$	0 - 5	Pomeroy *et al.*, (1991)	Canadian Prairies fallow

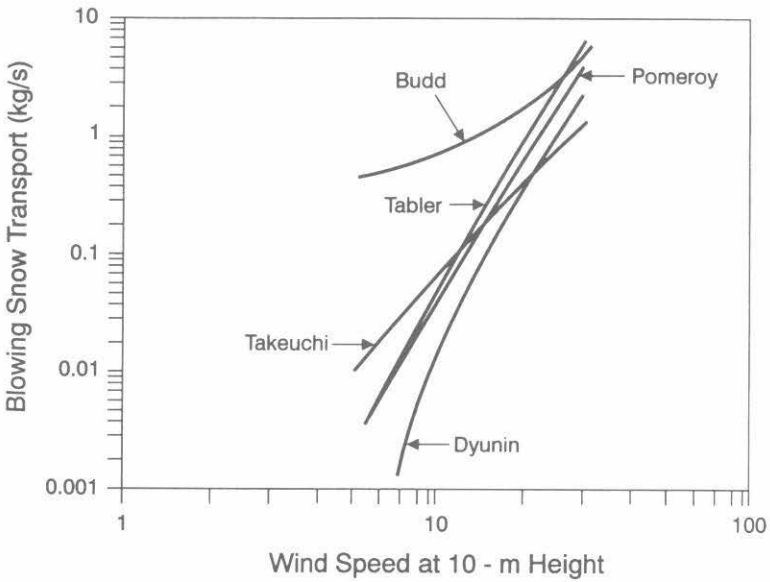

Figure 38 *Total snow transport rate as a function of 10-m wind speed calculated by various expressions developed in Antarctica (Budd et al., 1966), Siberia (Dyunin and Kotlyakov, 1980), Japan (Takeuchi, 1980), the United States (Tabler et al., 1990a,b) and Canada (Pomeroy et al., 1991).*

5.4 Sublimation

Although a large amount of research has focused on the saltation and suspension processes, equal attention has not been given to the loss of water by sublimation, the change in phase from ice to water vapour, during wind transport. The theory of sublimation of blowing snow is described by (Dyunin,1959; Schmidt, 1972, 1991; Male, 1980; Pomeroy, 1988).

Sublimation of a snow particle that is entrained in the atmosphere is governed by the laws of conservation of mass and energy. Consider a sphere of ice suspended in air. The rate that water vapour can be removed from the particle's surface-layer, dm/dt, is controlled by:

1. The radius of the sphere, r (m),
2. The diffusivity of water vapour in the atmosphere, D(m^2/s), $D = 2.06 \times 10^{-5}(T/273)^{1.75}$ (Thorpe and Mason, 1966).
3. The degree of turbulent transfer of water vapour from the particle surface to air indexed by the Sherwood number, Sh),
4. The water vapour density of the ambient air, ρ_{wa} (kg/m^3), and
5. The water vapour density at the particle surface, ρ_{wp} (kg/m^3), as:

$$\frac{dm}{dt} = 2\pi r D Sh(\rho_{wa} - \rho_{wp}) . \qquad (45)$$

However, dm/dt is also controlled by the rate that energy is delivered to the sphere. Considering only turbulent convective heat transfer, the energy balance for a sublimating ice sphere is:

$$h_s(\frac{dm}{dt}) = 2\pi \lambda_T r Nu(T_s - T_a) , \qquad (46)$$

where: h_s = latent heat of sublimation (2.838×10^6 J/kg),

λ_T = thermal conductivity of the atmosphere (J/(m·s·K)), ($\lambda_T = 0.00063T + 0.0673$),

Nu = Nusselt number,

T_s = surface temperature of the ice sphere (K), and

T_a = ambient atmospheric temperature (K).

Schmidt (1972;1991) combined Equations 45 and 46 using the Clausius-Clapeyron equation and the assumption that snow particles remain in thermodynamic equilibrium. He also included short-wave radiation absorbed by the particle, Q_s (W/m^2), in the energy balance. The sublimation rate, or time rate of change in the mass of a single ice crystal is given by Schmidt as:

$$\frac{dm}{dt} = \frac{2\pi\, r\, \sigma - \dfrac{Q_s}{\lambda_T\, T_a\, Nu}\left[\dfrac{h_s\, M}{R\, T_a} - 1\right]}{\dfrac{h_s}{\lambda_T\, T_a\, Nu}\left[\dfrac{h_s\, M}{R\, T_a} - 1\right] + \dfrac{1}{D\, \rho_s\, Sh}}, \qquad (47)$$

in which σ is the ambient atmospheric undersaturation of water vapour with respect to ice (0.01RH -1, in which RH = relative humidity (%)), M is the molecular weight of water (18.01 kg/kmole), R is the universal gas constant (8313 J/kmoleK), and ρ_s is the saturation density of water vapour at T_a.

The sublimation rate per unit area of snowcover, q_{subl} ($kg/m^2 \cdot s$), of a column of blowing snow that extends from the snow surface to the top of the boundary layer for suspended snow is determined by summation. This involves integrating the product of the ratio of the time rate of change in mass of the blowing snow particle of mean particle mass at height z, $d\bar{m}(z)/dt$, to its mass, $\bar{m}(z)$, and the mass concentration of blowing snow at height z, n(z), from the snow surface to the height, z_b. That is,

$$q_{subl} = \int_o^{z_b} \frac{d\bar{m}(z)/dt}{\bar{m}(z)} \eta(z)\, dz, \quad and$$
$$q_{subl} = \int_o^{z_b} V_s(z) \eta(z)\, dz\,. \qquad (48)$$

$V_s(z)$ (s^{-1}) is the sublimation loss rate coefficient at a specific height and equal to:

$$V_s(z) = \frac{d(\bar{m}(z))/dt}{\bar{m}(z)}\,. \qquad (49)$$

The sublimation loss rate coefficient at any height z is estimated from Equation 47 using r = $\bar{r}(z)$, the radius of a particle of mean particle mass at height, z, and estimates of σ, Nu, λ_T, T, D and Sh at the specific height. The following relationships can be used for these calculations.

Radius of particle, $\bar{r}(z)$, of mean particle mass, $\bar{m}(z)$, at height, z.

$$\bar{r}(z) = \left(\frac{3\bar{m}(z)}{4\,\pi\rho} \right)^{0.33}, \quad and \tag{50}$$

$$\bar{m}(z) = \frac{4}{3}\pi\,\rho_i\,\bar{r}_r(z)^3\left(1+\frac{3}{\alpha}+\frac{2}{\alpha^2}\right), \tag{51}$$

in which ρ_i is the density of ice (kg/m^3), α is a coefficient and $\bar{r}_r(z)$ is the mean radius of snow particles at height, z. α and $\bar{r}_r(z)$ can be determined as:

$$\alpha = 4.08 + 12.6z, \quad and \tag{52}$$

$$\bar{r}_r(z) = 4.6\text{x}10^{-5}\,z^{-0.258}, \tag{53}$$

in which z is in metres.

Nusselt and Sherwood Numbers, Nu, Sh

Lee (1975) confirmed that adjacent to a blowing snow particle in a turbulent atmosphere Nu ≡ Sh. Both terms are related to the particle Reynold's number, N_R, and for N_R between 0.7 and 10:

$$Nu(z) = Sh(z) = 1.79 + 0.606\,N_R(z)^{0.5}, \tag{54}$$

in which,

$$N_R(z) = \frac{2\bar{r}(z)\;V_r(z)}{\nu}, \tag{55}$$

where $V_r(z)$ is the ventilation velocity and ν is the kinematic viscosity of air. $V_r(z)$ is the sum of the mean terminal fall velocity, $\bar{w}(z)$ and the root mean square fluctuating velocity relative to the atmosphere. Lee (1975) found:

$$V_r(z) = \bar{w}(z) + 3\,x_r(z)\,\text{Cos}\left(\frac{\pi}{4}\right), \tag{56}$$

in which $x_r(z)$ is a component of the root mean square particle velocity relative to the atmosphere in one cartesian direction. An expression for the mean terminal fall velocity of suspended snow is given by Pomeroy and Male (1986) as:

$$\bar{w}(z) = 1.1 \times 10^{7}\ \bar{r}(z)^{1.8}\ . \tag{57}$$

Lee's model for fluctuating relative wind speeds was simplified by Pomeroy(1988) for mean prairie surface roughness conditions during drifting snow as:

$$x_r(z) = 0.005 u_z^{1.36}, \tag{58}$$

where $x_r(z)$ and u_z are in m/s.

For *saltating snow* the ventilation velocity is separated into vertical and horizontal mean components. The vertical component is taken as $0.68u^*$ (Pomeroy and Gray, 1990) and the horizontal component as $2.3.u_t^*$

Therefore:

$$V_r(salt) = 0.68u^* + 2.3u_t^*\ . \tag{59}$$

Temperature, $T_a(z)$

The ambient air temperature at any height, $T_a(z)$, can be calculated from the lapse rate. Measurements of vertical temperature profiles over three winters in southern Saskatchewan showed relative cooling near the snow surface during the majority of blowing snow events; however, there was no overall consistency in the stability of the gradients. Therefore, the effects of a gradient in temperature on sublimation rate are often neglected.

Undersaturation of water vapour with respect to ice, $\sigma(z)$

The undersaturation of water vapour in the atmosphere is calculated from the actual water vapour density, ρ_{wa}, and the saturation vapour density, ρ_s, at temperature, T_a, in the expression:

$$\sigma = \frac{\rho_{wa}}{\rho_s} - 1. \tag{60}$$

For practical applications, ρ_{wa}/ρ_s may be approximated by the relative humidity, RH (%), divided by 100.

Measurements of vertical humidity profiles over three winters on the Prairies consistently showed a decrease in relative humidity with increasing height during blowing snow. The most common gradient, expressed in terms of the undersaturation of water vapour at any height, $\sigma(z)$, is approximated by:

$$\sigma(z) = \sigma(z = 2)\,(1.02 - 0.027\,\ell nz)\,, \qquad (61)$$

where $\sigma(z = 2)$ is the undersaturation at a height of two metres.

Sublimation rate, q_{subl}

Combining $V_s(z)$ with the mass concentrations of blowing snow for saltation (Equations 34, 36) and for suspension (Equation 40) in Equation 48 gives the blowing snow sublimation rate for a column extending from the surface to the top of the boundary-layer. Figure 39 shows q_{subl} for a fully-developed column of blowing snow plotted with the 10-m wind speed, for a fetch distance of 500 m, an incoming solar radiation of 120 W/m^2, and three air temperatures and relative humidities. Note, in western

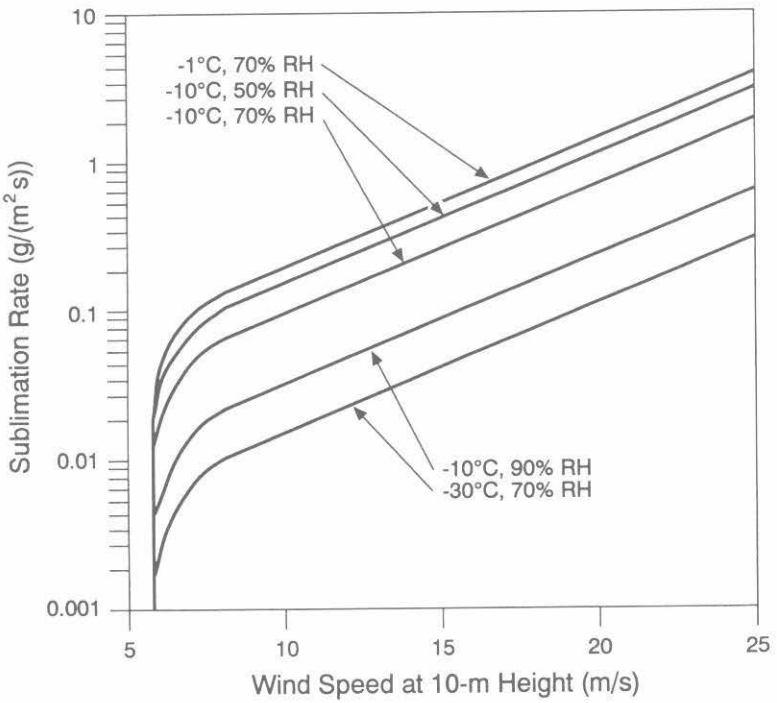

Figure 39 Variation in the sublimation rate in a column of blowing snow with 10-m wind speed, air temperature, and relative humidity. The calculations assume a fetch distance of 500 m and a solar radiation flux = 120 W/m^2.

Canada, variations in temperature or humidity through their normal range cause at least an order of magnitude change in the sublimation rate, whereas variations in daily radiation input cause only a small change in this rate. The sublimation rate increases exponentially with wind speed.

5.5 Snow Erosion and Deposition

Under invariant atmospheric and surface conditions and an adequate fetch of mobile snow, an equilibrium (steady-state) flow condition will develop where the mass of snow in saltation and suspension remains constant and the surface erosion rate is equal to the evaporation/sublimation rate.

Consider a control volume of the atmosphere that extends vertically from the snow surface to the top of the surface boundary-layer for blowing snow where the vertical flux of snow by diffusion is zero (Figure 40). Assume the snow fluxes perpendicular to the direction of transport are negligible and the reference for z, the vertical direction, is the snow surface. The surface erosion/deposition rate at a distance, x, downwind of the leading edge of a fetch, $q_v(x,0)$, is established by the net mass of snow entering or

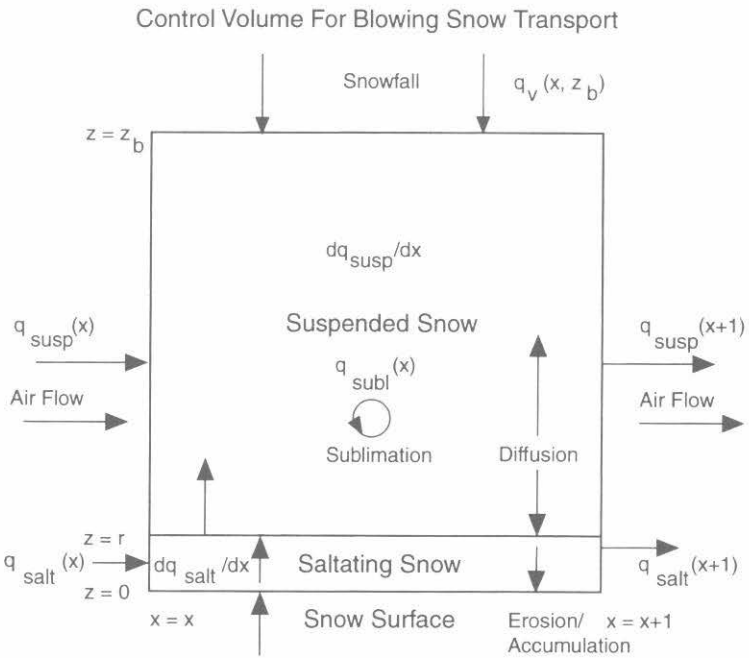

Figure 40 *Control volume for blowing snow transport and sublimation.*

leaving the volume in the x and z directions and sublimation occurring within the volume. The mass balance for the volume gives the surface erosion/deposition rate per unit area as:

$$q_v(x,0) = \frac{dq_{salt}}{dx}(x) + \frac{dq_{susp}}{dx}(x) + q_{subl}(x) + q_v(x,z_b)\,, \tag{62}$$

in which the vertical flux at the top of the volume, $q_v(x,z_b)$, equals the negative of the snowfall rate. Under fully-developed flow, the surface erosion rate is equal to the sublimation rate less the snowfall rate. Atmospheric conditions, surface roughness, snow supply and land use influence the length of fetch required to attain steady transport. Takeuchi (1980) reports distances varying from 150 to 300 m for transport rates to reach equilibrium in the lowest 0.3 m of the atmosphere; Pomeroy (1988) suggests a distance of 500 m for full development to a height of 5 m.

Snow accumulation occurs where surface roughness elements or topographic depressions cause decreases in wind speed and in saltation and suspension transport rates, or when the snowfall rate is greater than the sum of the surface erosion rate and the sublimation rate.

Chapter 6

ESTIMATING BLOWING SNOW TRANSPORT AND SUBLIMATION RATES ON THE PRAIRIES OF WESTERN CANADA

6.1 Introduction

The western Canadian Prairies are located in an open, arid and wind-swept environment where snowfall comprises, on average, about 39% of the annual precipitation. The region is extensively cultivated to cereal grains for which a fallow-crop rotation is often practised. These farming practices result in a land surface in winter that alternates large fields of grain stubble with large fields of bare soil (fallow). There is interest in managing snowcover by modifying land use patterns to maintain snow-covered fields, to reduce soil erosion, and to enhance soil water recharge by meltwater infiltration. To aid the design of snow management practices, calculations of snow transport and sublimation that consider the effects of surface roughness and aerodynamic fetch are necessary. Therefore, the physically-based algorithms for estimating saltation, suspension and sublimation rates of blowing snow due to wind transport presented in Section 5 were assembled into a model, the Prairie Blowing Snow Model, PBSM (Pomeroy, 1988; 1989). Landine and Gray (1989) applied the PBSM to calculate the disposition of seasonal snowfall over level, flat surfaces in the agricultural areas of the Canadian Prairies. Specifics on the implementation of the system for this purpose are provided by Pomeroy *et al.*(1993). Information was obtained on the wind transport of snow from stubble and fallow surfaces during the six-year

period, 1970-76, using meteorological observations reported by the Atmospheric Environment Service, Environment Canada, at sixteen stations in the prairie and parkland regions of western Canada. A summary of the findings of the analyses is presented below.

6.2 Annual Fluxes

Table 4 lists the average annual "modelled" blowing snow fluxes on 1-km fetches of stubble (stalk height = 25 cm) and fallow (surface roughness equivalent to grain stalk height = 1 cm) at four stations in Saskatchewan. These data show:

1. On average at Prince Albert, Swift Current and Yorkton at least 8% (range of 8-11%) of annual snowfall is removed from a 1-km fetch of 25-cm stubble by saltation and suspension; at Regina about double this percentage (19%).

2. Blowing snow fluxes are greater on fallow than stubble. The largest increases, with a change in surface condition from stubble to fallow, occur at Regina and Swift Current where the transport fluxes are at least double and the sublimation losses increase by 7%.

3. The percentage of annual snowfall lost to sublimation from a 1-km fetch is equal to or greater than (ranging to 2.6 times) the amount of snow transported in saltation and suspension. The results from 16 stations show that the average annual amount of snow water lost to sublimation from a 1-km fetch may be up to 5 times the amount of snow transported in saltation and suspension, independent of land use.

Blowing snow fluxes on the Prairies generally tend to decrease with increasing latitude from the grassland to boreal forest region due to differences in climate and changes in vegetation. Lower wind speeds, air temperatures and vapour pressure deficits prevail at the northerly stations and the vegetation changes from open grassland to mixed grassland, deciduous and boreal forest. Further north, in Arctic regions blowing snow fluxes may also be large, despite low temperatures and humidity, because of the open exposure, high winds and reduced bonding of snow crystals.

The mean annual (1970 to 1976) simulated snow transport (saltation + suspension) and sublimation losses from 1-km fetches of stubble and fallow at various sites in western Canada are summarized in Figures 41, 42, 43 and 44. They assume: (a) a stubble with a height of 25 cm, a plant density of 320 stalks/m^2 and an average stalk diameter equal to 3 mm; and (b) a surface roughness for fallow land equivalent to the roughness of a field of stubble having a uniform height of 1 cm.

Table 4 *Blowing snow fluxes as a percentage of annual snowfall, over 1 km fetches of stubble and fallow at four stations in the Province of Saskatchewan, Canada.*

		Climatic Statistics[a]			Land-use	Transport Fluxes		Sublimation (%)	
Station	Coordinates	Snowfall Water Equivalent (mm)	Mean Temperature °C	Mean Wind speed (m/s)		Saltation (%)	Suspension (%)		Region
Prince Albert	Lat. 53°13'N Long. 105°41'W	103	-11.6	4.5	Stubble	3	6	23	parkland region, mixed grassland and deciduous/Boreal forest; snowpack tends to be permanent during winter
					Fallow	4	9	27	
Yorkton	Lat. 51°16'N Long. 102°28'W	125	-10.6	4.7	Stubble	3	5	15	parkland region, mixed grassland and deciduous/Boreal forest; snowpack tends to be permanent during winter
					Fallow	4	9	23	
Regina	Lat. 50°26'N Long. 104°40'W	113	-8.9	6.0	Stubble	6	13	34	prairie region; infrequent occurrence of Chinook[b] winds; snowcover tends to be permanent during winter
					Fallow	10	26	41	
Swift Current	Lat. 50°17'N Long. 107°45'W	132	-6.7	6.6	Stubble	4	7	22	prairie region; frequent occurrence of Chinook winds; snowcover frequently lost during winter
					Fallow	8	21	29	

[a] October - March inclusive.

[b] Chinook - warm dry, winter winds that flow down the eastern slopes of the Rocky Mountains and move out onto the Prairies. They may cause appreciable melting of a snowcover.

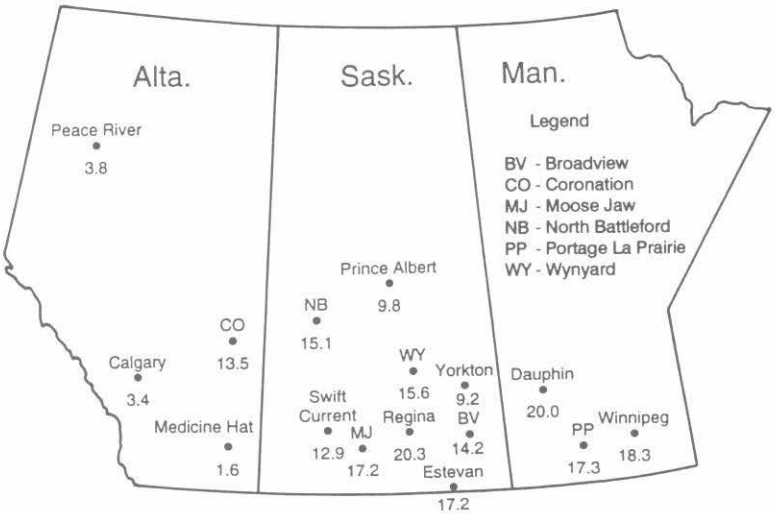

Figure 41 *Mean annual snow transport (saltation and suspension) from a 1-km fetch of stubble at various locations in the Prairie Provinces, 1970-76. Units are Megagram per metre width (Mg/m). Note: a flux of 1 Mg/m on a fetch of 1 km is equal to 1 mm of snow water equivalent over the fetch distance.*

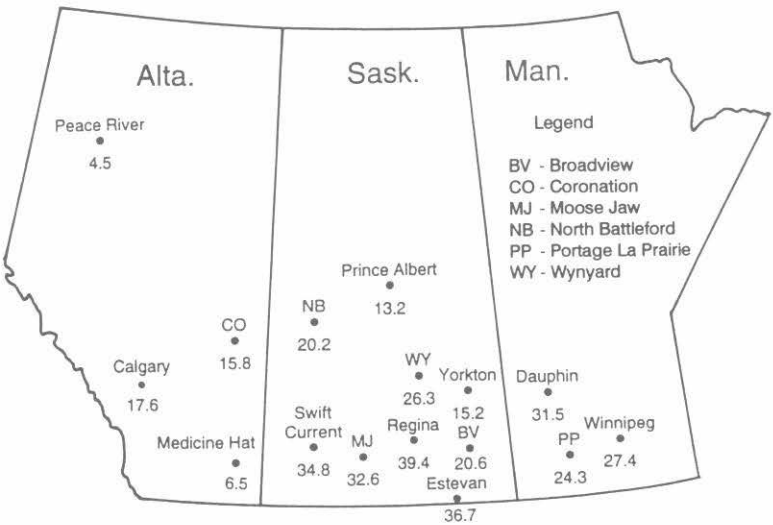

Figure 42 *Mean annual snow transport (saltation and suspension) from a 1-km fetch of fallow at various locations in the Prairie Provinces, 1970-76. Units are Megagram per metre width (Mg/m). Note: a flux of 1 Mg/m on a fetch of 1 km is equal to 1 mm of snow water equivalent over the fetch distance.*

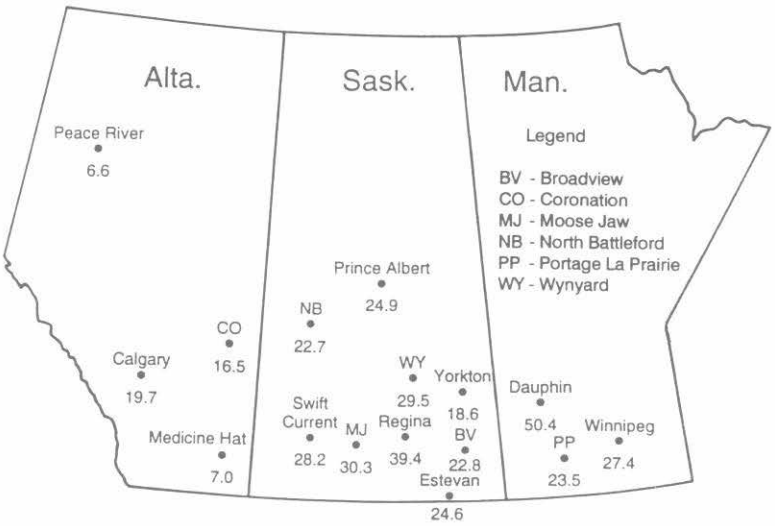

Figure 43 *Mean annual blowing snow sublimation from a 1-km fetch of stubble at various locations in the Prairie Provinces, 1970-76. Units are Megagram per metre width (Mg/m). Note: a flux of 1 Mg/m on a fetch of 1 km is equal to 1 mm of snow water over the fetch distance.*

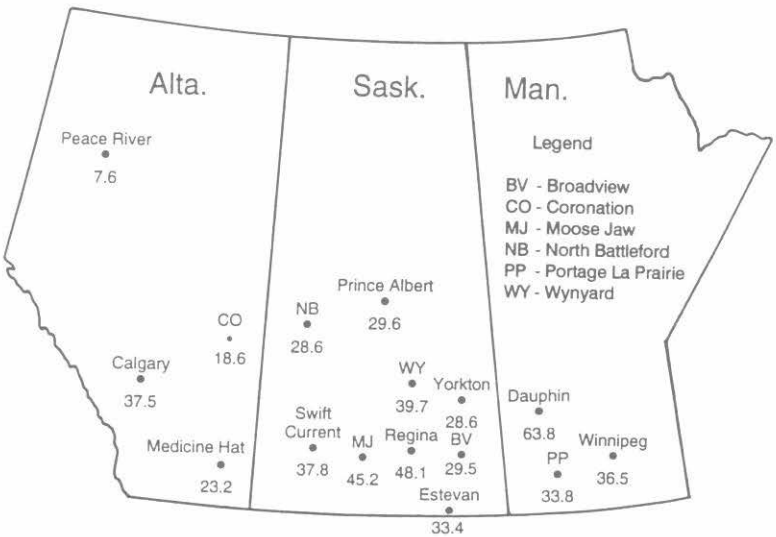

Figure 44 *Mean annual blowing snow sublimation from a 1-km fetch of fallow at various locations in the Prairie Provinces, 1970-76. Units are Megagram per metre width (Mg/m). Note: a flux of 1 Mg/m on a fetch of 1 km is equal to 1 mm of snow water over the fetch distance.*

Orientation of Snow Control and Management Works

Knowledge of the directional components of snow transport is useful for establishing the "best" orientation and alignment of barriers for snow control and management. Figures 45 and 46 show roses of the directional frequency of hourly wind and the average annual snow transport (saltation + suspension) to a height of 5 m on a 1-km fetch of fallow at Regina and Prince Albert, Saskatchewan. Figure 45a shows winds at Regina occurred from the NW, W, E and SE directions 75.4% of the time and these winds produced, on average, about 88.6% of the annual saltation and suspension flux (Figure 45b). The shapes of the roses of wind and snow transport are reasonably similar, with the exception of the SW and S directions, where winds with a frequency of 14.1% produced only about 2.6% of the annual flux. SW and S winds at Regina often bring "chinook" conditions and mid-winter warming, which produce low transport. At Regina, the most effective orientation of a snow control device would be SW to NE, i.e., in the direction perpendicular to the predominant prevailing winds and fluxes.

Matching symmetry in the directional distributions of wind and snow transport should not be assumed. Wind speeds may exhibit directional bias, as may snowfall, the persistence of snowcover, snow surface cohesion, and other factors affecting transport. Also, infrequent strong winds from a few directions usually cause a disproportionate amount of the annual transport. The roses of wind frequency and snow transport at Prince Albert (Figure 46) exhibit major departures in their directional distributions. Winds from the NE, which occurred with a frequency of 13.1%, produced 17.7% of the annual amount of snow transported in saltation and suspension. Those from the SW, which occurred with approximately the same directional frequency (13.3%), produced only 0.6% of the annual flux. As at Regina, the warmer S-SW winds at Prince Albert are the likely cause of the difference. The wind rose suggests that barriers placed on any alignment within a segment bounded by NE-SW and NW-SE directions should provide an equal measure of exposure to blowing snow. However, the flux rose rules out a NW-SE orientation because of the small amounts of snow transported from S and SE directions. A control placed with an N-S alignment would provide protection and "trapping" action against 85.4% of the winds and 90.5% of the annual flux of blowing snow in saltation and in suspension to a height of 5 m.

The directional distributions of the annual snow transport on 1-km fetches of stubble and fallow at sixteen stations in western Canada are summarized in Table 5. At most stations, the effect of land cover on the directional distribution is small. However, there are a few exceptions. At Calgary, 43% of the annual transport flux on fallow occurred from the north, compared to only 34% from the same direction on stubble. One possible cause for the difference may be a seasonal shift in wind speed and

direction over winter. Because a vegetative cover must first fill before significant transport begins, it is likely that transport on stubble occurs later in winter than transport on fallow. Therefore, the wind regimes contributing the annual flux on the two landscapes may not be the same. Analyses of data from all sixteen stations suggest that barriers placed with an alignment falling within the sector bounded by N-S and NE-SW co-ordinates will usually provide the greatest exposure to blowing snow in the prairie region.

Table 5 *Directional distribution of the mean annual snow transport (saltation and suspension) on 1000-m fetches of stubble and fallow at sixteen locations in western Canada. Values are a percentage of the total annual transport.*

Location	NE	E	SE	S	SW	W	NW	N
Stubble								
Broadview	4.4	13.5	18.5	4.2	2.6	17.5	28.6	10.7
Calgary	1.4	0.3	1.3	2.0	2.1	26.8	31.5	34.4
Coronation	3.0	3.1	9.6	5.7	1.0	1.5	38.7	37.5
Dauphin	1.2	6.0	2.0	6.2	38.9	32.0	7.8	5.9
Estevan	2.6	17.4	9.7	2.1	4.8	26.6	33.3	3.6
Medicine Hat	13.9	1.9	0.4	8.6	30.5	13.7	12.3	18.7
Moose Jaw	2.0	14.2	13.8	4.1	8.6	26.5	27.6	3.1
North Battleford	1.9	42.4	36.2	0.1	0.0	5.4	10.9	3.1
Peace River	16.0	0.7	0.0	0.0	2.8	10.5	21.7	48.2
Portage la Prairie	1.1	2.0	5.1	3.0	0.0	18.5	41.9	24.2
Prince Albert	16.8	31.9	7.8	0.4	0.8	11.7	20.6	10.2
Regina	3.2	20.7	22.2	1.0	0.9	18.3	28.5	5.2
Swift Current	4.4	12.4	12.9	12.2	9.5	26.2	19.8	2.6
Winnipeg	7.1	2.2	11.2	22.8	1.2	8.8	25.4	21.4
Wynyard	1.0	15.8	22.2	14.2	15.8	17.7	10.3	3.0
Yorkton	3.0	6.9	13.9	6.3	1.5	25.3	33.0	9.8
Fallow								
Broadview	3.4	11.1	17.4	4.5	2.2	19.6	32.4	9.4
Calgary	4.8	0.5	1.6	1.1	2.0	16.3	30.5	43.3
Coronation	3.5	3.5	8.7	5.6	0.9	11.4	29.0	37.4
Dauphin	1.6	5.7	2.2	5.8	36.7	33.0	8.1	7.0
Estevan	3.1	17.8	9.3	2.1	4.5	25.8	34.1	3.4
Medicine Hat	6.3	4.6	.6	12.3	25.9	15.8	17.1	17.4
Moose Jaw	3.0	15.3	13.3	4.1	7.5	25.9	26.9	4.0
North Battleford	2.8	40.1	34.9	0.8	0.0	5.5	12.0	3.8
Peace River	16.0	0.7	0.0	0.0	22.5	11.5	0.0	49.5
Portage la Prairie	1.0	2.2	5.8	3.7	3.8	19.7	41.0	22.8
Prince Albert	17.7	29.8	7.7	0.3	0.6	12.2	22.8	9.2
Regina	3.2	20.0	23.1	1.6	1.0	16.8	28.7	5.5
Swift Current	3.3	10.9	10.9	10.7	8.5	27.4	25.2	3.1
Winnipeg	6.4	2.5	11.2	23.8	1.5	9.3	25.3	20.0
Wynyard	1.3	13.5	20.7	13.5	14.6	19.1	14.0	3.3
Yorkton	3.9	6.8	13.4	5.9	1.3	25.3	32.6	10.8

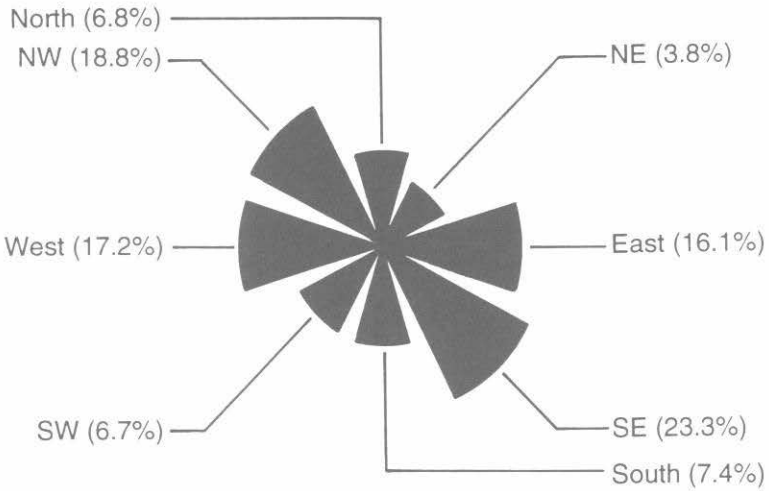

(a) Hourly Wind

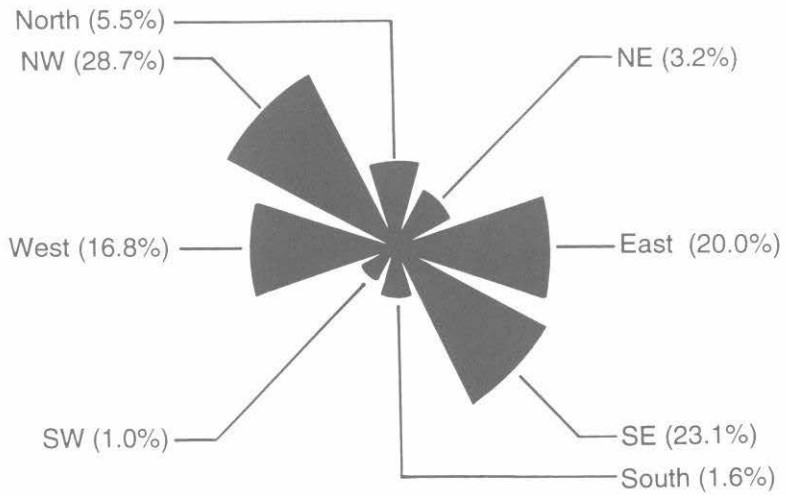

(b) Annual Snow Transport

Figure 45 *Roses showing the mean directional distributions of:* ***(a)*** *hourly wind and* ***(b)*** *annual snow transport on a 1-km fetch of fallow at Regina, Saskatchewan (Nov. through April, 1970-1976).*

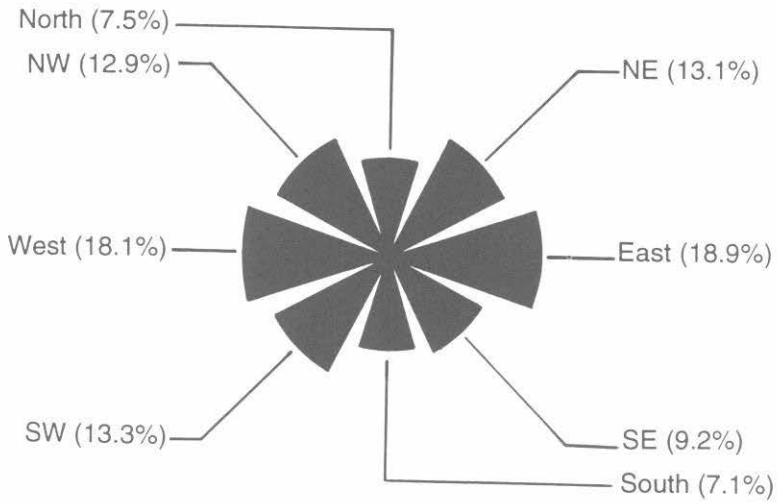

(a) Hourly Wind

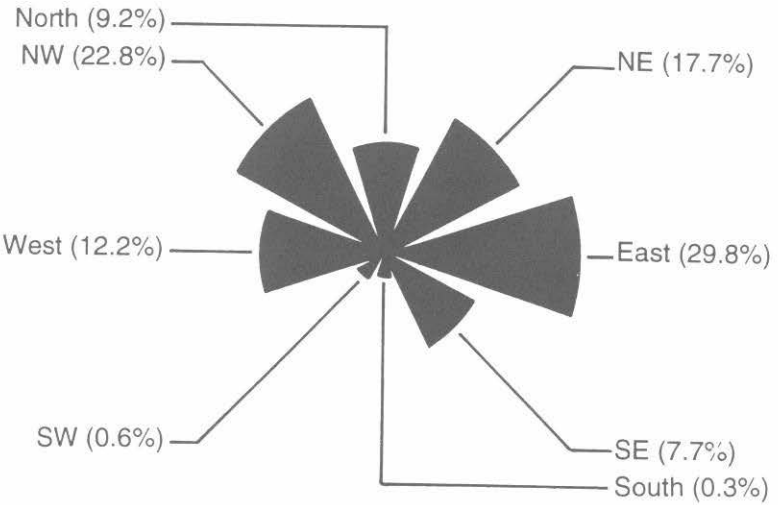

(b) Annual Snow Transport

Figure 46 *Roses showing the mean directional distributions of:* ***(a)*** *hourly wind and* ***(b)*** *annual snow transport on a 1-km fetch of fallow at Prince Albert, Saskatchewan (Nov. through April, 1970-1976).*

6.3 Adjustments to the Annual Blowing Snow Fluxes

Roughness Height

Snow transport and sublimation rates decrease with increasing height of vegetation because of increasing surface roughness due to exposed vegetation. At Regina, the annual flux of saltating and suspended snow on a 1-km fetch of stubble decreased by 25,300 kg/m width perpendicular to the wind with an increase in stubble height from 1 to 40 cm. At Prince Albert, the decrease was 6,800 kg/m for the same change in height of vegetation (Figure 47a). Figure 47b shows sublimation from a 1-km fetch at both Regina and Prince Albert decreasing slowly with increasing stubble height. For a given height of stubble the flux at Regina is roughly 1.75 times that at Prince Albert. Changes in snow transport and sublimation with a change in the height of stubble between 1 and 40 cm, can be approximated by:

$$\Delta TRAN = 207 - 0.0252\ TRAN(1,1), \quad \textit{and} \qquad (63)$$

$$\Delta SUB = 5.38 - 0.0103\ SUB(1,1), \qquad (64)$$

in which ΔTRAN is the change in snow transport rate per metre width perpendicular to the wind from a 1-km (kg/m) fetch *for each centimetre change in stubble height* (kg/cmm); TRAN (1,1) is the annual snow transport rate to a height of 5 m per metre width perpendicular to the wind from a 1-km fetch of 1-cm stubble (kg/m) (see fallow transport in Figure 42); ΔSUB is the change in sublimation rate per metre width perpendicular to the wind from a 1-km fetch *for each centimetre change in stubble height* (kg/cmm), and SUB(1,1) is the annual sublimation rate per metre width perpendicular to the wind from a 1-km fetch of 1-cm stubble (kg/m)(see fallow sublimation in Figure 44).

Fetch Distance

Snow Transport Rate - Stubble

Variations in the mean annual snow transport (saltation + suspension) with fetch distance on stubble at Prince Albert, Regina, Swift Current and Yorkton are shown in Figure 48a. For fetches greater than 300 m, the data show snow transport on stubble at Prince Albert and Yorkton remains reasonably constant between 9,000 and 10,000 kg/m, independent of fetch distance. At Regina and Swift Current, the flux decreases slowly with increasing fetch at distances greater than ≈1 km. These trends are due to sublimation becoming the dominant process governing transport for most combinations of wind speed, temperature and relative humidity.

For practical computations the 1-km snow transport flux *on stubble* can be used as an estimate for fetches ranging from 300 m to 4 km in length.

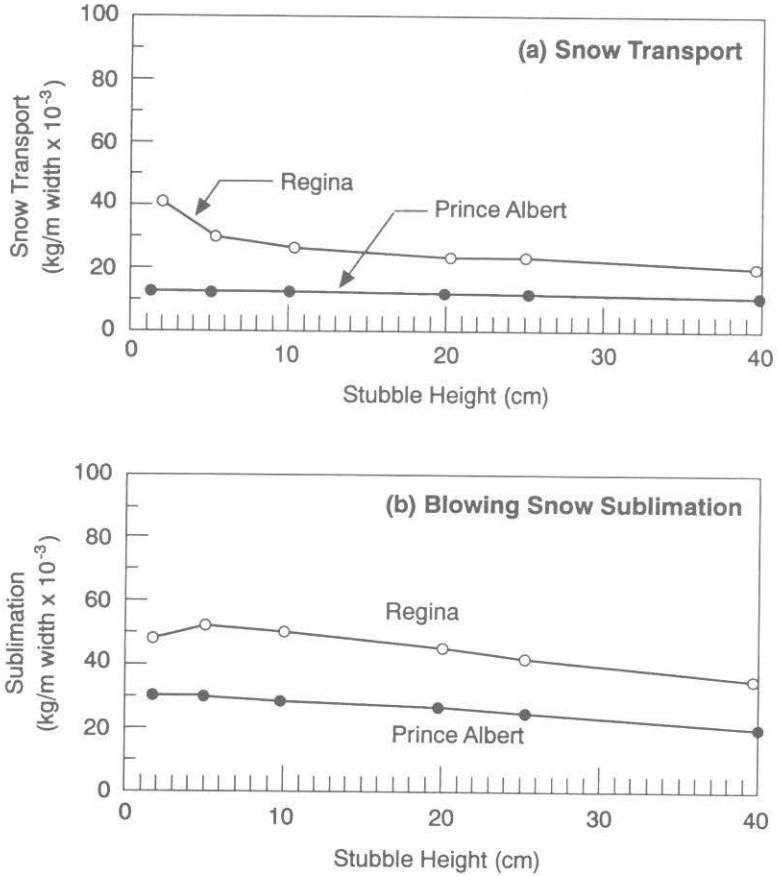

Figure 47 *Variation in mean-annual 1-km blowing snow flux with stubble height from 1-km fetches at Regina and Prince Albert, Saskatchewan:* ***(a)*** *snow transport and* ***(b)*** *sublimation. Note: a flux of 1000 kg per metre width on a fetch of 1 km is equal to 1 mm of snow water over the fetch distance.*

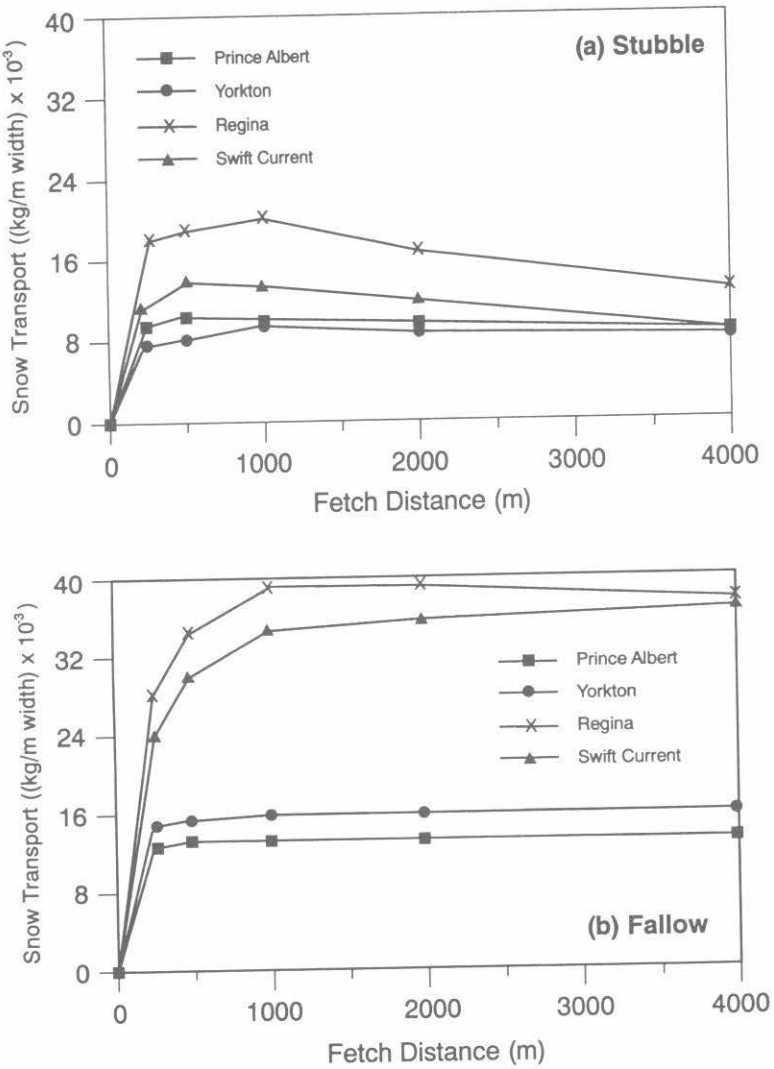

Figure 48 *Variation in mean annual snow transport with fetch distance at four stations in Saskatchewan, 1970-76:* ***(a)*** *stubble (25 cm) and* ***(b)*** *fallow. Note: a flux of 1000 kg per metre width on a fetch of 1 km is equal to 1 mm of snow water over the fetch distance.*

Snow Transport Rate - Fallow

The variation in mean annual snow transport (saltation + suspension) with fetch distance on fallow land at Prince Albert, Regina, Swift Current and Yorkton are shown in Figure 48b. At Regina and Swift Current on fetches ranging from 300 m to 1 km in length, snow transport increases appreciably with increasing fetch distance. At Regina, the maximum rate occurs at 1 km, whereas at Swift Current it is not reached in 4 km. The rapid increase in transport rate with distance on fetches between 300 m and 1 km at these stations is attributed to the combined effects on transport of high winds and the lack of snowcover to satisfy steady-state conditions. Because the requirements for fully-developed flow are given priority by the model, if there is not an adequate supply of snow available on the first three elements to satisfy steady-state requirements for saltation and suspension, elements are added. The probability of achieving steady flow increases with increasing fetch.

As a rule, the 1-km data can be used as practical estimates of snow transport rates on fallow for fetch distances between 300 m and 4 km. The locations where they do not apply are those where the annual 1-km flux on fallow exceeds 20,000 kg/m (e.g., Regina, Swift Current and Dauphin). For these locations, and for fetches with lengths 0.3 km $\leq$ FD $\leq$ 1 km, the annual snow transport can be estimated as:

$$\mathrm{TRAN}(1,\mathrm{FD}) = 4600(1-\mathrm{FD}) + [(0.58+0.42\mathrm{FD})\mathrm{TRAN}(1,1)], \quad (65)$$

in which TRAN(1,FD) is the snow transport in kg/m perpendicular to the wind from a field with fetch distance, FD, and TRAN(1,1) is the transport flux in kg/m perpendicular to the wind from a 1-km fetch (see Figure 42).

Sublimation Rate

The sublimation rate on stubble and fallow surfaces increases monotonically with fetch distance (Figure 49). At Regina, over a distance of 4 km the mean annual value is about 254,000 kg/m (~64 mm water equivalent). In contrast, the loss over the same distance at Yorkton is only 112,000 kg/m (~28 mm water equivalent). The higher sublimation rates at Regina and Swift Current are due primarily to the extremes of winds at these stations. Each year, several high winds usually occur that scour snow from previously-filled vegetation and produce large sublimation losses from this snow due to high particle ventilation rates. As a consequence, winds following these events that would normally cause saltation, do not, because of the increased surface roughness produced by scouring.

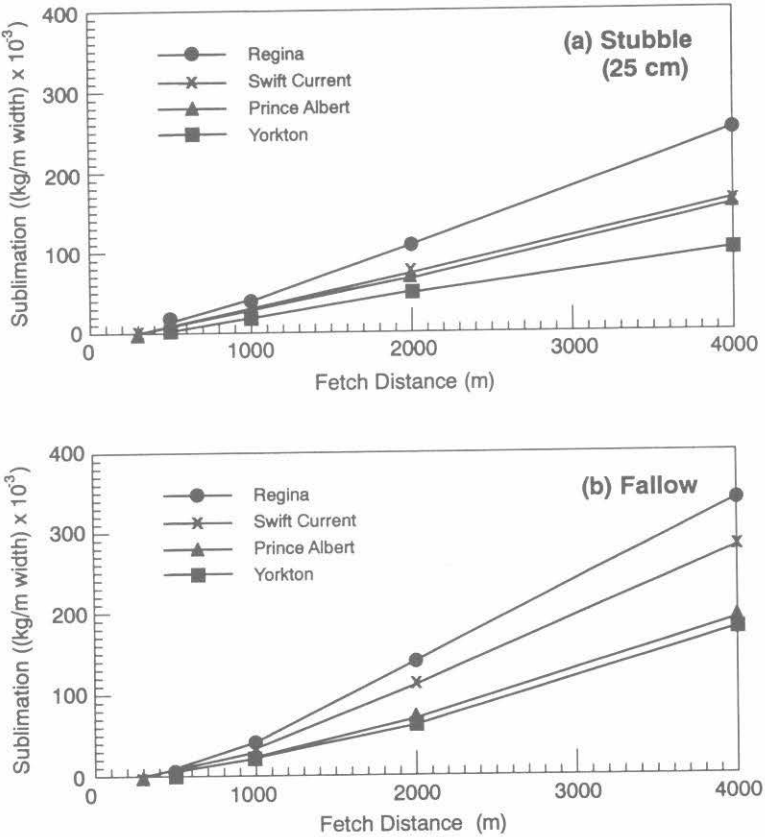

Figure 49 *Variation in mean annual sublimation with fetch distance at four stations in Saskatchewan, 1970-76:* ***(a)*** *stubble and* ***(b)*** *fallow. Note: a flux of 1000 kg per metre width on a fetch of 1 km is equal to 1 mm of snow water over the fetch distance.*

The variation in sublimation rates on stubble and fallow surfaces with fetch distance can be approximated from the 1-km rate by:

$$SUB(h,FD) = SUB(h,1)[-0.457 + 1.37FD + 0.125FD^2], \quad (66)$$

in which SUB(h,FD) is the sublimation rate in kg/m perpendicular to the wind from a field with a height of stubble, h, and fetch distance, FD, and Sub(h,1) is the sublimation loss in kg/m perpendicular to the wind from a 1-km fetch with stubble height, h.

Application of Fetch Relationships to Determine Disposition of Eroded Snow

The variations in mean annual snow transport and sublimation with roughness and fetch length can be used to assess the relative disposition of eroded snow as either snow that blows to the field edge (transport) or snow that sublimates in transit (sublimation). Transport (kg/m) and sublimation (kg/m) may be expressed as an average equivalent depth of water over a fetch by dividing the respective quantity by the product of the fetch length (m) and a reference density for ice (1000 kg/m^3). Figure 50 plots these values for various fetches and land uses at Prince Albert and Regina. Snowcover erosion contributing to snow transport off a fetch dominates for fetches up to about 600-1000 m in length. This dominance is prominent in the zone of developing flow that generally occupies the first 300 m of fetch. Snow lost to transport in this zone (0-300 m) is much greater at Regina than at Prince Albert: for example, on fallow, 85% of annual snowfall compared to 38% of annual snowfall. At Regina, a cover of 25-cm stubble produces a greater reduction in transport, relative to total snowfall than at Prince Albert. These differences are attributed to stronger winds at Regina.

For fetches longer than 600-1000 m, the amount of erosion contributing snow for sublimation increases and controls the depletion of snowcover. Sublimation losses equal to 74% of annual snowfall occur from a 4000-m fetch of fallow at Regina, whereas Prince Albert experiences only a 44% loss for this land use and fetch distance. The higher sublimation losses at Regina are associated with the larger transport losses caused by the extremes of wind speed at that location.

At all stations used in the study, total snowcover erosion that contributes to transport and sublimation does not change appreciably from the 1000-m fetch values for fetches from 500 to 4000 m. The implication of the transition from snow erosion contributing primarily to transport on fetches less than 1000 m to snow erosion contributing primarily to sublimation on longer fetches is most striking at larger scales rather than the small scale of the fetch itself. Snow eroded and transported from a fetch is available

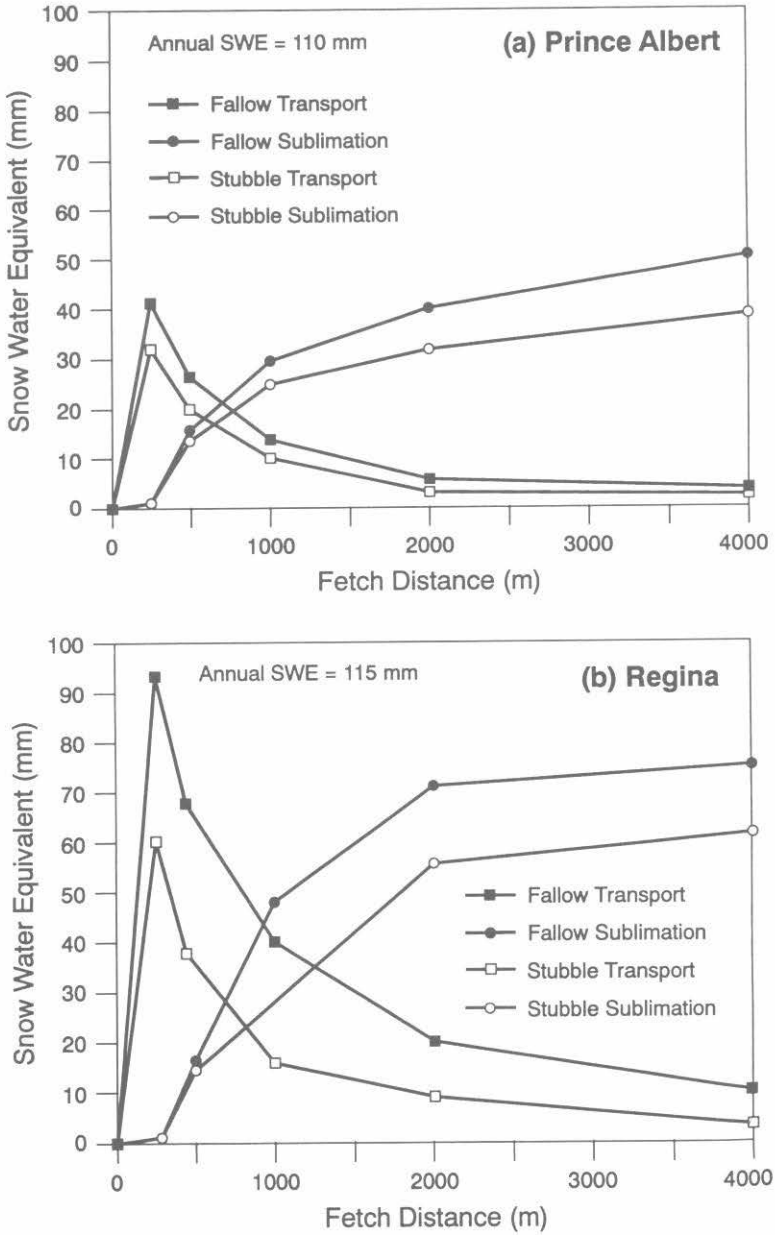

Figure 50 *Variation in mean annual snow transport and mean annual sublimation on stubble and fallow, expressed as the average depth of water on a fetch, with fetch distance, 1970-76;* ***(a)*** *Prince Albert and* ***(b)*** *Regina, Saskatchewan.*

for trapping by bushes, hedges, snowfences, woodlands and topographic depressions and serves as a source of water for recharging surface and soil water supplies. Snow eroded and then sublimated is removed from surficial water supplies, even at very large scales.

6.4 Mean Monthly Fluxes

The Prairie Blowing Snow Model is a complex computer model that requires large amounts of data. For practical applications, empirical expressions relating mean monthly transport and sublimation modelled by PBSM to mean monthly climatic data were derived by trial and error. At AES stations, temperature and relative humidity are measured at a 2-m height, wind speed and direction are measured at a 10-m height, snowfall water equivalent is measured by a Nipher precipitation gauge, and snowcover depth is measured with a ruler.

The best-fit regression equations for monthly snow transport (saltation and suspension), $TRAN_m(h,1)$ and sublimation, $SUB_m(h,1)$ expressed as an average depth of snow water (mm) over a 1-km fetch, 1 m in width, are:

Stubble

$$TRAN_m(25,1) = -8.26 + 0.89u_{10} + 5.70\exp[-10(T_{max} + 20)] + 0.041RH_{max} + 3.32\exp[\frac{-8.72}{d}]. \quad (67)$$

correlation coefficient, r = 0.83,
mean difference (PBSM -regression), $\Delta = -1.4 * 10^{-7}$ mm, and
standard deviation of difference, $s_\Delta = 1.13$ mm.

$$SUB_m(25,1) = -6.93 + 1.85u_{10} - 0.17T_{min} - 0.074RH_{min} + 0.010P_m + 5.22\exp[\frac{-6.12}{d}]. \quad (68)$$

r = 0.83, $\Delta = -4.2 * 10^{-7}$ mm, and $s_\Delta = 1.75$ mm.

Fallow

$$\mathrm{TRAN}_m(1,1) = 14.33 + 2.26u_{10} - 0.25T_{\max} + 0.046RH_{\max} + 0.079P_m \cdot \quad (69)$$

r = 0.90, $\Delta = 4.7 * 10^{-7}$ mm, and $s_\Delta = 1.19$ mm.

$$\mathrm{SUB}_m(1,1) = 7.21 + 1.76u_{10} - 0.16T_{\max} - 0.18RH_{\max} + 0.19P_m \cdot \quad (70)$$

r = 0.80; $\Delta = 2.9 * 10^{-8}$ mm, and $s_\Delta = 1.94$ mm.

In Equations 67 to 70:

u_{10} = mean monthly wind speed at 10 m height, (m/s),

T_{max} = monthly mean of daily maximum air temperature, (°C),

T_{min} = monthly mean of daily minimum air temperature, (°C),

RH_{max} = monthly mean of daily maximum relative humidity (%),

RH_{min} = monthly mean of daily minimum relative humidity (%),

P_m = mean monthly snowfall (mm snow water equivalent) which must be greater than 0, and

d = mean monthly depth of snowcover (mm snow water equivalent), which must be greater than 0.

The effects on monthly snow transport and sublimation of the variables used in the regressions are discussed briefly below.

Wind speed

The models assume a linear increase in blowing snow fluxes with increasing wind speed.

Temperature

Mean monthly snow transport and sublimation increase with decreasing mean monthly minimum or maximum temperature (below 0°C). Regarding sublimation, this trend is the opposite to the effect of temperature on the sublimation rate for an ice sphere. One plausible explanation for this difference is demonstrated in the data in Figure 51 that

plots mean monthly temperature against monthly hours of blowing snow at Regina and Prince Albert. Both stations show the variables are inversely related during the winter months: that is, a larger number of hours of blowing snow occur during months with low temperatures. Low air temperatures result in snowcovers with low cohesion and low transport thresholds. The increase in frequency of blowing snow events more than compensates the lowering of the sublimation rate due to a decrease in temperature.

The effect of decreasing air temperature on snow transport is most important at low wind speeds. For a mean monthly wind speed of 5 m/s, transport quadruples as the monthly mean of daily maximum air temperature drops from -2 to -25 °C.

Mean monthly snow transport on stubble displays a strong temperature dependence due to the effect of mid-season melts in re-exposing buried vegetation. The frequency of these melts increases as temperature increases and transport increases dramatically as monthly mean daily maximum temperature drops below -10 °C.

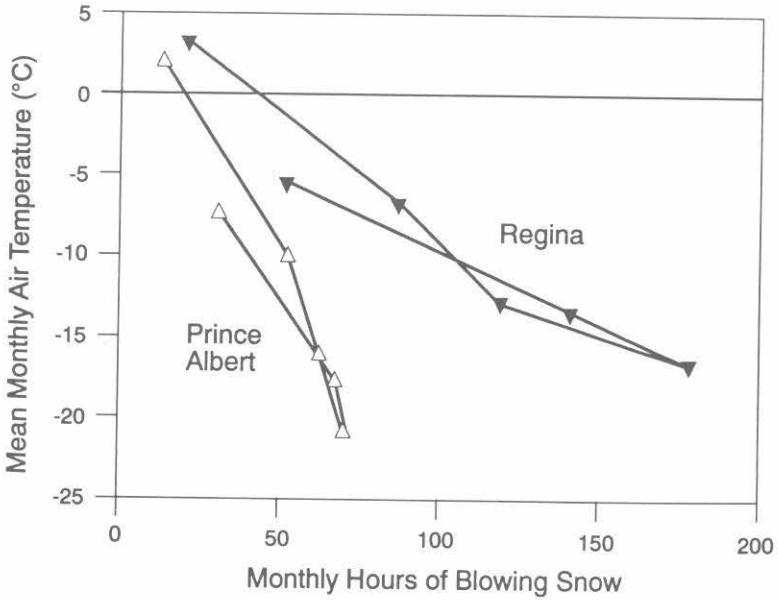

Figure 51 *Monthly variation in mean monthly temperature during blowing snow events and number of hours of blowing snow at Regina and Prince Albert, Saskatchewan during winter season.*

Relative Humidity

There is a slight increase in snow transport on both stubble and fallow land with increasing relative humidity. This trend is presumed due to higher humidities that suppress sublimation, leaving more snow available for transport.

Snowfall and Snow depth

On stubble land the mean monthly snow transport and sublimation rates increase exponentially with increasing depth of snow on the ground. The largest increases occur when the snowcover water equivalent is less than 30 mm because stalks of vegetation are exposed to the wind. At greater depths of snowcover the vegetation is inundated and snow transport will be similar to that on a field of fallow. On fallow land, the transport and sublimation fluxes increase with increasing mean monthly snowfall. Sublimation rate exhibits the greatest increase per unit increase in snowfall.

Chapter 7

SNOW MANAGEMENT AND CONTROL PRACTICES

7.1 Forest Management Practices

Snow supply in forest lands is important not only as a source of local soil moisture after melt but in its contribution to stream flow in North America. Goodell (1966) estimated that 90% of the runoff from above 2740 m elevation in the Colorado Rockies is derived from snow. Over 70% of the streamflow in major rivers (Saskatchewan, Missouri) draining the western North American mountains and plains originates in forests that consist largely of conifers. Much of this water is used for municipal and irrigation supplies in the more arid prairies and deserts surrounding the forested uplands. Strong demand for runoff from forested mountain watersheds in the arid West has led to many decades of research on coniferous forest management techniques to increase snow accumulation and meltwater runoff from these areas. Knowledge of the effect of forest management on snow accumulation is useful in directing forest logging operations, either to increase snow accumulation or to mitigate the changes in basin snow accumulation that occur after logging. This knowledge is particularly necessary in anticipating downstream changes in discharge regime.

Alexander *et al.* (1985) and Meiman (1987) reviewed the results of fifty years of research conducted in watersheds of pine, fir and spruce in the Fraser Experimental Forest, located in the Rocky Mountains, 120 km west of Denver, Colorado. The coniferous forest management techniques tested at this research facility are the same as those used to increase snow

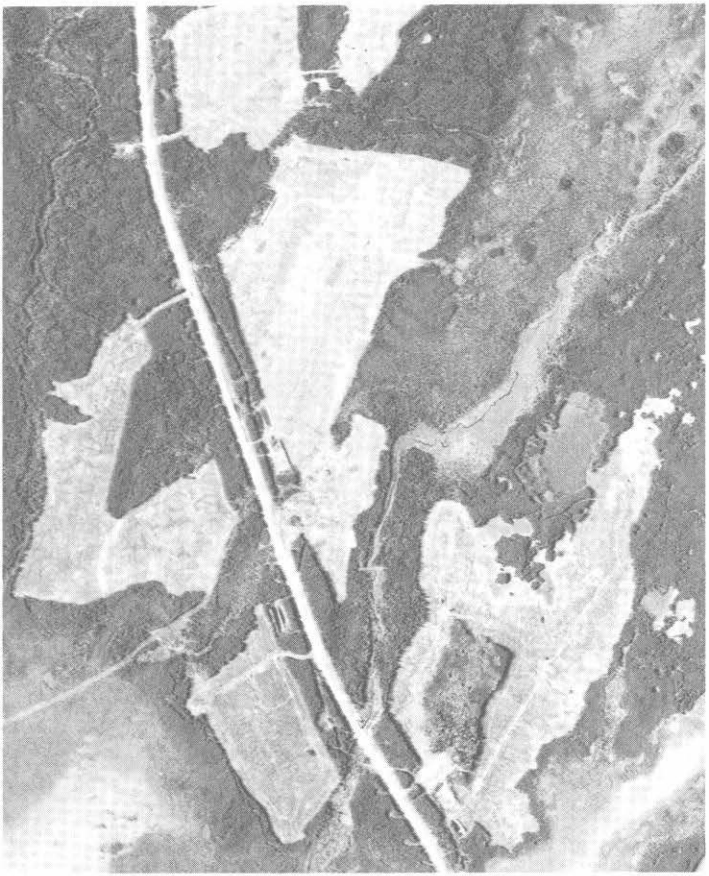

Figure 52 *Forest cut-blocks, from aerial photographs near Montreal Lake, Saskatchewan.*

accumulation in the United States (especially Colorado, Wyoming) and in Canada (especially Alberta). They are:

1. Cut-blocks - roughly square areas of forest are clear-cut in an alternating, "chequer-board" pattern, (see Figure 52)
2. Alternate strip clear-cutting - strips of forest 20-m to 120-m wide are clear-cut with uncut or slightly-thinned strips in between
3. Group selection cutting - irregular to circular 20-m to 120-m diameter openings are cut in the forest, and
4. Individual tree selection (thinning) -uniform removal of trees.

The first three techniques involve clear-cutting and typically result in the removal of 60% of the timber volume, about 50% from the clear cuts themselves and an additional 10% from thinning of the larger trees from the uncut areas. The individual tree selection technique can preserve some of the original forest structure; from 50% to 85% of timber volume is removed. Alexander *et al.*(1985) summarize that for a selected volume of spruce-timber removed, roughly the same increase in snow water equivalent occurs for alternate strip clear-cutting and group selection cutting. They reported 60% removal of timber volume resulted in a 20-23% increase in snow water equivalent. The increase in snow water equivalent with tree removal is not as pronounced for pine forests. Fifty-three percent removal by group selection cutting resulted in only a 16.8% increase in water equivalent and 85% removal by thinning lead to a 23% increase. The last is roughly equivalent to the increase experienced by 60% thinning of a spruce forest.

Troendle (1987) suggests a linear approximation between the percentage basal area of conifers removed and percentage increase in peak snow water equivalent using the results of forest management experiments in Colorado (see Figure 53). The relationship predicts a maximum increase in snow water equivalent of 35% for the complete removal of conifers, and has the form,

$$\Delta SWE = 34.3 - 0.038\ \Delta A_C\,, \qquad (71)$$

where ΔSWE represents the percent increase in snowcover water equivalent (%) and ΔA_c is the percent basal area of conifers removed (%).

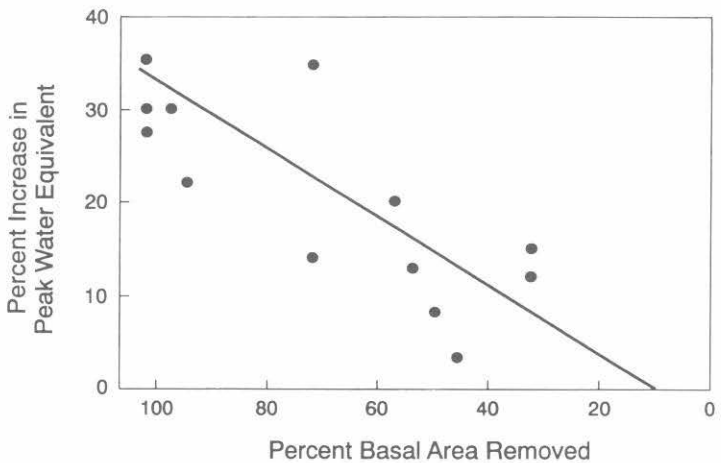

Figure 53 *Effect of forest cutting on snow accumulation. Increase in peak water equivalent with basal area removed (after Troendle, 1987).*

The size of a forest clearing affects the change in snow water equivalent. Figure 54 shows transects of snow water equivalent in alternate forested and clear-cut strips (Alexander *et al.*, 1985). More snow accumulates in cut strips than the uncut forest. Snow distribution patterns in both cut and uncut strips are irregular and vary with the width of the strip. For 20-m wide clear-cuts, the maximum water accumulations occur near the centre of 20-m wide strip whereas for the forested strips they occur near the edges. For 120-m wide strips, the maxima for both clear-cuts and forest are at the edges with minima in the centres. On the basis of measurements in Colorado, Troendle (1983) recommends an optimal diameter of a forest clearing for snow accumulation equal to 5 times the tree height, H. Openings larger than 15H retained lower snow accumulations than adjacent forest. Larger openings contain less snow because wind removes and sublimates snow. Toews and Gluns (1986) found no reduction in ΔSWE with clearing size for interior British Columbia clear-cuts up to 21H. Cleared areas showed an increase of 37% in snow water equivalent. The relatively moist and low-wind-speed environment of interior British Columbia probably accounts for the lack of significant wind transport from large clear-cuts in their study. Troendle and Meiman (1984) report that by leaving "non-commercial" trees and logging "slash" to increase surface roughness, snow can be effectively retained in large clear-cuts until the snow accumulation has buried the slash.

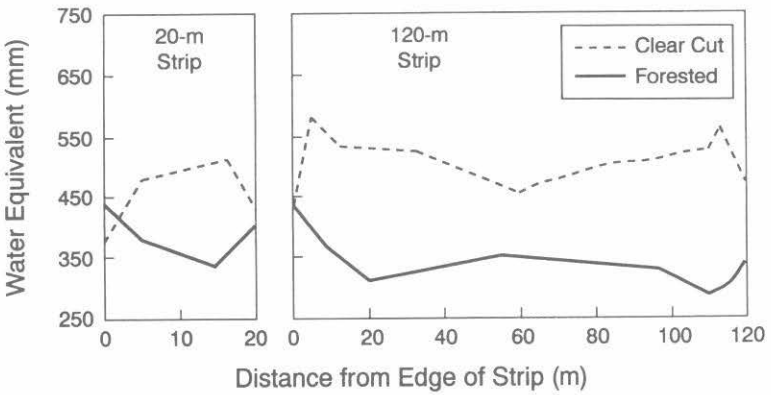

Figure 54 *Transects of snow water equivalent monitored in alternate forested and clear-cut strips.*

7.2 Stubble Management and Vegetative Practices

The importance of water to the production of crops in drought-prone, semi-arid and sub-humid regions of western Canada is well-known. The Saskatchewan Advisory Council on Soils and Agronomy (1982) recommends that root-zone water reserves of 125 mm and 100 mm are needed in the brown and dark brown soil zones of the Province at the time of seeding to achieve average yields of cereal grains. This recommendation is based on the expectation of normal (between 175 and 195 mm), or near normal, rainfall during the crop growing season. When combined with the recommended reserves, these data suggest that the amount of water required for an average crop is of the order of 300 mm.

Staple and Lehane (1954) suggest water additions above specific base levels increase yields by varying amounts. For example, each additional 25 mm of water to a moisture reserve of 252 mm, up to a maximum of 412 mm, increases the yield of spring wheat by 230 to 400 kg/ha. Similarly, de Jong and Rennie (1969) report increases in the yield of spring wheat in the sub-humid, east-central region of Saskatchewan of between 200 and 275 kg/ha for each additional 25 mm of water above the long-term normal precipitation. These findings and the results of other research illustrate the variable nature of the interaction between the yield of spring wheat and added water in dryland areas (usually between 38 and 406 kg/ha per 25 mm) depending on year, location, soil, and other factors. Nevertheless, because the yield-water relationship is positive, producers are always searching for better and more efficient water conservation practices to increase the amount of water available for crop growth.

The average annual precipitation received throughout much of the prairie region ranges from 300 to 380 mm. Of this total, the relative amounts occurring as snow and rain vary widely from year to year. On average, about 39% occurs as snow. Since snow is manageable, there is considerable interest in its potential for increasing soil water reserves, although the exact role of snow as a water resource for agricultural production is not well-understood. The basic principle employed by a snow management practice involves increasing the roughness of the land surface to trap blowing snow. Three commonly-used practices are:

(a) **windbreaks** of tall, woody (caragana, ash, maple or other trees) or non-woody (sudan grass, tall wheatgrass, uncut strips of grain) within cultivated areas,

(b) **stubble management practices,** for example, tall stubble, alternate height stubble, and trap strips, and

(c) **snow ridges.** These measures also reduce sublimation and soil erosion losses.

Where the primary objective is to obtain a uniform snowcover over a field, the optimum spacing of barriers will likely be determined by economics. Tabler and Schmidt (1986) recommend a spacing for hedgerows, grass barriers and shelterbelts of about 10 - 15H on level terrain. H is the height of the obstacle. Spacings of 20H have proven beneficial for wheat production on the Prairies.

Stubble management practices for snow trapping are popular on the Canadian Prairies because they are easily applied to cereal grains, use existing harvesting equipment, and create snow-barriers that are non-competitive with the cultivated crop (in terms of water consumption). They have also been adopted in the U.S. Great Plains (Black and Siddoway, 1971) and the northern steppes of Europe and Asia (Petropavlovskaya and Kalyuzhny, 1986)

Tall Stubble

The term tall stubble is used in a "relative" sense to describe the condition where a crop is cut to leave a field with a "high" stubble. Normally, this practice is followed when the crop is straight-combined. The actual height of a "tall" stubble usually falls in the range of 30 to 70 cm, but will vary with the type, density and height of crop.

The stubble of most cereal crops is usually sufficiently dense to retain snow to a depth nearly equal to the stubble height. Thus, a cropped field downwind of an adequate fetch of snow will tend to fill from trapping of

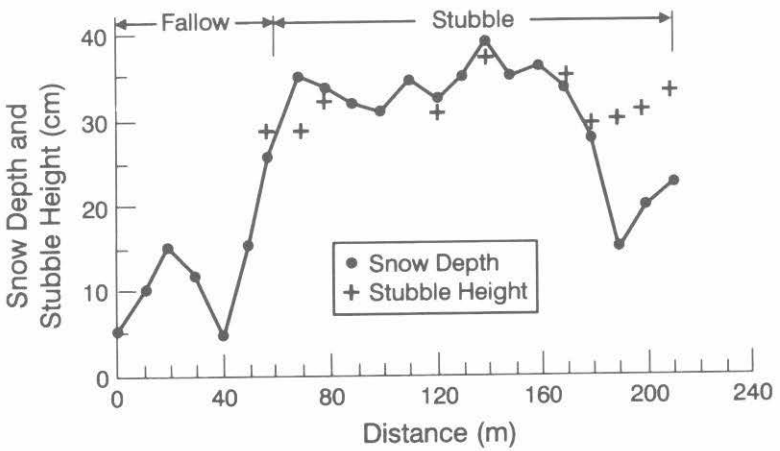

Figure 55 *Snowcover accumulation in adjacent fallow and stubble fields, Richlea, Saskatchewan, 1983.*

wind-transported snow. The "filling process" is relatively orderly, especially when winds are predominately from one direction. Figure 55 shows a typical snow accumulation pattern on flat terrain due to a change in land use from fallow to canary grass stubble. The data show: (a) less snow on fallow than on stubble - snow having been eroded from the fallow and deposited in the stubble; (b) a depth of snow downwind of the leading edge of stubble approximately equal to the height of vegetation; and (c) a sharp decrease in snow depth (from about 29 cm to 17 cm) at the leading edge of the advancing front of "trapped" snow (~180 m). Before melting starts, average densities for a prairie snowcover typically range between 225 and 325 kg/m^3 on fallow and between 175 and 275 kg/m^3 on uniform - height stubble.

Raupach *et al.* (1993) studied the effect of roughness elements on the wind erosion threshold and adopted the roughness density, λ, defined by:

$$\lambda = \frac{nbh}{S}, \tag{72}$$

where: n = number of roughness elements (stalks),

b = mean width of stalk,

h = mean height of stalk above the surface, and

S = ground area occupied by the n roughness elements.

λ can be assumed to be directly related to the mass of residue per unit surface area with a proportionality coefficient dependent on the stubble height. Based on trials conducted on cylinders and hemispheres, Raupach *et al.* found that when λ was greater than 0.03, the ratio of the shear stress imparted to the non-erodible surface elements to the atmospheric shear stress imparted to the surface, $\tau_n/\tau \approx 1$. Thus, an approximation of the maximum mean depth of snow $\overline{d_s}$ retained by a uniform tall stubble is:

$$\overline{d_s} = H - 0.03\frac{A_s}{S_d}, \tag{73}$$

where: H = height of the stubble above ground,

A_s = average ground surface area occupied by each plant, and

S_d = stalk diameter or width of plant.

Alternate-Height Stubble

This practice involves harvesting a crop to leave bands of stubble of alternate height within a field. The height of cut of the swather is changed on each round of the field to produce a series of bands, each the width of the swather, of "low" (15 cm to 30 cm) and "high" (30 cm to 60 cm) stubble. Figure 56 shows the snow accumulation pattern under this practice in which snow has filled the vegetation. Additional drifting would lead to increased accumulation on the low stubble. The average density of the snow in the "low" stubble was 207 kg/m^3 and in the "tall" stubble it was 248 kg/m^3. The bands of "tall" stubble would result in an estimated increase of about 30 mm of snow water over that obtained had the field been harvested at a uniform low height.

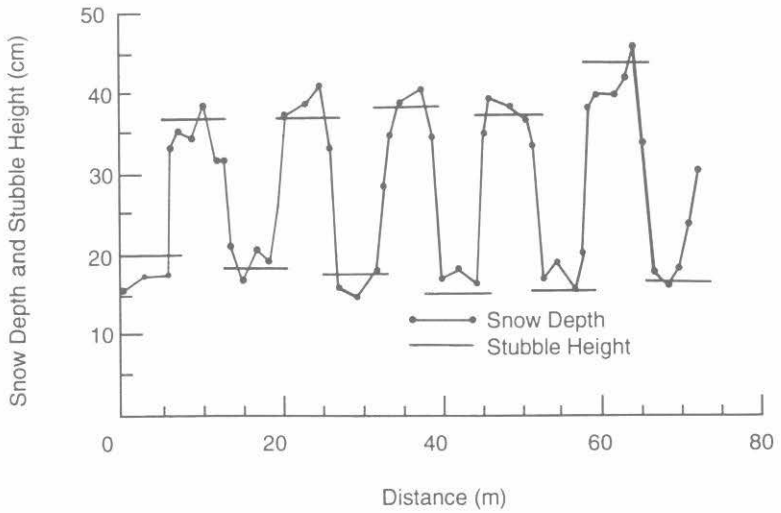

Figure 56 *Snowcover accumulation pattern on a wheat-field cut with alternate-height stubble management practice, Eston, Saskatchewan.*

Trap Strips

This harvesting practice, also referred to as deflector strips, involves leaving narrow strips of tall stubble in a field. These strips, usually 40 to 60 cm wide, are made by attaching a deflector unit (usually Vee-shaped) to a swather or to the header of a combine. As the swather travels through the crop, the deflector separates and bends the stems of the crop sideways where they are cut to form a strip of stubble having the shape of an inverted "V" that is 250-350 mm higher than the adjacent stubble. Figure 57 shows larger accumulations of snow in a field with trap strips than in an adjacent field of "tall" stubble. The data also show the effects on snow accumulation of reducing the width and spacing of strips by one-half. The accumulations in the strips on the wide spacing exhibit an undulating pattern because of scour and erosion of snow from between the strips. On the area of the field having the narrower strips, the depth of snowcover is more uniform and deeper: the average increase in depth being about 5 cm. Table 6 compares the effects of various stubble management practices and grass barriers on snow accumulation in Saskatchewan.

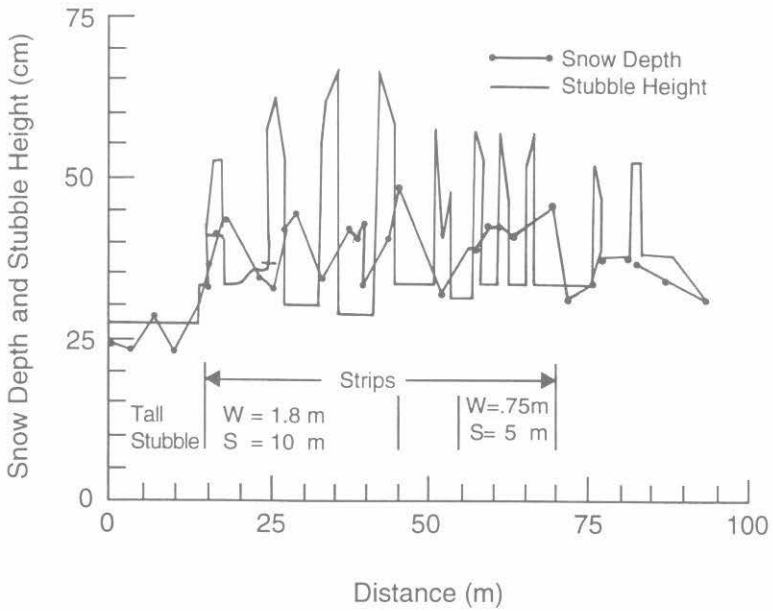

Figure 57 *Snowcover accumulation patterns on a wheat-field cut with "hi-low" stubble management practice at Saskatoon, Saskatchewan, 1983. W = width of the deflector strip; S = distance between strips.*

Table 6 *Field comparisons of the effects of various stubble management practices and grass barriers on snow accumulation in Saskatchewan.*

Location	Years	Treatment	Snow Water (mm)		% Snowfall Trapped[a]	
			Range	Mean	Range	Mean
Central	1980-84	Tall Stubble	48-86	66		
		Control[b]	26-71	50		
Central and Western	1980-84	Trap Strips[c]	32-99	61		
		Control	20-99	50		
Swift Current	1972-85	Alternate Height	16-119	62	21-113	66
		Control	13-77	47	17-82	51
Swift Current	1979-85	Barriers[d]	27-129	77	45-129	94
		Control	16-66	35	24-66	43

[a] % Snowfall Trapped = % of total snowfall water equivalent monitored with a Nipher gauge.

[b] Control = accumulation monitored in an adjacent area of uniform-height stubble.

[c] Trap Strips = deflector strips.

[d] Barrier = tall wheatgrass.

Sparse Vegetation and Objects

For sparse vegetation and objects whose exposed silhouettes provide a rectangular profile and a drag coefficient similar to cylinders (for example, crested wheatgrass, sagebrush, corn stalks), Tabler and Schmidt (1986) suggest the mean snow depth at the time of peak accumulation, $\overline{d_s}$, can be estimated as:

$$\overline{d_s} = H - 0.01\frac{A_s}{S_d}, \tag{74}$$

where: H = height of the element above ground,
A_s = average ground surface area occupied by each element, and
S_d = stalk diameter or width of plant.

The coefficient, 0.01, is lower than the 0.03 recommended from Raupach *et al.'s* (1993) theory (Equation 73) because sparse objects induce flow separation and scouring in addition and in opposition of effect to the reduced atmospheric shear stress on the surface.

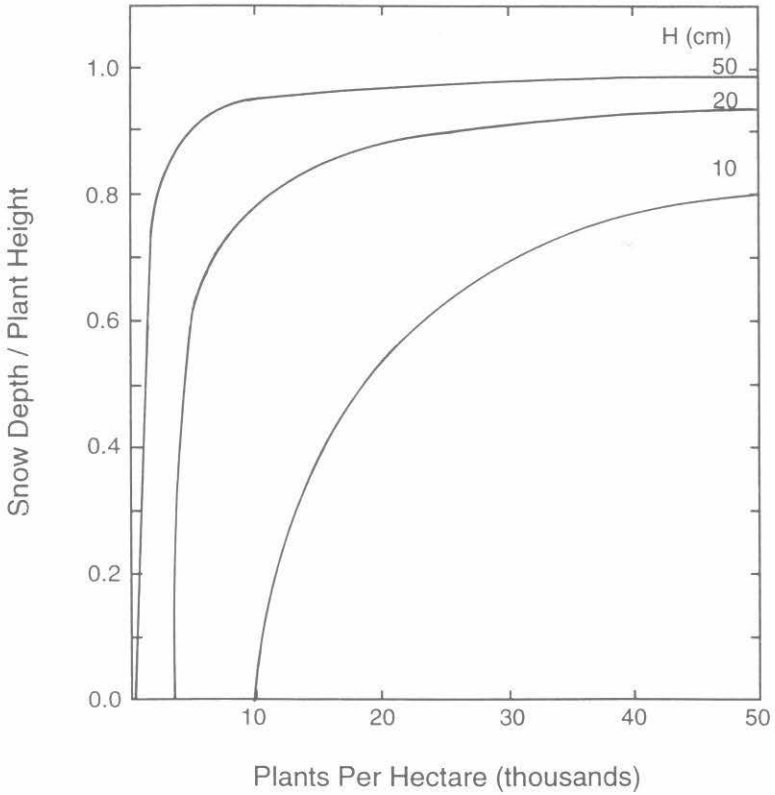

Figure 58 *The ratio of snow depth to plant height as a function of plant density in wind-swept Wyoming sagebrush rangelands (after Tabler and Schmidt, 1986).*

In Figure 58, Equation 74, presuming typical Wyoming sagebrush plant dimensions and placement, is used to show the ratio of retained snow depth to plant height as a function of the density of sagebrush plants that are found in the pastures of Wyoming, USA. It is evident from those data that short plants (10 cm high) fill in much less effectively than do tall plants (50 cm high).

Snow Ridging

Snow ridging is the practice of constructing a series of parallel ridges of snow in a field to trap snow. The trapping action of a ridge is similar to that of a solid fence. The total length of the drift formed on level terrain is of the order of 20H, which is equally divided between the windward and leeward sides. Ridges placed at a spacing of approximately 10H should provide a reasonably uniform depth of snow between ridges having a volume of about $10H^2$ per unit length of ridge. Practical aspects of snow ridging that limit its use are densification of ridges over time and mid-winter melts that reduce their size and collection capacity.

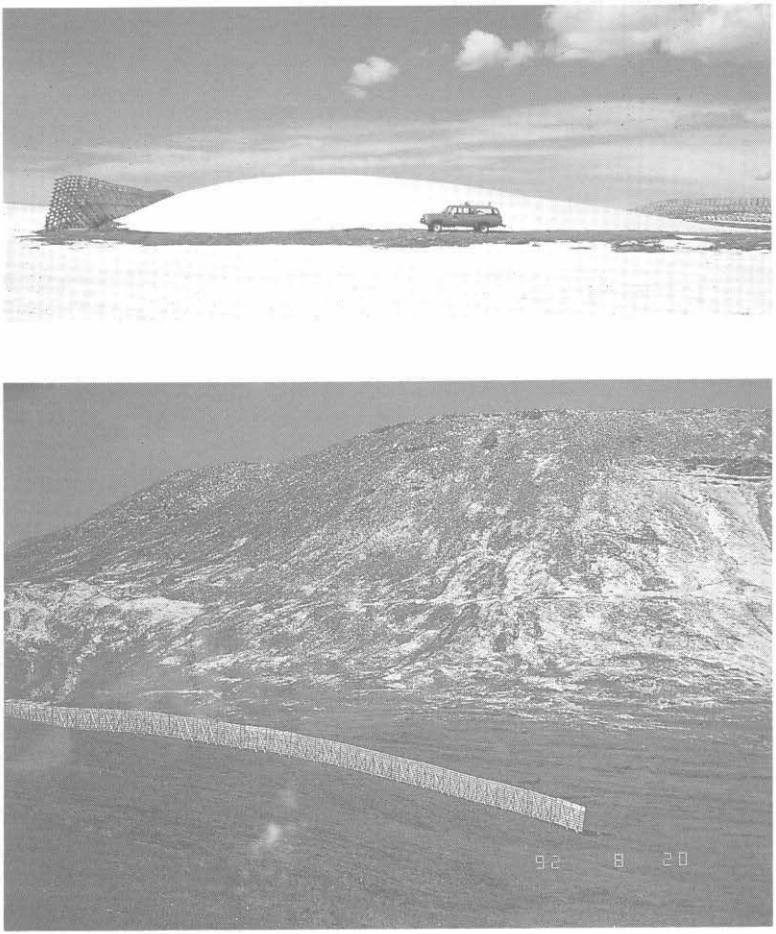

Figure 59 *(**a**) A snow drift near Laramie, Wyoming, photograph by R.D. Tabler. (**b**) A "Wyoming-style" snow fence along the Demptster Highway in the Richardson Mountains, N.W.T.*

7.3 Topographic and Mechanical Barriers

Topographic

Tabler and Schmidt (1986) show that the profile of snowdrifts formed by topographic features can be estimated from the empirical equation:

$$S_s = 0.25x_1 + 0.55x_2 + 0.15x_3 + 0.05x_4 \ , \qquad (75)$$

where S_s is the snow slope (%) over the main portion of the drift, x_1 is the average ground slope (%) over a distance of 45 m upwind of the feature causing deposition, and x_2, x_3 and x_4 are the average ground slopes (%) over distances of 0-15 m, 15-30 m and 30-45 m downwind. When applying Equation 75, if x_2, x_3 or x_4 is less than -20, then set x_2, x_3 or x_4 to -20. Slopes upward in the direction of the wind are taken as positive, and downward slopes are negative.

Snow Fences and Shelterbelts

Snow fences and shelterbelts are often used to prevent the formation of snow drifts on roads and around buildings and to enhance drift formation as a local water source. An equilibrium snow drift is one whose shape minimizes the combined wind resistance of drift and snow fence and creates a relatively uniform surface shear stress over the drift snow surface. The size and shape of equilibrium drifts are quite distinctive and repeatable when wind directions are consistent as shown in the example near Laramie, Wyoming, USA in Figure 59a. Proper installation of such a fence in northern Canada is shown in Figure 59b.

Shelterbelts of conifers or deciduous trees can also form large equilibrium drifts as shown in Figure 60 of a conifer-induced drift near Loreburn, Saskatchewan and a carragana hedge drift near Bradwell, Saskatchewan. The depth and densities of snow that a shelterbelt can induce on agricultural land are shown in Figure 61. Depth increases 8-10 fold and density increases by one-third over adjacent stubble and fallow land, though the effects are limited to about 50 m in width.

The following discussion refers to principles that may be applied equally to snow fences or to shelterbelts, though only the term snow fence is used here. The equilibrium drift is approximately the largest snow drift that can be retained by a fence, if blowing snow supply is not limiting. The shape of the equilibrium drift behind these types of barriers depends primarily on the height, H, length, L, and the porosity, F, of the obstructing barrier. In general: (a) all drift dimensions are approximately proportional to the height of the barrier above the ambient snow depth, (b) all drift dimensions are reduced for fences with lengths less than 30H, (c) lee drifts behind

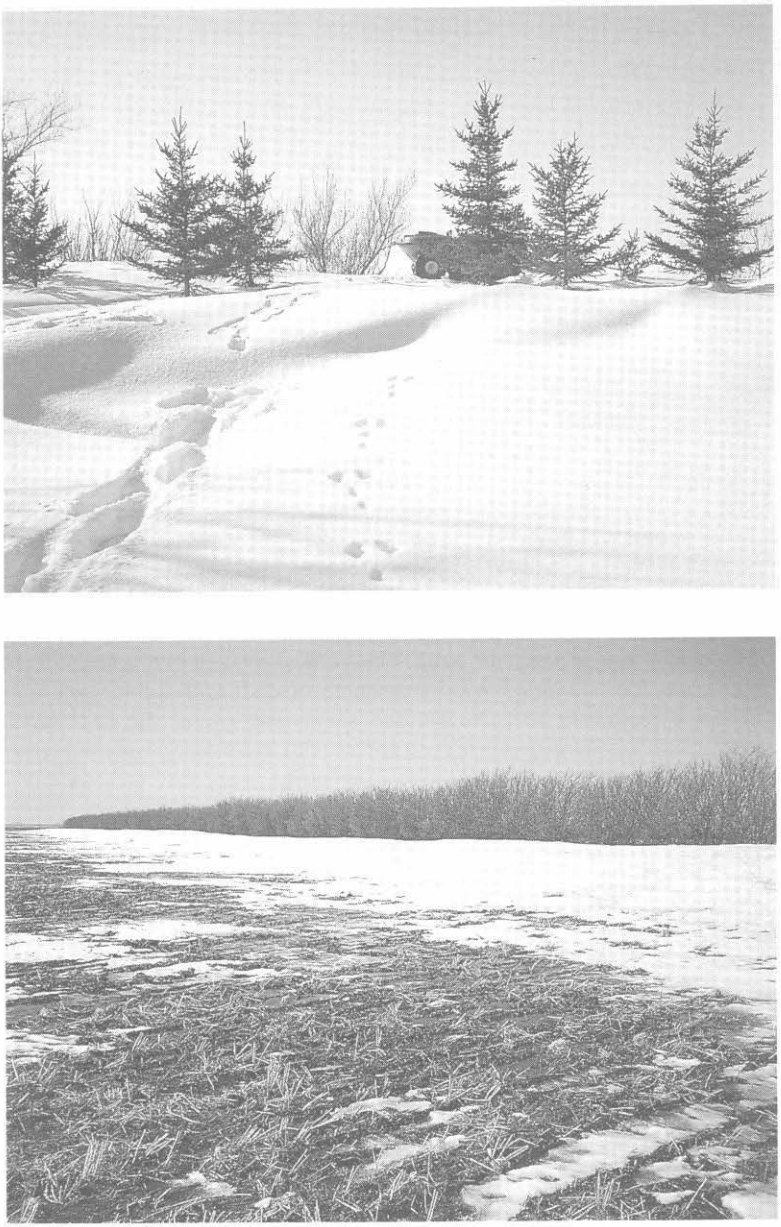

Figure 60 *Drifts formed by shelterbelts:* ***(a)*** *spruce row near Loreburn, Saskatchewan;* ***(b)*** *carragana hedgerow near Bradwell, Saskatchewan.*

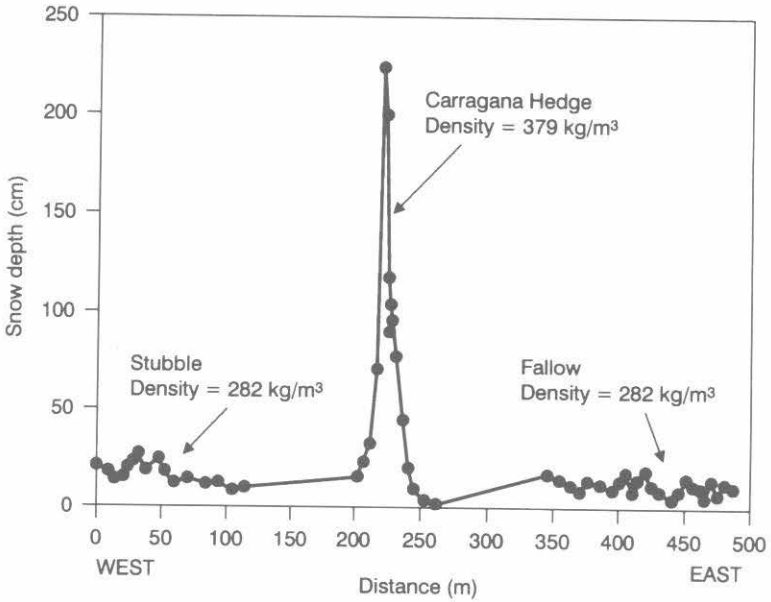

Figure 61 *Snow accumulation in an agricultural field near a carragana shelterbelt, noting changes in depth and density of snow. Near Saskatoon, Saskatchewan, 1989 (after Pomeroy et al., 1993).*

porous fences are more than twice as long as those behind solid barriers, and (d) drift depths decrease for porosities greater than about 50%.

Tabler and Schmidt (1986) and Tabler *et al.* (1990) describe the geometry of drifts formed by 50% porous snow fences on flat terrain that are oriented perpendicular to the wind and uninfluenced by the ends of the fence: that is, no closer to the ends than 12H. The dimensions are for sites where the wind direction during snow storms is relatively unvarying. They show that the windward drift, which forms as a result of deflection and reduction in the surface shear stress as flow approaches the barrier, is about 15H long and has a maximum depth of about 0.5H at the fence. Takeuchi (1989) suggests that the windward drift is composed primarily of saltating snow deposits; hence, its size is sensitive to upwind snowcover conditions. For a given wind regime, the size increases when hard, "high transport threshold" snow is upwind. For dry snow conditions, the windward drift has a longitudinal cross-sectional area of about $3.6H^2$. The windward drift contains about 15% as much snow as the drift on the lee side of the fence. This drift, the leeward drift, is about 35H long, with a maximum depth of about 1.2H at 6H from the fence and a longitudinal cross-sectional area of about $21.5H^2$. The shape of the lee drift is approximated by:

$$\frac{d_s}{H} = 0.43 + 0.303\frac{x}{H} - 0.0412\left(\frac{x}{H}\right)^2 + 0.002193\left(\frac{x}{H}\right)^3$$
$$-5.421 * 10^{-5}\left(\frac{x}{H}\right)^4 + 5.105 * 10^{-7}\left(\frac{x}{H}\right)^5, \quad (76)$$

where d_s is the snow depth at a distance x from the fence and (x/H)<34 (Tabler 1980a, Tabler *et al.*, 1990). The dimensions of equilibrium drifts formed behind 50% porous snow fences as described here are shown in Figure 62 (Tabler *et al.*, 1990).

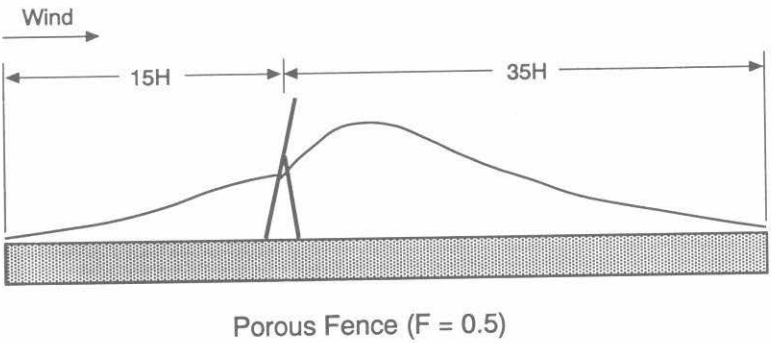

Figure 62 *Dimensions of equilibrium drift formed behind a 50% porous snow fence (Tabler et al., 1990a).*

The capacity of a 50% porosity snow fence, V_c, which includes both windward and leeward drifts, expressed as m^3 of water per metre of fence length can be approximated by the equation:

$$V_c = 8.5H^{2.2}, \quad (77)$$

in which H is the height to the top of the fence measured from ground level (m). This relationship assumes the density of drifted snow, before melting begins, is approximated by Equation 4, and that fence length is essentially infinite.

The drift characteristics described above apply only to fences that are not buried by snow. An opening ("bottom gap") is usually left under the fences to reduce the tendency for burial. Equations 76 and 77 apply to fences having a bottom gap in the range from 0.10H to 0.15H. As the bottom gap is increased to more than 0.15H: (a) the depths of both the

windward and leeward drifts are reduced, (b) the windward edge of the lee drift is displaced downwind, (c) the total drift length remains the same, and (d) the total snow storage capacity is reduced.

Tabler and Schmidt (1986) suggest that a fence should be sufficiently long to protect an area from snow transported by winds varying 25° on either side of the prevailing wind direction. A properly-designed fence allows for this variation and provides an overlap to compensate for the reduced capacity near the ends. Therefore, the recommended length of a snow fence is equal to the sum of the required protection width plus the distance between the fence and the downwind end of protected area. Fence lengths shorter than 20 to 25H have overlapping effects from both ends, resulting in large reductions in drift size and storage capacity. The reduction in storage capacity caused by insufficient length is approximated (Tabler and Schmidt, 1986) for fence length to height ratios from 5 to 50 as,

(78)

$$\frac{V_C(L)}{V_C} = 0.288 + 0.039(\frac{L}{H}) - 0.0009(\frac{L}{H})^2 + 0.0000075(\frac{L}{H})^3$$

where $V_c(L)$ is the storage capacity for a fence of length L.

Snow fences having porosities, F, between 0.4 and 0.6 accumulate the largest drifts. Solid fences, F=0, develop equilibrium drifts about 24H long, which are equally divided between windward and leeward sides. The volume of snow accumulated, $V_c(F=0)$, in m^3 per metre of solid fence length can be approximated to be $V_c(F=0) = 3H^{2.2}$, with H in metres. The dimensions of an equilibrium drift formed by a solid fence are shown in Figure 63. The windward drift is slightly larger than that formed by a porous fence but the leeward drift is much smaller.

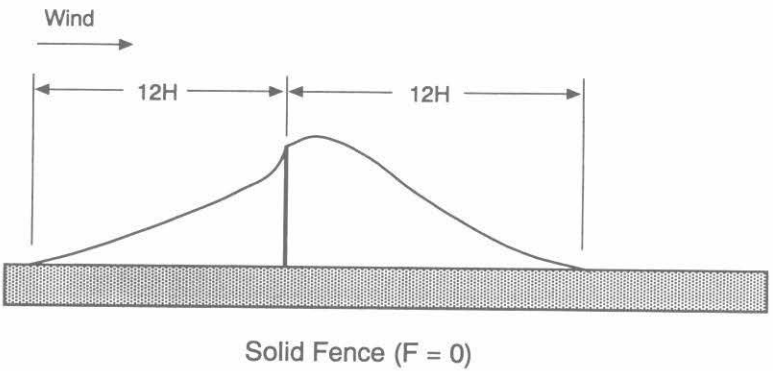

Figure 63 *Dimension of equilibrium drift formed behind a solid snow fence (Tabler et al., 1990a).*

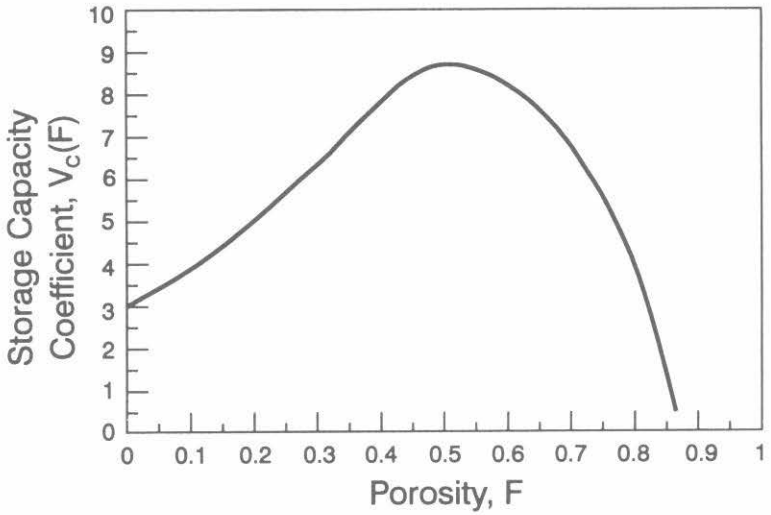

Figure 64 *Variation in snow storage coefficient with fence porosity for H=1, (after Tabler, 1994).*

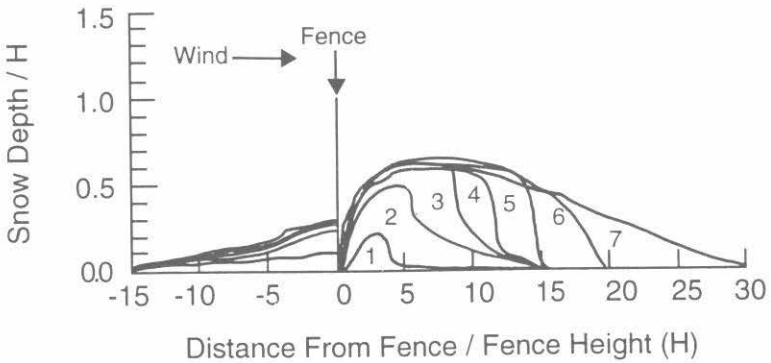

Figure 65 *Stages in "growth" of a snow drift formed by a 3.8-m tall "Wyoming-style" fence with a 15-cm bottom gap (after Tabler, 1989).*

The effect of varying fence porosity on snow storage for an H=1 is shown in Figure 64. The influence of this variation on the storage of a fence can be approximated by the expression:

$$V_c(F) = (3 + 4F + 44F^2 - 60F^3)H^{2.2} . \qquad (79)$$

in which $V_c(F)$ is the storage capacity of a fence porosity, F. The snow storage capacity of a solid fence is about one-third that of a fence with a porosity of 50%.

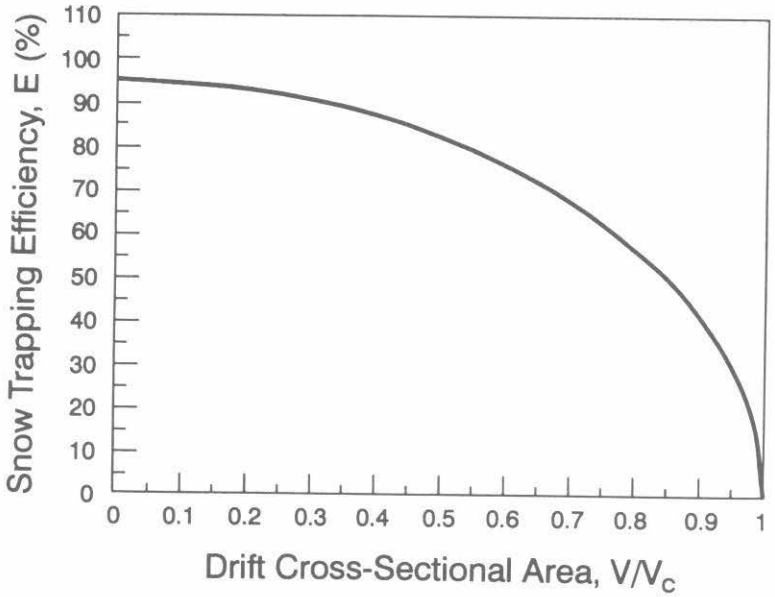

Figure 66 *Decay in the trapping efficiency of a snow fence with a porosity of 50% as it fills with snow.*

The efficiency of snow trapping by a fence diminishes as the snow drift grows. Figure 65 shows the stages of drift formation as a result of unidirectional transport to a fence. The trapping efficiency of a snow fence, E (%), is the percentage of incoming blowing snow at heights below that of the fence top that is retained by the fence as a snow drift. Tabler (1994) shows that trapping efficiency declines with increasing wind speed. Tabler and Jairell (1993) demonstrate the decay in trapping efficiency during snow drift growth as shown in Figure 66 which describes the decrease as

$$E = 95[1-(\frac{V}{V_C})^2]^{0.5}\ , \qquad (80)$$

in which V = the drift volume. Equation 80 assumes an initial 95% trapping efficiency for the snow fence which is typical for a variety of common conditions.

For a 2-m fence having a porosity F = 0.5 and a wind speed of about 14 m/s, the trapping efficiency remains above 70% until the drift is at 70% of capacity and then drops rapidly. The decline in trapping efficiency as

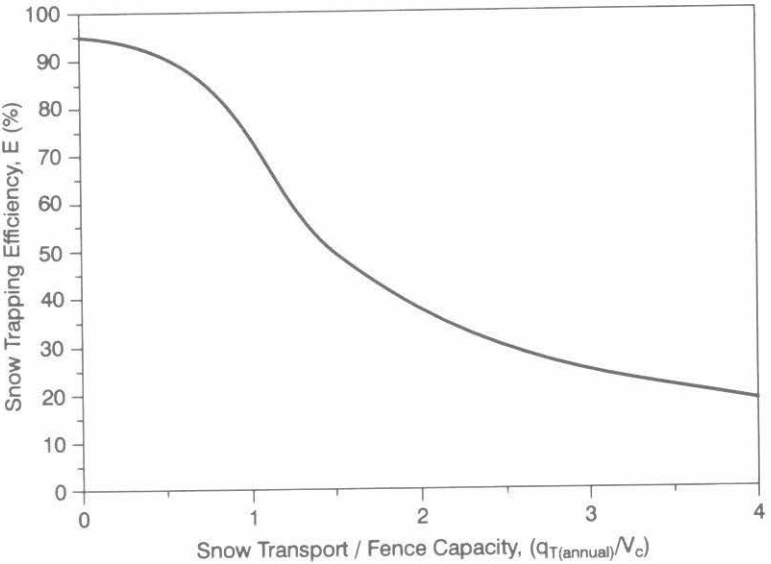

Figure 67 *Snow trapping efficiency as a function of snow transport relative to snow fence capacity (after Tabler and Jairell, 1993).*

a snow fence fills and eventually has its storage capacity exceeded is shown in Figure 67. When the unidirectional annual snow transport to the fence is just sufficient to fill the fence, average annual trapping efficiencies of 75% are suggested (Tabler and Jairell, 1993). As annual snow transport exceeds the snow storage capacity, then E(annual) = 0.75 [V_c/q_T(annual)]. This results in a 38% trapping efficiency when annual snow transport is twice the size of snow storage capacity. To retain average annual trapping efficiencies of greater than 50%, the snow storage capacity of a fence should be at least two-thirds of the average annual unidirectional snow transport.

Chapter 8

Conclusion

Snow is one of the lowest density materials on the Earth's surface; hence, snow accumulation processes largely involve interception of snow by vegetation and relocation of snow by the wind. Effective snow management consists of manipulating vegetation and placing man-made structures to modify the area of surfaces that intercept snow and the magnitude of lift and shear forces exerted by the wind. Snow accumulation is highly sensitive to climatic conditions; thus, climate regime and changes to this regime should be considered in interpreting interception and relocation processes and in appropriately managing snow. Because snow accumulation can often be managed with subtle changes in the spatial distribution and geometry of vegetation or with modest engineering structures, snow management techniques present an opportunity to augment water supply at the surface without irrigation and to ameliorate excess runoff without dams or other water control structures.

This Science Report has reviewed the major processes and factors that affect the spacing and timing of snow accumulation. The density of snow usually increases after its initial deposition, the rate of increase dependent upon climate and vegetation conditions in various geographic regions. Even in windswept regions, snow density has little covariance with snow depth for depths less than 60 cm. Hence, in calculating the snow water equivalent, mean snow densities appropriate to the landscape type can be assigned for depths in this range. For depths greater than 60 cm in windblown landscapes, there are relationships between depth and density that can be used to calculate snow water equivalent from depth measurements. For landscapes that are not subject to strong wind at the surface, snow densities are a function of vegetation type and snow depth.

Because of these relationships, snow-water-equivalent measurement strategies that stratify sampling by landscape units are the most efficient and successful.

Snowcover distribution is strongly affected by topography and vegetation, though as these factors are not independent the interaction is often complex and specific effects are difficult to ascertain from field data. Elevation alone is not a causative factor in snow distribution, winter orographic precipitation being related more to wind flow and slope than to elevation. Other factors such as frequency of melt and rain and exposure to the wind correlate with elevation and cause the perceived trends in snow accumulation along mountain slopes.

Snow falling into a vegetation canopy is redistributed by turbulent air flow associated with the canopy and direct interception of snow by the canopy. Hence, the water equivalent under a canopy varies with distance to individual trees and between stands of different tree species. In dense spruce forests, over 60% of cumulative snowfall can be intercepted in mid-winter. Intercepted snow is subject to sublimation rates much higher than snow on the ground. In continental North America, about one-third of annual snowfall is sublimated from intercepted snow in conifer stands, while less than 10% is similarly sublimated from deciduous stands. Clear-cuts in coniferous forests show a one-third increase in snow water equivalent compared to adjacent forests. In windy environments, this increase diminishes where clear-cut size is greater than about five times the tree height.

Blowing snow in open areas can remove up to three-fourths of annual snowfall. If fetches are large, most of this snow sublimates in transit; for short fetches, most snow is deposited in drifts. The transport rate of blowing snow increases with the fourth power of wind speed; thus, when snow is sufficient, the local wind, climatology and landscape exposure control the annual transport. Wind relocation of snow is also extremely sensitive to surface roughness, such as caused by standing stubble, because this roughness can reduce the wind force applied to the surface. Wheat stubble in southern Saskatchewan reduces snow transport by half compared to that on fallow fields. Though the sublimation rate increases with increasing temperature, monthly sublimation losses increase with decreasing monthly temperature because the frequency of blowing snow increases as the mean monthly temperature becomes colder. Because of these balancing factors, similar high sublimation rates are found in both the southern prairies and in the Arctic. However, as winds from specific directions tend to be either warmer or colder, the direction of snow transport does not match that of wind directional frequency and simple wind roses cannot always be used to design windblown snow-control structures.

In landscapes that display a mixture of windswept and forested locations, snow water equivalent increases with the density of vegetation and in sheltered valleys and gullies. In sub-arctic environments, water vapour fluxes from soils to snow may increase the snow water equivalent above that contributed by snowfall. These factors permit the development of landscape classification schemes in which characteristic depths, accumulations and the small-scale variation of these parameters can be assigned to readily-determined landscape types (tundra plains, prairie hillslopes, taiga, hilltops, valley bottoms, etc.). Such schemes can be used to assess the impact of land use changes, and, when coupled to physically-based snow relocation models can assess the concomitant impact of changing climate and vegetation cover.

Various management strategies have been designed for controlling snow accumulation. In forests, cut blocks and thinning are used to enhance snow accumulation. For windy environments, cut blocks less than 12H are most effective. Where forest thinning is applied, there is a linear increase in snow water equivalent and the basal area of conifers removed with up to 35% increase in snow achieved for complete conifer removal. Snow management on agricultural lands can increase the yield of spring wheat by more than 10 kg/ha per mm of additional snow water equivalent. Alternate height stubble and trap strips are generally more effective than level tall stubble in trapping snow, though the benefits vary with snowfall and wind regime. Typically up to 60 mm additional water equivalent over a field in southern Saskatchewan can be gained by appropriate stubble management techniques. Snow fences and shelterbelts limit the fetch of blowing snow and cause transported snow to be deposited rather than sublimated. The capacity of a porous snow fence or shelterbelt to trap snow increases with the square of its height; hence, one tall barrier is usually more effective than several shorter barriers. Porous fences are more efficient than solid fences in trapping snow and maximum drift lengths of 35 times the fence height can be obtained. The snow trapping efficiency of a barrier declines exponentially as the drift approaches its capacity size; therefore, fences should have capacities well in excess of annual transport in order to trap snow throughout the winter.

The authors hope that the principles and practices outlined in this Science Report will continue to develop. Recent advances in understanding the physics of snow hydrology should lead to improved and more physically-based hydrological simulations and snow management schemes. A particular improvement to the work outlined in this report will stem from a more rigorous assessment of the implications of air and snow flow over irregular terrain, and the coupling of spatially-distributed snow-surface process models with global circulation models and numerical weather prediction models.

Chapter 9

BIBLIOGRAPHY

Abbott, J.R. and J.R.D. Francis. 1977. Saltation and suspension trajectories of solid grains in a water stream. Philosophical Transcripts of Royal Society, London, Series A, 284:225-254.

Adams, W.P. and B.F. Findlay. 1966. Snow measurement in the vicinity of Knob Lake, central Labrador-Ungava. In *Proceedings of the 25th Annual Meeting of the Eastern Snow Conference*, 110-139.

Alexander, R.R., C.A. Troendle, M.R. Kaufmann, et al. 1985. The Fraser Experimental Forest, Colorado: Research program and published research 1937-1985. General Technical Report RM-118. Fort Collins, Colorado, USDA Forest Service, Rocky Mountain Forest and Range Experiment Station. 46 p.

Bagnold, R.A. 1941. The Physics of Blown Sand and Desert Dunes. Chapman and Hall, London. 255 p.

Barnsley, M. 1988. Fractals Everywhere. Academic Press Inc., San Diego, California.

Barry, P.J. 1991. Discussion paper on the report by H.G. Jones entitled 'Snow chemistry and biological activity: A particular perspective on nutrient cycling'. In *T.D. Davies, M. Tranter, H.G. Jones (eds.), Seasonal Snowpacks: Processes of Compositional Change*. NATO ASI Series G(28). Berlin: Springer-Verlag. 229-235.

Black, A.L. and F.H. Siddoway. 1971. Tall wheatgrass barriers for soil erosion control and water conservation. Journal of Soil and Water Conservation, 26:107-111.

Budd, W.R., R. Dingle and U. Radok. 1966. The Byrd snowdrift project: Outline and basic results. Studies in Antarctic Meteorology, American Geophysical Union, Antarctica Research Service 9:71-134.

Calder, I.R. 1990. Evaporation in the Uplands. John Wiley and Sons, Chichester, U.K. 148 p.

Carroll, T.R. 1987. Operational airborne measurements of snow water equivalent and soil moisture using terrestrial gamma radiation. In *Proceedings of the Large Scale Effects of Seasonal Snow Cover. International Association of Scientific Hydrologists*. No. 166:213-223.

Carroll, T.R. 1991. Operational airborne and satellite snow cover products of the National Operational Hydrologic Remote Sensing Center. In *Proceedings of the 47th Annual Eastern Snow Conference*, 87-98.

Chang, A.T.C., J.L. Foster, D.K. Hall et al. 1982. Snow water equivalent estimation by microwave radiometry. Cold Regions Science and Technology, 259-267.

Chang, A.T.C., J.L. Foster, P. Gloersen, et al. 1987. Estimating snowpack parameters in the Colorado River basin. In *Large Scale Effects of Seasonal Snow Cover. Proceedings of the Symposium of the International Association of Hydrological Sciences*, Vancouver. AISH Publication No. 166:343-352.

Chepil, W.S. 1945. Dynamics of erosion, II: Initiation of soil movement. Canadian Journal of Soil Science, 610(5):397-411.

Colbeck, S.C. 1986. Statistics of coarsening in water-saturated snow. Acta Metallica, 34(3):347-352.

Cork, H.F. and H.S. Loijens. 1980. The effect of snow drifting on gamma snow survey results. Journal of Hydrology, 48:41-51.

de Jong, E. and D.A. Rennie. 1969. Effect of soil profile type and fertilizer on moisture use by wheat grown on fallow or stubble. Canadian Journal of Soil Science, 44:189-197.

Donald, J.R., E.D. Soulis, F. Seglenieks and N. Kouwen. 1991. Snow depth estimates for shallow snowpacks from GOES visible imagery. In *Proceedings of the 48th Eastern Snow Conference*, 149-161.

Dickinson, W.T. and F.G. Theakston. 1982. Snow-flume modelling of snow accumulation in forest openings. In *Hydrological Processes of Forested Areas. Proceedings of the Canadian Hydrology Symposium, Fredericton, NB*, National Research Council, Ottawa, No. 20548, 113-129.

Dozier, J. and D. Marks. 1987. Snow mapping and classification from Landsat thematic mapper data. Annals of Glaciology, 9:1-7.

Dyunin, A.K. 1959. Fundamentals of the theory of snow drifting. Izvest. SIbirsk, Otdel. Akad. Nauk. U.S.S.R. No. 12:11-24. [English Translation by G. Belkov, National Research Council, Ottawa, Technical Translation, 952, 1961].

Dyunin, A.K. and V.M. Kotlyakov. 1980. Redistribution of snow in mountains under the effect of heavy snow-storms. Cold Regions Science and Technology, 3:287-294.

Dyunin, A.K., Ya.D. Kvon, A.M. Zhilin and A.A. Komarov. 1991. Effect of snow drifting on large-scale aridization. In *V.M Kotlyakov, A. Ushakov and A. Glazovsky (eds.), Glaciers-Ocean-Atmosphere Interactions*. IAHS Publication No. 208, IAHS Press, Wallingford, U.K., 489-494.

Ellerbruch, D.A. and H.S. Boyne. 1979. Snow stratigraphy and water-equivalence measured with an active microwave system. Journal of Glaciology, 194:225-234.

Föhn, P.M.B. and R. Meister. 1983. Distribution of snow drifts on ridge slopes: measurements and theoretical approximations. Annals of Glaciology, 4:52-57.

Gary, H.L. 1974. Snow accumulation and melt as influenced by a small clearing in lodgepole pine. Water Resources Research, 10:345-353.

Gary, H.L. 1975. Airflow patterns and snow accumulation in a forest clearing. In *Proceedings of the 43rd Annual Meeting of the Western Snow Conference*, 106-113.

Golding, D.L. and R.H. Swanson. 1986. Snow distribution patterns in clearings and adjacent forest. Water Resources Research, 22(13):1931-1940.

Goodell, B.C. 1966. Watershed treatment effects on evapotranspiration. In *W. Sooper and H. Lull, (eds.), Forest Hydrology*. Pergamon Press, New York, NY, 477-482.

Goodison, B.E., H.L. Ferguson and G.A. McKay. 1981. Measurement and data analysis. In *D.M. Gray and D.H. Male, (eds.), Handbook of Snow: Principles, Processes, Management and Use*. Pergamon Press, Toronto, 191-274.

Goodison, B.E., B. Wilson, K. Wu and J. Metcalfe. 1984. An inexpensive remote snow gauge: an assessment. In *Proceedings of the 52nd Annual Western Snow Conference*, 188-191.

Goodison, B.E., I. Rubinstein, F.W. Thirkettle and E.J. Langham. 1986. Determination of snow water equivalent on the Canadian Prairies using microwave radiometry. Modelling Snowmelt Induced Processes. IAHS Publication No. 155:163-173.

Goodison, B.E., J.R. Metcalfe, R.A. Wilson and K. Jones. 1988. The Canadian automatic snow depth sensor: A performance update. In *Proceedings of the 56th Annual Western Snow Conference*, 178-181.

Granberg, H.B. 1978. Snow accumulation and roughness changes through winter at a forest-tundra site near Shefferville, Quebec. In *S.C. Colbeck and M. Ray, (eds.), Proceedings, Modeling of Snow Cover Runoff*. U.S. Army Cold Regions Research Laboratory, Hanover, NH, 83-92.

Gray, D.M., P.G. Landine and R.J. Granger. 1985. Simulating infiltration into frozen prairie soils in streamflow models. Canadian Journal of Earth Sciences, 22(3):464-474.

Gray, D.M. and others. 1979. Snow accumulation and distribution. In *S.C. Colbeck and M. Ray (eds.), Proceedings, Modeling Snow Cover Runoff*. U.S. Army Cold Region Research Laboratory, Hanover, NH, 3-33.

Gray, D.M., D.I. Norum and G.E. Dyck. 1970. Densities of prairie snowpacks. In *Proceedings of the 38th Annual Meeting of the Western Snow Conference*, 24-30.

Gray, D.M., R.J. Granger and G.E. Dyck. 1985. Overwinter soil moisture changes. Transactions of the American Society of Agricultural Engineers, 28(2):442-447.

Greeley, R. and J.D. Iversen. 1985. Wind as a Geological Process on Earth, Mars, Venus and Titan. Cambridge University Press, New York, NY. 333 p.

Gubler, H. 1981. An inexpensive snow depth gauge based on ultrasonic wave reflection from the snow surface. Journal of Glaciology, 127(95):157-163.

Gubler, H. and M. Hiller. 1984. The use of microwave FMCW radar in snow and avalanche research. Cold Regions Science and Technology, 9:109-119.

Gubler, H. and J. Rychetnik. 1991. Effects of forests near the timberline on avalanche formation. In *Snow, Hydrology and Forests in High Alpine Areas*. IAHS Publication No. 205. IAHS Press: Wallingford, U.K., 19-38.

Haan, C.T. 1977. Statistical Methods in Hydrology. Iowa State University Press, Ames, IA.

Hall, D.K. and J. Martinec. 1985. Remote Sensing of Ice and Snow. Chapman and Hall Ltd., New York.

Holroyd, E.W. and T.R. Carroll. 1990. Refinements in the remote sensing of snow-covered area. In *Proceedings of the 58th Annual Western Snow Conference*, 79-86.

Hoover, M.D. and C.F. Leaf. 1967. Process and significance of interception in Colorado subalpine forest. In *W.E. Sopper and H.W. Lull (eds.), Forest Hydrology*. Pergamon Press, New York, NY, 213-223.

IAHS/UNESCO/WMO. 1973. The Role of Snow and Ice in Hydrology. Proceedings of the Banff Symposia, September, 1972, 2 Vols. IAHS Publication No. 107.

Jeffrey, W.W. 1968. Snow hydrology in the forest environment. In *Snow Hydrology, Proceedings of a Workshop Seminar*. Canadian National Committee for the International Hydrological Decade. Queen's Printer, Ottawa, 1-19.

Jones, H.G. 1987. Chemical dynamics of snowcover and snowmelt in a boreal forest. In *H.G. Jones and W.J. Orville-Thomas (eds.), Seasonal Snowcovers: Physics, Chemistry, Hydrology*. NATO ASI Series C(211). Dordrecht: Reidel, 531-574.

Jones, H.G. 1991. Snow chemistry and biological activity: a particular perspective on nutrient cycling. In *T.D. Davies, M. Tranter and H.G. Jones (eds.), Seasonal Snowpacks: Processes of Compositional Change*. Springer-Verlag: Berlin, 173-228.

Killingtveit, A. and K. Sand. 1991. On areal distribution of snowcover in a mountainous area. In *T.D. Prowse and C.S.L. Ommanney (eds.), Northern Hydrology, Selected Perspectives*. NHRI Symposium No. 6, 189-203.

Kind, R.J. 1981. Chapter 8. Drifting snow. In *D.M. Gray and D.H. Male (eds.), Handbook of Snow, Principles, Processes, Management and Use*. Pergamon Press: Toronto, 338-359.

Kobayashi, S. 1971. Development and movement of wavy features on the snow surface during drifting. Low Temperature Science Series A, Physical Sciences. No. 29, 81-92.

Kobayashi, D. 1972. Studies of Snow Transport in Low-Level Drifting Snow. Contributions from the Institute for Low Temperature Science, Series A(24), 1-58.

Kotlyakov, V.M. 1961. Results of study of the ice sheet in Eastern Antarctica. Antarctic Glaciology, IAHS/AISH Publication 55, 88-99.

Kuz'min, P.P. 1963. Formirovanie Snezhnogo Pokrova i Metody Opredeleniya Snegozapasov (Snow Cover and Snow Reserves). [English Translation by Israel Program for Scientific Translation, Jerusalem]. 139 p.

Landine, P.G. and D.M. Gray. 1989. Snow Transport and Management. Internal Report, Division of Hydrology, University of Saskatchewan, Saskatoon, Saskatchewan. 80 p.

Langham, E.J. 1981. Physics and properties of snowcover. *In D.M. Gray and D.H. Male (eds.), Handbook of Snow, Principles, Processes, Management and Use*. Pergamon Press: Toronto, 275-337.

Lee, L.W. 1975. Sublimation of Snow in a Turbulent Atmosphere. Unpublished Ph.D. Thesis. University of Wyoming, Laramie, Wyoming. 162 p.

Lettau, H. 1969. Note on aerodynamic roughness-parameter estimation on the basis of roughness element description. Journal of Applied Meterology, 8:828-832.

Lyles, L. and B.E. Allison. 1976. Wind erosion: The protective role of simulated standing stubble. Transactions of the American Society of Agricultural Engineering, 19:61-64.

Male, D.H. 1980. The seasonal snowcover. In *S.C. Colbeck (ed.), Dynamics of Snow and Ice Masses*. Academic Press, New York, NY, 305-395.

Mandelbrot, B.B. 1983. The Fractal Geometry of Nature. W.H. Freeman and Co. New York, NY. 468 p.

Maeno, N., Araoka, K., Nishimura, K. and Y. Kaneda. 1979. Physical aspects of the wind-snow interaction in blowing snow. Journal of the Faculty of Science, Hokkaido University Series VII (Geophysics), 6(1):127-141.

Martinec J. and A. Rango. 1991. Indirect evaluation of snow reserves in mountain basins. Snow, Hydrology and Forests in High Alpine Areas. IAHS Publication No. 205:111-119.

Martinec, J., K. Seidel, U. Burkhart and R. Baumann. 1991. Areal modelling of snow water equivalent based on remote sensing techniques. Snow, Hydrology and Forests in High Alpine Areas. IAHS Publication No. 205:121-129.

McGinnis, D.F., J.R. Pritchard and D.R. Weisnet. 1975. Determination of snow depth and snow extent from NOAA 2 satellite very high resolution radiometer. Water Resources Research, 11(6):897-902.

McKay, G.A. 1970. Precipitation. In *D.M. Gray (ed.), Handbook on the Principles of Hydrology*. Water Information Center, Syosset, NY, 2.1 - 2.111.

McNay, R.S., L.D. Petersen and J.B. Nyberg. 1988. The influence of forest stand characteristics on snow interception in the coastal forests of British Columbia. Canadian Journal of Forest Research, Vol. 18:566-573.

Meiman, J.R. 1970. Snow accumulation related to elevation, aspect and forest canopy. In *Snow Hydrology, Proceedings of a Workshop Seminar, 1968*. Canadian National Committee for the International Hydrological Decade, Queen's Printer, Ottawa, 35-47.

Meiman, J.R. 1987. Influence of forests on snowpack accumulation. In *Management of Subalpine Forests: Building on 50 years of Research.* General Technical Report RM-149. USDA Forest Service, Rocky Mountain Forest and Range Experiment Station. Fort Collins, CO, 61-67.

Miller, D.H. 1962. Snow in trees - where did it go? Proceedings of the 30th Annual Meeting of the Western Snow Conference, 30:21-29.

Miner, N.H. and J.M. Trappe. 1957. Snow Interception, Accumulation and Melt in Lodgepole Pine Forests in the Blue Mountains of Eastern Oregon. USDA Forest Research Service, Forest Range Experimental Station, Research Note No. 143. 4 p.

Pasquill, F. 1974. Atmospheric Diffusion, Second Edition. Ellis Horweed Ltd., Chichester, U.K. 429 p.

Patch, J.R. 1981. Effects of forest cover on snow distribution in the Nashwaak experimental watershed project. Proceedings of the 38th Eastern Snow Conference, 76-87.

Petropavlovskaya, M.S. and I.L. Kalyuzhnyi, 1986. Drifting of snow in northern Kazakhstan. Meteorologiya i Gidrologiya, 2:81-90.

Pomeroy, J.W. 1988. Wind Transport of Snow. Ph.D. Thesis, University of Saskatchewan, Saskatoon, Saskatchewan. 226 p.

Pomeroy, J.W. 1989. A process-based model of snow drifting. Annals of Glaciology, 13:237-240.

Pomeroy, J.W. 1991. Transport and sublimation of snow in wind-scoured alpine terrain. In *H. Bergmann, H. Lang, W. Frey, D. Issler and B. Salm (eds.), Snow Hydrology and Forests in High Alpine Areas.* IAHS Publication No. 205, IAHS, Wallingford, 131-140.

Pomeroy, J.W. and D.M. Gray. 1990. Saltation of snow. Water Resources Research, 26(7):1583-1594.

Pomeroy, J.W. and D.H. Male. 1986. Physical modelling of blowing snow for agricultural production. In *H. Steppuhn and W. Nicholaichuk (eds.), Proceedings of the Symposium of Snow Management for the Great Plains Agriculture Council.* Publication No. 120, Water Studies Institute, Saskatoon, Saskatchewan, 73-108.

Pomeroy, J.W. and D.H. Male. 1992. Steady-state suspension of snow. Journal of Hydrology, 136:275-301.

Pomeroy, J.W. and R.A. Schmidt. 1993. The use of fractal geometry in modelling intercepted snow accumulation and sublimation. In *Proceedings of the Joint Meeting, Eastern/Western Snow Conference*, 1-10.

Pomeroy, J.W., D.M. Gray and P.G. Landine. 1991. Modelling the transport and sublimation of blowing snow on the prairies. In *Proceedings of the 48th Eastern Snow Conference*, 175-188.

Pomeroy, J.W., D.M. Gray and P.G. Landine. 1993. The Prairie Blowing Snow Model: characteristics, validation, operation. Journal of Hydrology, 144:165-192.

Raupach, M.R., D.A. Gillette and J.F. Leys. 1993. The effect of roughness elements on wind erosion threshold. Journal of Geophysical Research, 98(D2):3023-3029

Rees, W.G. 1990. Physical Principles of Remote Sensing. Cambridge University Press. 247 p.

Rhea, J.O. and L.O. Grant. 1974. Topographic influences on snowfall patterns in mountainous terrain. Advance Concepts in Technical Study of Snow Ice Resources, Interdisciplinary Symposium, U.S. National Academy of Sciences, Washington D.C., 182-192.

Santeford, H.S. 1978. Snow soil interactions in interior Alaska. In *S. Colbeck and M. Ray (eds.), Proceedings, Modeling of Snow Cover Runoff.* U.S. Army Cold Regions Research and Engineering Laboratory, Hanover, NH, 311-318.

Saskatchewan Advisory Council on Soils and Agronomy. 1982. Saskatchewan fertilizer and cropping practices, 1982-83. Saskatchewan Department of Agriculture and Extension Division, University of Saskatchewan, Saskatoon, Saskatchewan.

Satterlund, D.R. and H.F. Haupt. 1970. The disposition of snow caught by conifer crowns. Water Resources Research 6:649-652.

Schmidt, R.A., Jr. 1972. Sublimation of wind-transported snow - "A model". Research Paper RM-90, USDA Forestry Service, Rocky Mountain Forest and Range Experimental Station, Fort Collins, CO.

Schmidt, R.A. 1982. Properties of blowing snow. Review of Geophysics and Space Physics, 20:39-44.

Schmidt, R.A. 1986. Transport rate of drifting snow and the mean wind speed profile. Boundary Layer Meteorology, 34:213-241.

Schmidt, R.A. 1991. Sublimation of snow intercepted by an artifical conifer. Agriculture and Forest Meteorology, Vol. 54:1-27.

Schmidt, R.A. and D.R. Gluns. 1991. Snowfall interception on branches of three conifer species. Canadian Journal of Forest Research, Vol. 21:1262-1269.

Schmidt R.A. and J.W. Pomeroy. 1990. Bending of a conifer branch at subfreezing temperatures: implications for snow interception. Canadian Journal of Forest Research, Vol. 20:1250-1253.

Schmidt, R.A. and C.A. Troendle. 1989. Snowfall into a forest and clearing. Journal of Hydrology, 110:335-348.

Schmidt, R.A. and C.A. Troendle. 1992. Sublimation of intercepted snow as a global source of water vapour. In *Proceedings of the 60th Western Snow Conference*, 1-9.

Schmidt, R.A., R.L. Jairell and J.W. Pomeroy. 1988. Measuring snow interception and loss from an artificial conifer. In *Proceedings of the 56th Annual Meeting of the Western Snow Conference*, Kalispell, MT, 166-169.

Seligman, G. 1980. Snow Structure and Ski Fields. International Glaciological Society, Cambridge, England. 555 p.

Shook, K. and D.M. Gray. 1994. Determining the snow water equivalent of shallow prairie snowcovers. In *Proceedings of the 51st Eastern Snow Conference*. In press.

Shook, K., D.M. Gray and J.W. Pomeroy. 1993. Temporal variation in snowcover area during melt in Prairie and Alpine environments. Nordic Hydrology, 24:183-198.

Smith, J.L., H.G. Halverson and R.A. Jones. 1972. Central Sierra profiling snow gauge: A guide to fabrication and operation. USAEC Report. TID-25986, National Technical Information Services, U.S. Department of Commerce, Washington, DC.

Staple, W.J. and J.J. Lehane. 1954. Wheat yield and use of water on substations in Southern Saskatchewan. Canadian Journal of Soil Science, 34:460-468.

Steppuhn, H. 1981. Snow and agriculture. In *D.M. Gray and D.H. Male (eds.) Handbook of Snow, Principles, Processes, Management and Use*. Pergamon, Toronto, 60-126.

Steppuhn, H.W. 1976. Areal water equivalents for prairie snowcovers by centralized sampling. In *Proceedings of the 44th Annual Meeting of the Western Snow Conference*, 63-68.

Steppuhn, H.W. and G.E. Dyck. 1974. Estimating true basin snowcover. Advance Concepts in Technical Study of Snow Ice Resources, Interdisciplary Symposium, U.S. National Academy of Science, Washington, DC, 314-328.

Strobel, T. 1978. Schneeinterzeption in Fichten-Bestaenden in den Voralpen des Kantons Schwyz. In *Proceedings, IUFRO Seminar Mountain, Forests and Avalanches*. Davos, Switzerland, 63-79.

Sturm, M. 1991. The Role of Thermal Convection in Heat and Mass Transport in the Subarctic Snow Cover. CRREL Report 91-19. U.S. Army Cold Regions Research and Engineering Laboratory, Hanover, NH, 84 p.

Sturm, M. 1992. Snow distribution and heat flow in the taiga. Arctic and Alpine Research, 24(2):145-152.

Swanson, R.H. 1988. The effect of *in situ* evaporation on perceived snow distribution in partially clear-cut forests. In *Proceedings of the 56th Annual Western Snow Conference*, 87-92.

Tabler, R.D. 1971. Design of a watershed snow fence system and first-year snow accumulation. In *Proceedings of the 39th Annual Meeting of the Western Snow Conference*, 50-55.

Tabler, R.D. 1980a. Geometry and density of drifts formed by snow fences. Journal of Glaciology 26(94):405-419.

Tabler, R.D. 1980b. Self-similarity of wind profiles in blowing snow allows outdoor modeling. Journal of Glaciology, 26(94):421-434.

Tabler, R.D. 1989. Snow fence technology: state of the art. First International Conference on Snow Engineering. CRREL Special Report 89-6. US Army Cold Regions Research and Engineering Laboratory, Hanover, NH, 297-306.

Tabler, R.D. 1994. Design Guidelines for the Control of Blowing and Drifting Snow. Report prepared for Strategic Highway Research Program, SHRP-H-381, National Research Council, Washington, D.C., 391 p.

Tabler, R.D. and R.L. Jairell. 1993. Trapping efficiency of snow fences and implications for system design. Transportation Research Record, 1387:108-114.

Tabler, R.D. and R.A. Schmidt. 1986. Snow erosion, transport and deposition. In *H. Steppuhn and W. Nicholaichuk, (eds.), Proceedings of the Symposium on Snow Management for Agriculture*, Great Plains Agricultural Council Publication No. 120, University of Nebraska, Lincoln, NB, 12-58.

Tabler, R.D., J.W. Pomeroy and B.W. Santana. 1990a. Drifting snow. In *W.L. Ryan and R.D. Crissman (eds.), Cold Regions Hydrology and Hydraulics*. American Society of Civil Engineers, New York, 95-146.

Tabler, R.D., C.S. Benson, B.W. Santana and P. Ganguly. 1990b. Estimating snow transport from wind speed records: Estimates versus measurements at Prudhoe Bay, Alaska. In *Proceedings of the 58th Annual Meeting of the Western Snow Conference*, 61-78.

Takeuchi, M. 1989. Vertical profiles and horizontal increase of drift snow transport. Journal of Glaciology, 26(94):481-492.

Thorpe, A.D. and B.J. Mason. 1966. The evaporation of ice spheres and ice crystals. Journal of Applied Physics, 17:541-548.

Toews, D.A. and D.R. Gluns. 1986. Snow accumulation and ablation on adjacent forested and clearcut sites in southeastern British Columbia. In *Proceedings of the 54th Western Snow Conference*, 101-111.

Troendle, C.A. 1983. The potential for water yield augmentation from forest management in the Rocky Mountains. Water Resources Bulletin, 19, 359-373.

Troendle, C.A. 1987. Effect of clearcutting on streamflow generating processes from a subalpine forest slope. In *Forest Hydrology and Watershed Management*. IAHS Publication No. 167, 545-552.

Troendle, C.A. and C.F. Leaf. 1980. Hydrology. An Approach to Water Resources Evaluation of Non-point Silvicultural Sources. Athens, GA. U.S. Environmental Protection Agency, 1-173.

Troendle, C.A. and J.R. Meiman. 1984. Options for harvesting timber to control snowpack. In *Proceedings of the 52nd Annual Meeting of the Western Snow Conference*, 86-98.

Troendle, C.A., R.A. Schmidt and M.H. Martinez. 1988. Snow deposition processes in a forest stand with a clearing. In *Proceedings of the 56th Annual Meeting of the Western Snow Conference*, Kalispell, MT, 78-88.

U.S. Army Corps of Engineers. 1956. Snow Hydrology: Summary Report of the Snow Investigations. North Pacific Division, Portland, Oregon. 437 p.

Wankiewicz, A. 1991. Mountain snowpack observations by microwave satellite. Snow, Hydrology and Forests in High Alpine Areas. IAHS Publication No. 205, 151-160.

Wheeler, E. 1987. Interception and redistribution of snow in a subalpine forest on a storm-by-storm basis. In *Proceedings of the 55th Annual Meeting of the Western Snow Conference*, 70-77.

Wilm, H.G. and E.F. Dunford. 1945. Effect of Timber Cutting on Water Available for Streamflow from a Lodgepole Pine Forest. USDA Technical Bulletin No. 965. 43 p.

Woo, M-K. and P. Marsh. 1978. Analysis of error in the determination of snow storage for small high arctic basin. Journal of Applied Meteorology, 17(10):1537-1541.

Woo, M.K. and P. Steer. 1986. Monte Carlo simulation of snow depth in a forest. Water Resources Research, 22(6):864-868.

Woo, M-K., R. Heron, P. Marsh and P. Steer. 1983. Comparison of weather station snowfall with winter snow accumulation in high Arctic basins. Atmosphere-Ocean, 21(3):312-325.

Notes: